

**HYDROGEOCHEMICAL AND WATER
QUALITY INVESTIGATION ON
IRRIGATION AND DRINKING WATER
SUPPLIES IN THE MEKELLE REGION,
NORTHERN ETHIOPIA**

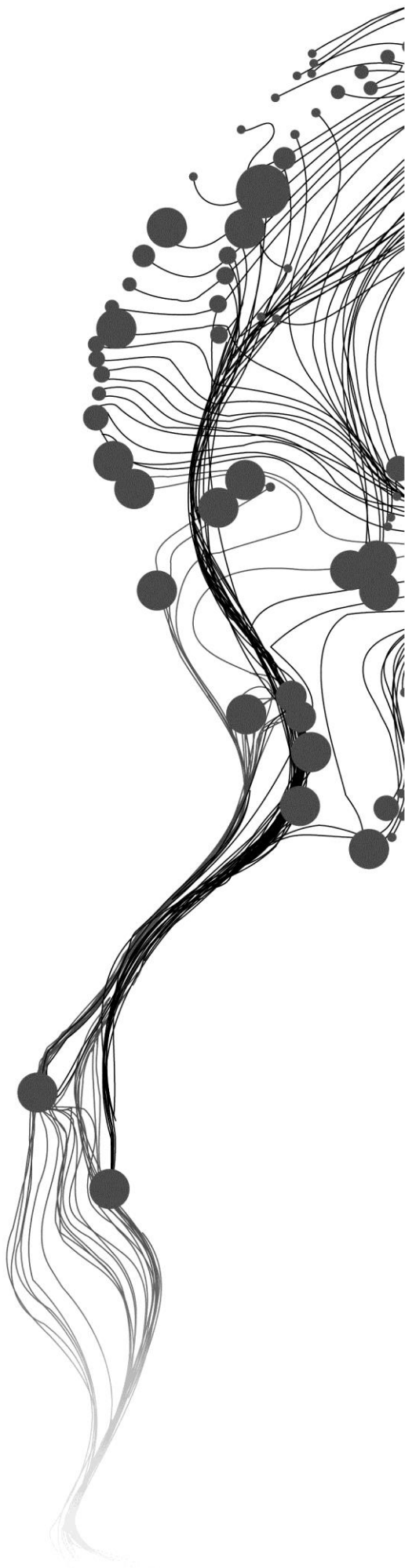
ASMELASH GEBREYOHANNS ABREHA

March, 2014

SUPERVISORS:

Dr. ir. C.M.M. Mannaerts

Drs. J.B. de Smeth



HYDROGEOCHEMICAL AND WATER QUALITY INVESTIGATION ON IRRIGATION AND DRINKING WATER SUPPLIES IN THE MEKELLE REGION, NORTHERN ETHIOPIA

ASMELASH GEBREYOHANNS ABREHA
Enschede, The Netherlands, March, 2014

Thesis submitted to the Faculty of Geo-Information Science and Earth
Observation of the University of Twente in partial fulfilment of the
requirements for the degree of Master of Science in Geo-information Science
and Earth Observation.
Specialization: Water Resource and Environmental Management

SUPERVISORS:
Dr. ir. C.M.M. Mannaerts
Drs. J.B. de Smeth

THESIS ASSESSMENT BOARD:
[Dr.Ir.M.S. Salama (Chair)]
[Prof.em.Dr.S.P. Vriend (External Examiner, University Utrecht, NARCIS,
Research group of Geochemistry)]
etc

DISCLAIMER

This document describes work undertaken as part of a programme of study at the Faculty of Geo-Information Science and Earth Observation of the University of Twente. All views and opinions expressed therein remain the sole responsibility of the author, and do not necessarily represent those of the Faculty.

ABSTRACT

This study focused on investigating water use problems, related to water quality and hydrogeochemical processes (evolutions, origins and mixing) of water resources in Mekelle region, Northern Ethiopia (Tigray). Hydrogeochemical (PHREEQC) and Aquachem modeling approaches combined with stable water isotopes and geospatial data analysis were employed for this purpose. Both primary and secondary geochemical data were used to understand the general hydrochemistry, correlation of major ions with TDS and types of water in the region. A statistical approach of hierarchical clustering analysis was also applied to classify the water resources into distinct groups and sub-groups, which are used to calculate hydrogeochemical equilibrium speciation, saturation indices of solid phases and inverse modeling among the sub-groups. Moreover, stable isotopes were used in the hydrogeochemical analysis. A water quality assessment was also carried out against WHO and Ethiopian standards for domestic use, irrigation and engineering works.

The findings of the study show that the water resources in the study area are evolved from Ca-HCO₃ water types to Ca-SO₄ water types through Ca-HCO₃-SO₄ and Ca-SO₄-HCO₃ water types. But small numbers of observations with distinct sodium, chloride and nitrate signal were also identified possibly indicating contamination by urban and agriculture. The result of the study further revealed that outgassing and dissolving of carbon dioxide, loss and dilution of water, dissolution and precipitation of carbonate and evaporite of halite and sylvite, and dissolution of sulphate minerals and anthropogenic effects are the main hydrogeochemical processes observed during hydrogeochemical evolution of the water resources. It is also observed that the isotopes signature of deuterium and oxygen-18 from water of boreholes, hand-dug wells, springs and rivers show depletion in deuterium and oxygen-18 when compared to VSMOW due to effects of evaporation processes. Moreover, lower D-excess was observed when compared to local rainfall of KOBO station data and this is mainly due to secondary fractionation effect and isotopic exchanges in the aquifer. The origin of the water resources in the study area is found to be primarily precipitation and there is mixing of ground and river waters.

By large, the study revealed that a significant number of water resources observations don't meet the WHO water quality standards for domestic uses including 38.5 % for TDS, 82.5 % for Total Hardness and 19 % for Nitrate. Moreover, 83% of the water resources data have corrosive character though 100 % not aggressive. Generally, the water resources in the region are characterized with high salinity and low alkalinity controlled by geology, land-use, water-rock interaction, evolution and anthropogenic effects.

Key words: - Water Quality, Hydrogeochemical processes, evolution, inverse modeling, isotopes fractionation, salinity, equilibrium speciation and saturation Indices.

ACKNOWLEDGEMENTS

I would like to express my sincere thanks to the Government of Netherlands and ITC (International Institution for Geo-information Science and Earth Observation) university of Twente for giving me an opportunity to pursue my Master program and financial support.

Above all, I would like to express my sincere thanks and appreciation to Dr. Ir. Chris Mannaerts for his scientific advice, guidance, critical comments and suggestions throughout my research work. I really appreciate his choosing the title and model because I gained a new knowledge and deeper insight in to water quality and PHREEQC model that makes me to have a new carrier to my work. I would like to say thank you to my second supervisor Drs. Boudewijn de Smeth for his commitment and extraordinary patience during laboratory works and for his constructive comments during my laboratory and research works.

This research work needs to collect primary and secondary water quality data from the study area. Hence, I would like to say thank you for Tigray Water Resource Bureau, Solomon Abera, Tedros Belay, Tadese and Alem for committed support during field work. I would like to extend my gratitude to Ataklti Gebretasdik and Kiros Tadesse for their unceasing support before, at and after field work.

My deepest gratitude also goes to Dr. Tagel Gebrehiwot for his precious time reading my thesis and constructive comments and also for his useful advice during my stay in ITC and thesis writing.

I want to express my appreciation to all my class mates for their friendship, socialization and support during stress times and my stay in ITC university of Twente.

I would like to thank the Ethiopian community students at ITC for love and providing me environment of home feeling during my stay at ITC university of Twente.

Finally, my special gratitude goes to all my family and my wife Almaz Gedy and my baby Hyab Asmelash for their love and moral support.

TABLE OF CONTENTS

1.	INTRODUCTION.....	1
1.1.	Background.....	1
1.2.	Research Problems.....	3
1.3.	Research Objectives.....	3
1.3.1.	General Objectives.....	3
1.3.2.	Specific Objectives.....	3
1.4.	Research Questions.....	4
1.5.	Organization of the Thesis.....	4
2.	LITERATURE REVIEW.....	7
2.1.	Water Quality.....	7
2.1.1.	Water Quality Sampling.....	7
2.1.2.	Water Quality Parameters.....	7
2.2.	Water Quality Analysis and Interpretation.....	8
2.3.	Hydrochemical Processes.....	9
2.4.	Geochemical Modeling.....	9
2.4.1.	Speciation Models.....	9
2.4.2.	Hydrochemical Equilibrium and geochemical Modeling.....	9
2.4.3.	Inverse Modeling.....	9
2.5.	Aquachem Water Quality Database.....	9
2.6.	Stable Isotopes.....	9
2.6.1.	Isotope Fractionation.....	9
2.7.	Previous works and studies.....	10
3.	STUDY AREA.....	11
3.1.	Location.....	11
3.2.	Physiography.....	11
3.3.	Climate.....	12
3.4.	Vegetation.....	12
3.5.	Land-use.....	12
3.6.	Stratigraphy of the study area.....	14
3.6.1.	Geology of the study area.....	14
3.7.	Hydrogeological Setting.....	15
3.8.	Hydrographic Setting.....	15
4.	DATA COLLECTION.....	17
4.1.	Field Data Collection.....	17
4.1.1.	Secondary Data.....	17
4.1.2.	In-situ Data.....	19
4.2.	Water Samples Collection.....	20
4.3.	Remote Sensing Data.....	22
5.	METHODS.....	23
5.1.	Laboratory Analysis.....	23
5.2.	Hydrochemical Data Reliability Check.....	24
5.3.	Hierarchical Cluster Analysis (HCA).....	25
5.4.	Source-rock Deduction.....	26
5.5.	Hydrogeochemical Modeling.....	26
5.5.1.	Aquachem 2012.1.....	26

5.5.2.	PHREEQC-2	26
5.5.3.	Inverse Modeling	27
5.6.	Relation and Fractionation of Stable Isotopes of Water (Oxygen and Hydrogen)	27
5.6.1.	Stable Isotopes Ratio.....	27
5.6.2.	Isotopic Fractionation.....	27
5.6.3.	The Meteoric Water Line	28
5.7.	Water Quality Assessment	29
5.7.1.	Domestic Use.....	29
5.7.2.	Irrigation Use.....	29
5.7.3.	Larson and Langelier Index	29
6.	RESULTS AND DISCUSSION	31
6.1.	General hydrogeochemistry.....	31
6.2.	Correlation of Total Dissolved Solids and Major Elements (Ions)	37
6.3.	Hydrogeochemical Water Classification using Piper Diagram and Mapping.....	39
6.4.	Comparison of groundwater and surface water hydrogeochemistry	41
6.5.	Hierarchical Cluster Analysis	43
6.5.1.	Source-rock Deduction and Chemical composition.....	46
6.6.	Hydrogeochemical Modeling	48
6.6.1.	Equilibrium Speciation and Saturation Indices of Mineral Phases in Solutions.....	48
6.6.2.	Inverse Modeling with Removal or Dilution of Water	50
6.7.	Relation and Fractionation Between Stable Isotopes Deuterium and Oxygen ($\delta^{18}\text{O}$).....	54
6.8.	Mixing of Water Among Different Resources.....	58
6.9.	Water Quality Assessment Evaluation (Criteria Testing).....	59
6.9.1.	Domestic Use.....	59
6.9.2.	Irrigation Use.....	61
6.9.3.	Implication of Groundwater Problems in Pipe Lines and Engineering Works	62
7.	CONCLUSION AND RECOMMENDATION	65
7.1.	Conclusions	65
7.2.	Recommendations.....	67

LIST OF FIGURES

Figure 1: Geological map of Mekelle outlier and its surrounding from geological map of Ethiopia (V.Kazmin, 1973).....	2
Figure 2: General structure of the thesis.....	5
Figure 3: Location map of the study area.....	11
Figure 4: Percentage of land-use/land-cover area of the region.....	12
Figure 5: Land-use/ Land-cover map of Mekelle region.....	13
Figure 6: Geological map of the study area.....	15
Figure 7: Topography and Groundwater Contour Map (A) and Drainage map (B) of the study area.....	16
Figure 8: Location and distribution of water points having secondary data.....	17
Figure 9: Images for Land-use from the study area.....	20
Figure 10: Field data collection flow chart.....	21
Figure 11: Location and distribution of water points from which water samples were collected in Sep, 2013.....	22
Figure 12: Laboratory Analysis, Data Control and Result Checks Flowchart.....	25
Figure 13: Aquachem Analysis, Geochemical Modeling and Isotope Fractionation Flow Chart.....	28
Figure 14: The distribution of pH with Geology (A) and Land-use (B) in Mekelle region.....	32
Figure 15: Graphs of correlation between measured, laboratory and model TDS and EC values.....	33
Figure 16: Spatial Variation of Electrical Conductivity (Salinity Hazard) with Geology (A) and Land-use (B) in the study area.....	35
Figure 17: Spatial Variation of Total Dissolved Solids with Geology (A) and Land-use (B) in the study area.....	37
Figure 18: Relationship between major ions concentration and TDS values of the water resources.....	38
Figure 19: Water type classification of water samples from Mekelle region using piper plot.....	40
Figure 20: Spatial distribution hydrochemical water types as a function of water resource type (River, Spring, Hand-dug Well & Borehole).....	41
Figure 21: Average concentration of major ions comparison with TDS for different water resources.....	43
Figure 22: Altitude effects on stable isotopes of oxygen-18 of boreholes, hand-dug wells, springs and rivers.....	43
Figure 23: Dendrogram of the hierarchical cluster analysis for groundwater samples classified in to groups and sub-groups.....	44
Figure 24: Water Type Classifications of the Sub-Groups using Piper Diagram.....	46
Figure 25: Stiff diagram shows Source-rocks of sub-groups in the study area.....	47
Figure 26: Spatial distribution map of sub-groups relative to the geology and drainage of the study area.....	48
Figure 27: Saturation indices of common minerals in Mekelle region: carbonate (Aragonite, Calcite, and Dolomite) and sulphate (Gypsum and Anhydrite) in the water samples.....	49
Figure 28: Example of sub-groups flow paths for inverse modeling from recharge to discharge areas.....	51
Figure 29: Plot of isotopic signature (LMWL) of rainfall year 2002 for KOBO and GMWL.....	55
Figure 30: Isotopes data sample point distribution in the study area.....	55
Figure 31: Plot of different water resource against LMWL using isotopes of deuterium versus oxygen-1856	
Figure 32: Evaporation trends for surface and groundwater samples in the study area.....	58
Figure 33: Linear correlation of stable isotopes of hydrogen and oxygen for different water resources in Mekelle region.....	58
Figure 34: Distribution of Nitrate with Geology (A) and Land-use (B) in the study area.....	61

Figure 35: Wilcox diagram of Sodium Adsorption ratio (Sodium Hazard) versus Salinity Hazard of Mekelle region.....62

Figure 36: Plots of Larson index (A) for corrosive and Langelier Index (B) for aggressive characteristics of observations63

Figure 37: Sodium Adsorption Ratio map with Geology (A) and Land-use (B) in the study area64

LIST OF TABLES

Table 1: Land-use classification accuracy analysis results	14
Table 2: Description of water points having secondary data	18
Table 3: Summary statistics of cations and anions of water resource constituents from 103 secondary data (Appendix-11)	18
Table 4: Summary statistics of the isotopes of water resources 2002 secondary data for the study area.....	18
Table 5: Isotopes of precipitation for KOBO area (2002) from IAEA	19
Table 6: Summary statistics of on the spot data measurements.....	19
Table 7: Description of the type of water points for water sample collection	21
Table 8: Summarized result of hydrogeochemical analysis in the laboratory and calculated Parameters for 40 water samples (Appendix-10)	24
Table 9: Maximum, Minimum and Mean value of water quality parameters for 143 primary and secondary data (Appendix- 10 and 11).....	34
Table 10: Correlation matrix of dissolved constituents (n = 143).....	39
Table 11: Mean hydrogeochemical composition of cluster sub-groups (except pH, EC ($\mu\text{S}/\text{cm}$), all others in mg/l)	45
Table 12: Description and interpretation of statistical sub-groups	45
Table 13: Source-rocks Deduction	47
Table 14: Chemical Composition of Source-rocks (Source Mesebo Cement Factory).....	47
Table 15: Pure solid mineral phases and their Initial saturation indices of sub-groups of the study area ...	49
Table 16: Equilibrium saturation indices and mineral phases of sub-groups	50
Table 17: Hydrogeochemistry data inputs for inverse modeling	50
Table 18: Outputs of inverse modeling flow path 1	51
Table 19: Outputs of inverse modeling flow path 2	52
Table 20: Outputs of inverse modeling flow path 3	52
Table 21: Outputs of inverse modeling flow path 4	53
Table 22: Isotopes abundances for precipitation of KOBO station.....	54
Table 23: Summary of Isotopes Deuterium and Oxygen-18 for the study area.....	56
Table 24: summary output of Anova (single factor) for Oxygen-18.....	56
Table 25: Study area parameters comparisons with guidelines of WHO (2011) and Ethiopian standards.	60
Table 26: Summarized values of LSI and LI for water resources in the study area.....	63

LIST OF ABBREVIATIONS

Abbreviations	Description
A	Aynalem
ANOVA	Analysis of Variance
A.S.L	Above Sea Level
At. Wt.	Atomic Weight
AQ-1	Aqua-1
BH	Borehole
CH	Chelekot
ET	Ethiopia
F	Flow path
G	Group
GIS	Global Information System
GLOVIS.USGS	USGS Global Visualization Viewer
GMWL	Global Meteoric Water Line
GNIP	Global Network of Isotopes in Precipitation
GPS	Global Positioning System
HACH	Spectrometry
HCA	Hierarchical Cluster Analysis
HDW	Hand-dug Well
IAEA	International Atomic Energy Agency
ICP-AES	Plasma Atomic Emission Spectrometry
IL	Ilala
ISO	Isotopes
LMWL	Local Meteoric Water Line
Log	Logarithm
M. Wt.	Molecular Weight
Meq/l	Mili Equivalent per Litter
Mg/l	Mili Gram per Litter
MM	May Mekden
MWL	Meteoric Water Line
NASA	National Aeronautics and Space Administration
ORG	Organization
RI	River
SAR	Sodium Absorption Ratio
S.NO	Serial Number
SG	Sub-Group
SMOW	Standard Mean Oceanic Water
SP	Spring
SRTM	Shuttle Radar Topography Mission
TH	Total Hardness
TM	Thematic Mapper
USGS	United States Geological Survey
VSMOW	Vienna Standard Mean Oceanic Water
WHO	World Health Organization
WMO	World Meteorological Organization
WQ	Water Quality

LIST OF SYMBOLS

Symbols	Description	Units
Al ³⁺	Aluminium Ion	Mg/l
Ca ²⁺	Calcium Ion	Mg/l
Cl ⁻	Chloride Ion	Mg/l
EC	Electrical Conductivity	μS/cm
F ⁻	Fluoride Ion	Mg/l
Fe ²⁺	Iron Ions	Mg/l
² H	Deuterium	‰
H ⁺	Hydrogen Ion	Mg/l
HCO ₃ ⁻	Bicarbonate Ion	Mg/l
IAP	Ionic Activity product	
K ⁺	Potassium Ion	Mg/l
K _{sat}	Solubility Product	
Mg ²⁺	Magnesium Ion	Mg/l
Mn ²⁺	Manganese	Mg/l
Na ⁺	Sodium Ions	Mg/l
NH ₄ ⁺	Ammonium Ion	Mg/l
NO ₃ ⁻	Nitrate Ions	Mg/l
¹⁸ O	Stable Isotope of Oxygen	‰
pH	Power of Hydrogen	
PO ₄ ³⁻	Phosphate Ion	Mg/l
SI	Saturation Index	
SiO ₂	Silicate	Mg/l
SO ₄ ²⁻	Sulphate Ion	Mg/l
TDS	Total Dissolved Solids	Mg/l

1. INTRODUCTION

1.1. Background

Water with good quality and sufficient quantity from different resources is a back bone for economic development of a country. The demand for water in Ethiopia has increased rapidly with the construction of power plant, development of industry, irrigated agriculture, urbanization, to improve in living standards and Eco-environmental construction. In Northern Ethiopia, particularly in the densely populated region of Mekelle, mainly four sub-basins i.e., the Aynalem, Chelekot, upper Geba (Agulae) and Ilala sub-basins from the main water supply sources for drinking and irrigation activities. They are part of the larger Geba basin and supply comes from pumped boreholes, springs, hand-dug wells and rivers.

Rapid increases in population and urbanization causes an increase in the demand for water and this in turn leads to over-pumping of ground and surface water (Lawrence et al., 2000). Land-use change for urbanization and agricultural activities commonly results in the deterioration of water quality (Sharp, 1997; Tewelde, 2012). Consequently, water quality issues like groundwater salinity is a major concern for water resources development projects (irrigation, floriculture) as well as for human health (drinking water supply). Furthermore, hydrogeological conditions and chemical compositions of groundwater are important constraints and limiting factors for development, the type of materials used for water distribution systems, the quality of constructions and local ecological values (Berhane et al., 2013; Carol et al., 2009). Hence, it is essential to understand the hydrogeochemical processes and its evolution that take place in both ground and surface water resources (Subramani et al., 2010).

The main processes which determine groundwater chemical composition are water-rock interaction, recharge and discharge (percolation and pumping), atmospheric inputs, inputs of chemicals by human activities, geological structure, mineralogy of aquifers and the geological processes within the aquifer. The interaction of all these factors leads to various water types and gives important clues for the geological history of the enclosing rocks (Freeze & Cherry, 1980; Hem, 1985; Jeong, 2001; Krishnaraj et al., 2011). Similarly, Prasanna et al. (2011) clearly demonstrates studies focused on quantity of water alone are not sufficient to solve water management problems. Besides, Subramani et al. (2010) emphasized the importance of hydrogeochemical studies to create suitable management plans to protect aquifers as well as to take remedial measures for contaminated water resources by natural and manmade activities.

A review of literature indicates that virtually no attempts have been made to investigate the hydrogeochemical process and evolution that control the groundwater chemistry, and origins of the water and mixing of water resources despite the fact that water quality issues are the main concern in the study area, Mekelle region. Mekelle region is located within the Mekelle geological outlier, which is fully covered with sedimentary rocks of limestone, shale, shale-gypsum intercalation, and dolerite sills and dykes. It is surrounded by volcanic, sedimentary rock of sandstone and metamorphic rocks as shown in Figure 1. As a result, Mekelle outlier faces water salinity problems due its special geological formations and rock-water interaction during groundwater flow and circulation, resulting in corrosion of metallic pipe lines of the water supply distribution systems (Appendix-8). Hence, the paper aims to study water use problems, related to water quality, hydrogeochemical processes (evolution), origins and mixing of water resources using geochemical modeling (PHREEQC) approaches combine with stable isotopes fractionation and geospatial data analysis.

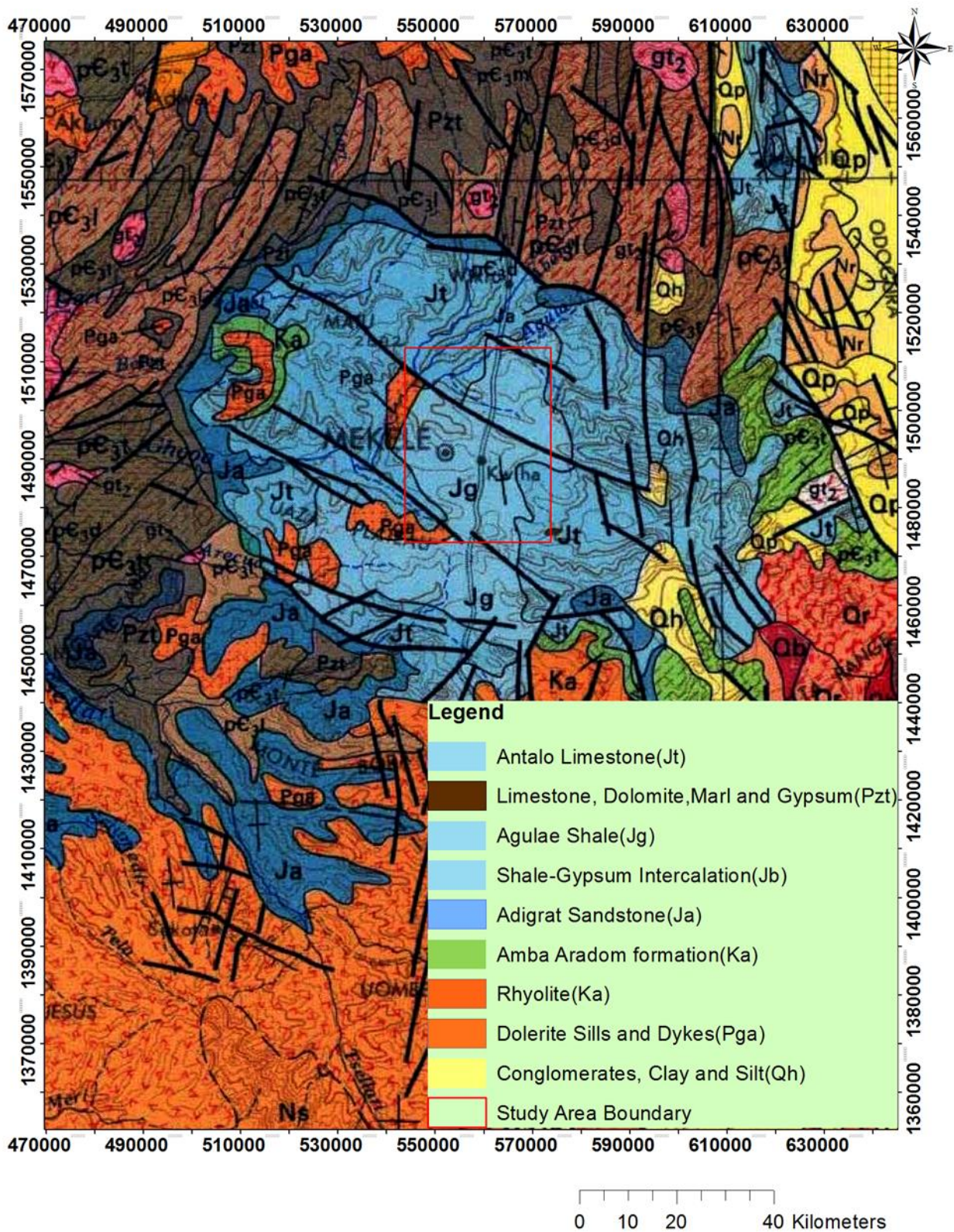


Figure 1: Geological map of Mekelle outlier and its surrounding from geological map of Ethiopia (V.Kazmin, 1973).

1.2. Research Problems

In the Northern parts of Ethiopia, water quality issues like groundwater salinity is a major concern for water resources development projects (such as irrigation, floriculture) as well as for human health (drinking water supply). The water resources in the Mekelle region are generally over-pumped. Despite the fact that there is major concern on water quality issues in the area, researches on hydrogeochemical and water quality studies are scanty. As a result, the hydrogeochemical processes (evolution), origins, mixing and quality of the water resource in Mekelle region are not well known. Moreover, the source of element concentrations and sensibility of the water resource to pollution is not clear. This causes a large uncertainty in understanding the main hydrogeochemical processes controlling the evolution of water chemistry and complicates planning and management of water resources in the area.

To the best of my knowledge no attempt has ever been made to identify the hydrogeochemical processes that control the groundwater chemistry, origins of the water and the mixing of water resources in Mekelle region. Important exceptions include Worash and Valera (2002), Kahsay (2008), Tewolde (2012), and Berhane et al. (2013). Worash and Valera (2002) studied the rare earth element geochemistry of the Antalo Supersequence in the Mekelle Outlier of Tigray region, northern Ethiopia. Kahsay (2008) assessed groundwater resource of Aynalem well field (Mekelle area) through distributed steady-state flow modeling. Tewolde (2012) has also studied regional groundwater flow modeling of the Geba basin, northern Ethiopia. Berhane et al. (2013) also investigated the implications of groundwater quality to corrosion problem and urban planning in Mekelle area. This apparent scarcity of information provided me with the starting point of the present study.

Therefore, studies aimed at identifying the hydrogeochemical process and evolution that control the groundwater chemistry, the origins of water and mixing of water resources of Mekelle region. The research is believed to fill the stated gap and provide policy makers with better information on water use and management in the area.

1.3. Research Objectives

1.3.1. General Objectives

This research aims to investigate water use problems related to water quality and hydrogeochemical processes and evolutions, origins and mixing of water resources using hydrogeochemical modeling (PHREEQC) approaches combined with stable isotopes fractionation and geospatial data analysis.

1.3.2. Specific Objectives

The specific objectives are:

- ✓ To analyze and interpret water quality parameters of water resource sample data.
- ✓ To determine hydrochemical water types, evaluate water quality criteria (drinking and irrigation) in relation to hydrogeochemical processes (chemical precipitation, dissolution of minerals, ion exchange reaction, oxidation/reduction, pollution and mixing of water) that affect the water quality.
- ✓ To evaluate the equilibrium conditions concentration of chemical species in solution (activities) and mineral saturation indices of solid phases in equilibrium with a solution and Source-rock origins.
- ✓ To determine geochemical reactions that led to a given water quality using inverse geochemical modeling.

- ✓ To map and plot the water quality parameters in relation to geology and land-use of Mekelle region.
- ✓ To provide scientific information for effective water resource management in the region using PHREEQC.

1.4. Research Questions

- ✓ How does geology and land-use affect water quality in the area?
- ✓ Where are the most severe water quality problems located in the study area?
- ✓ What is the spatial distribution of different water quality indicators (drinking and irrigation)?
- ✓ What are the main hydrogeochemical processes affecting water quality in the area?
- ✓ What are the origins of water at the different locations in the study area? How is water mixed from different resources in the area?
- ✓ Can the PHREEQC model improve our understanding of the effects of hydrogeochemical processes on use and management of the water resources?

1.5. Organization of the Thesis

The research is organized into seven chapters.

Chapter 1: Contains the introduction of the research that includes the background, research problems, objectives of the research and research questions in which the research tries to answer using the available data and methodologies.

Chapter 2: Deals with literature review related to definitions of water quality, principle of Aquachem modeling, geochemical process and modelling, and reviews previous works conducted in the study area.

Chapter 3: Presents a brief introduction of the study area description. It discusses the physiography, climate, vegetation, land-use, stratigraphy (geology), hydrogeological and hydrographic setting of the study area.

Chapter 4: This chapter is devoted to the method of data collection: on spot water quality data, water samples for laboratory analysis, geology and land-use information, and secondary data collection during the fieldwork.

Chapter 5: This chapter provides a brief description of the methods used in the study. It mainly focuses on the methods such as laboratory analysis, result and reliability checks, hierarchical cluster analysis (HCA), Source-rock deduction, Aquachem and PHREEQC modelling and isotopes fractionation, and water quality assessment.

Chapter 6: This chapter presents the main findings of the study. Results and discussion includes illustration and discussion of general hydrogeochemistry, hierarchical cluster analysis (HCA), Aquachem and PHREEQC modeling and calculation results, and result of the isotopes fractionation. Moreover, it discusses with water uses for domestic and irrigation and its implication in pipe lines and engineering works.

Chapter 7: The last chapter concludes by presenting the main issues discussed in this study as well as by providing recommendations for further improvement and researches.

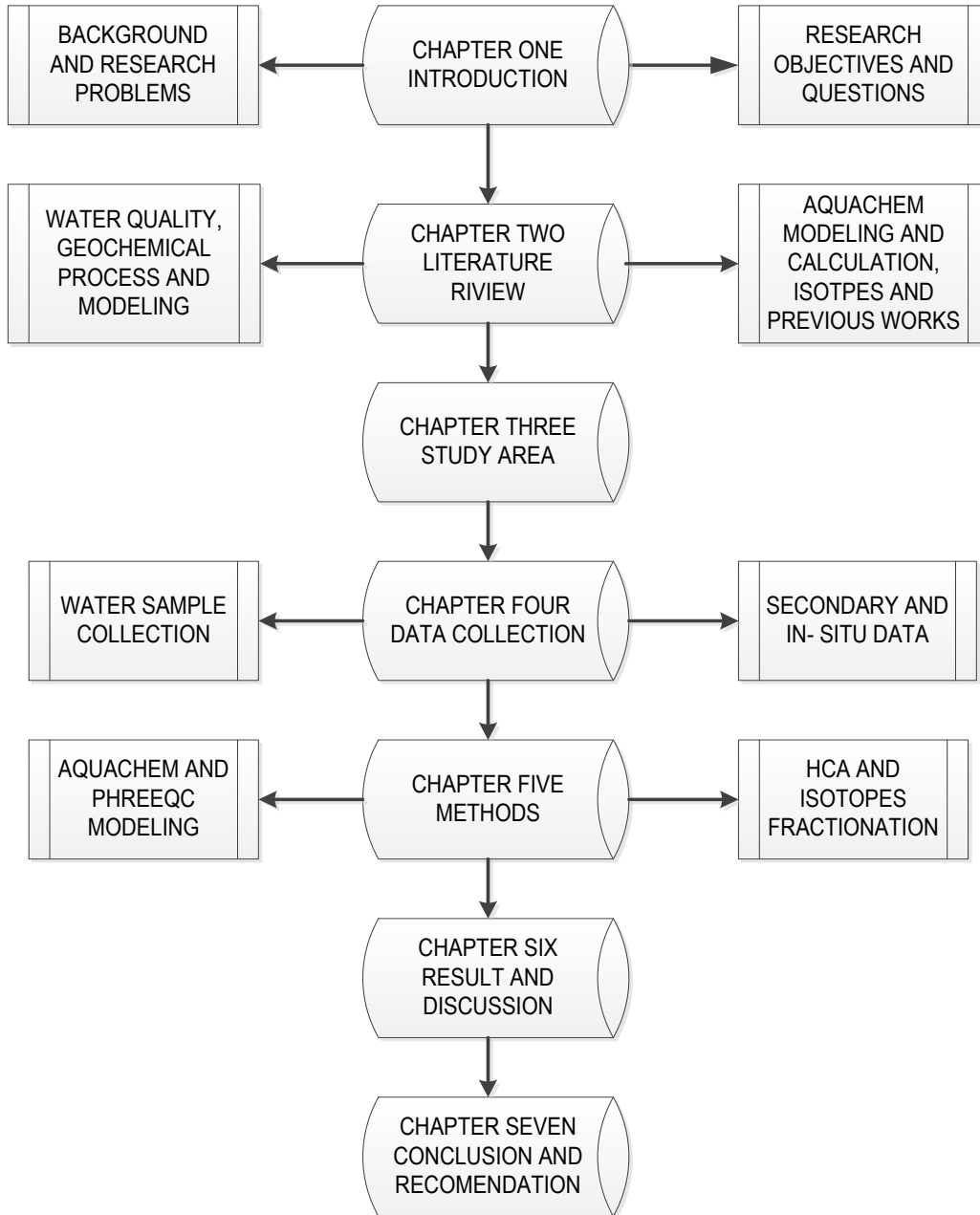


Figure 2: General structure of the thesis

2. LITERATURE REVIEW

2.1. Water Quality

According to Hounslow (1995), water quality is defined by the physical, chemical and biological characteristics and composition of a water sample. The chemical composition of groundwater is the combined result of water composition that enters the groundwater reservoir and the reactions with minerals present in the rocks (Iliopoulos et al., 2011; C. Zhu, 2002).

2.1.1. Water Quality Sampling

Sampling could be defined as a process of selecting a portion of material small enough in volume to be transported conveniently and handled in the laboratory. However, the main difficulties with sampling is representativeness and integrity (Madrid & Zayas, 2007). The number of samples to be taken for a given investigation must be determined from both statistical and economic considerations (Hounslow, 1995). Water sample collection procedures (how often and when), type of container and method of preservation must be decided before water sample collection. Besides, data must also be collected at a minimum level of sensitivity and completeness to satisfy the information needed for the sampling program (Barcelona et al., 1985). According to Hounslow (1995), some chemical variables including temperature, dissolved gases, pH and alkalinity must be determined in the field, at time of sampling.

2.1.2. Water Quality Parameters

Water sample parameters are analysed in a laboratory. Some parameters such as temperature, conductivity, alkalinity, dissolved oxygen, pH, cations and anions, hardness, TDS, sodium adsorption ratio, and saturation index are determined in the field (Hounslow, 1995).

- TDS

Dissolved solid content- TDS is calculated by adding the mass of ions plus SiO_2

$$\text{TDS} = \text{sum of ions} + \text{SiO}_2$$

- Temperature

Temperature data are need for water-rock equilibrium calculations, as well as for the identification of water groups, and the determination of water end member properties (Mazor, 1991).

- pH

The pH of a solution indicates effective concentration of the hydrogen ion H^+ . The units of pH are the negative logarithm of hydrogen ion concentration, expressed in moles per liter.

$$\text{pH} = -\log(H^+)$$

- Hardness

Hardness is the sum of the Ca and Mg concentrations expressed in terms of mg/l of calcium carbonate.

$$\text{Hardness} = \text{Ca} \left(\frac{\text{mg}}{\text{l}} \right) * \frac{\text{M.Wt. CaCO}_3}{\text{At.Wt. Ca}} + \text{Mg} \left(\frac{\text{mg}}{\text{l}} \right) * \frac{\text{M.Wt. CaCO}_3}{\text{At.Wt. Mg}}$$

- Conductivity

Conductivity, which is also called electrical conductivity (EC) is a reciprocal of the resistance in Ohms between the opposite faces of a 1 – cm cube of an aqueous solution at specified temperature (usually 25°C). It is temperature dependent and the international unit is Siemens/m that is numerically equivalent to the Mhos/m (Hounslow, 1995; Mazor, 1991).

Conductivity is a good estimator of TDS because TDS in mg/l is proportional to the conductivity in micromhos.

$$\text{TDS (mg/l)} = A * \text{conductivity } (\mu\text{Mhos/cm}), \text{ where } A = 0.54 - 0.96 \text{ usually } (0.55-0.76)$$

Conductivity may also be estimated from the sum of cation expressed in meq/l.

$$\text{Conductivity } (\mu\text{Mhos/cm}) = \text{sum cations (meq/l)} * 100$$

- Alkalinity

Alkalinity of a solution is the capacity of a solution to react with and neutralize acidity. It is determined by titration to specific end-points, namely, pH = 4.5 - methyl orange, and pH = 8.3 - phenolphthalein. It is commonly reported in terms of an equivalent amount of CaCO₃ usually meq/l CaCO₃ (Hounslow, 1995; Mazor, 1991).

$$\text{meq/l CaCO}_3 = \frac{\text{mg CaCO}_3}{50}, \text{ where 50 is the gram equivalent weight of CaCO}_3$$

- Dissolved oxygen

The concentration of dissolved oxygen in air-saturated water depends on pressure or altitude, temperature, salinity and aquifer lithology (Mazor, 1991).

- Sodium Adsorption ratio (SAR)

SAR measures the amount to which sodium in irrigation water replaces the adsorbed (Ca²⁺ + Mg²⁺) in the soil clays, and can damage the soil structure (Hounslow, 1995).

$$\text{SAR} = \frac{\text{Na}^+}{\sqrt{\frac{\text{Ca}^{2+} + \text{Mg}^{2+}}{2}}}$$

- Saturation index (SI)

When a mineral is dissolved in water, the cations and anions of which it is composed will attain a specific concentration. Their sum essentially equals the solubility of that mineral and it used to evaluate departure from equilibrium (Hem, 1985; Hounslow, 1995).

$$\text{Saturation index (SI)} = \log \frac{\text{IAP}}{K_{\text{sat}}} \text{ where IAP is ion activity product and } K_{\text{sat}} \text{ is solubility product.}$$

If the SI equals zero, that is, IAP = K_{sat} then the water is just saturated with the mineral phase in question. If SI is positive, or IAP > K_{sat}, then the water is over saturated, the water is under saturated with respect to the mineral in question if SI is negative and will tend to dissolve more of the mineral if it is present (Appelo & Postma, 1993; Hounslow, 1995).

- Ions

Ions are naturally very variable in surface and groundwater due to local geological, climatic and geographical conditions (Chapman, 1996). However, specific cations and anions concentrations are evaluated against drinking and irrigation water quality criteria.

- Nutrients

Nitrogen and phosphorus compounds are essential nutrients for living organisms. Nevertheless, increasing of nitrate levels can be problematic in groundwater as a result of soil leaching and in high fertiliser application and urban sewage infiltration areas (Chapman, 1996).

2.2. Water Quality Analysis and Interpretation

Analyses of individual water samples should be subject to accuracy and reliability checks. Moreover, the speciation and saturation index determinations of individual water samples should be done using mass

balance or hydrogeochemical equilibrium modeling techniques (Barcelona et al., 1985; Hounslow, 1995). Water samples can be examined and interpreted using graphical plots, diagrams, maps and statistical analyses (Hounslow, 1995).

2.3. Hydrochemical Processes

The chemical quality of water results from hydrogeochemical processes of solution or precipitation of solid minerals, reduction and oxidation compounds, solution or evolution of gases, sorption or ion exchange, pollution, leaching fertilisers or manure, and mixing of different waters (Appelo & Postma, 1993; Hounslow, 1995). These processes are dependent on water and rock interaction, atmospheric inputs, inputs of chemicals by human activities, precipitation, geological structure, mineralogy of aquifers (Freeze & Cherry, 1980; Hem, 1985; Jeong, 2001; Krishnaraj et al., 2011).

2.4. Geochemical Modeling

Geochemical models can be used to assess the bioavailability and mobility of contaminants in a particular geochemical environment by predicting the behaviour of the contaminants based on the chemical and physical properties of local soils, sediments, and solutions (precipitation and surface and groundwaters) (Bricker, 1999).

2.4.1. Speciation Models

According to Bricker (1999), speciation models are used to determine the partitioning of an element among different aqueous species and complexes. They also determine, to the extent of the thermodynamic information in the program, the saturation state of the solution with respect to solid phases and gases.

2.4.2. Hydrochemical Equilibrium and geochemical Modeling

PHREEQC was developed for determining and simulating 'real world' hydrogeochemistry. Its outputs are chemical speciation and saturation indices of chemical species (Hounslow, 1995; Parkhurst & Appelo, 1999).

2.4.3. Inverse Modeling

Inverse modelling determines mixing fractions for the aqueous solutions and mole transfers of the gases and minerals that produce the composition of an aqueous solution (Parkhurst & Appelo, 1999).

2.5. Aquachem Water Quality Database

Aquachem is a water quality database software package with functionality for graphical and numerical analysis and modeling of water quality data. Its feature has a fully customizable database of physical and chemical parameters and provides a comprehensive selection of analytical tools (such as calculations and graphs) for interpreting water quality data (Hounslow, 1995; Nies et al., 2011).

2.6. Stable Isotopes

Environmental isotopes have been extensively used during the past decades to address key aspects of the water cycle, such as for studying the origin, dynamics and interconnections groundwater, surface water and atmosphere (Mook, 2000). In addition, stable isotopes are chemically conservative elements, and can be used for hydrogeological investigations and to trace environmental phenomena (Krishnaraj et al., 2011).

2.6.1. Isotope Fractionation

Isotope fractionation addresses tiny differences in chemical as well as physical behaviour of molecules (Mook, 2000). Fractionation of isotopic composition of a water resource is caused by different physical

environmental processes (Krishnaraj et al., 2011). Hence, chemical composition and isotropic gradients show differences between water resources and this can be quantified by comparing the signatures of the stable water isotopes ($\delta^{18}\text{O}$, $\delta^2\text{H}$) (Nies et al., 2011).

2.7. Previous works and studies

Based on the hydrochemistry analysis of the groundwater samples, the major water types in Mekelle region are Ca-SO₄, Ca-HCO₃-SO₄, Ca-SO₄-HCO₃ and Ca-HCO₃ waters (Kahsay, 2008).

In the Geba basin, water samples from shale or shale-marl layers are mainly dominated by Ca-HCO₃, Ca-HCO₃-SO₄ or Ca-SO₄ and from dolerite also have similar properties, but groundwater in limestone is mainly of the Ca-Mg-HCO₃-(SO₄) type (Tewolde, 2012). Moreover, the geochemical characteristics of the aquifers in Geba basin are the main cause for changes in groundwater quality except in some rare cases where chemical fertilizers and urban sewage are affecting the water quality.

Previous researches in the study area indicate that the pH varies from 6.9 to 8.6 with a mean value of 7.6 and Electrical Conductivity (EC) varying from 542 to 5300 $\mu\text{S}/\text{cm}$ with a mean value of 1289.7 $\mu\text{S}/\text{cm}$. The Total dissolved solids (TDS) range from 330–1,312 mg/l for spring, 436-13,007.13 mg/l for hand-dug wells and 350-2,195 mg/l for boreholes (Berhane et al., 2013).

Quartz and the clay minerals montmorillonite, kaolinite and illite are the dominant soil minerals. Moreover, Potassium feldspar, occasionally albite, goethite, hematite and scarce glauconite and the carbonate mineral calcite are also found in the Mekelle outlier (Worash & Valera, 2002).

Some similar work were done in Ethiopia, which included studies on groundwater recharge, circulation and geochemical evolution in the source region of the Blue Nile River, Ethiopia (Kebede et al., 2005). Hydrogeological and Hydrochemical framework of Upper Awash River Basin, Ethiopia: with special emphasis on inter-basin groundwater transfer between Blue Nile and Awash River (Yitbarek et al., 2012). Major ion hydrochemistry and environmental isotope signatures as a tool in assessing groundwater occurrence and its dynamics in fractured volcanic aquifer system located within a heavily urbanized catchment, central Ethiopia (Demlie et al., 2008). Hydrogeochemical and Isotope Hydrology in Investigating Groundwater Recharge and Flow Processes, South Afar, Eastern Ethiopia (Addisu, 2012).

3. STUDY AREA

3.1. Location

The study area is geographically bounded between Latitudes 1472872 and 1512872 m N and Longitudes 543650 and 573650 m E and covers a total land area of 1,200 square kilometres. Mekelle region is found on the north-eastern part of the central plateau west of the Rift valley, and is 776 km north of Addis Ababa. Mekelle town is geographical located at coordinates of 1491663 m N, Latitude and 551089 m E, Longitude with elevation of 2000 meter above sea level.

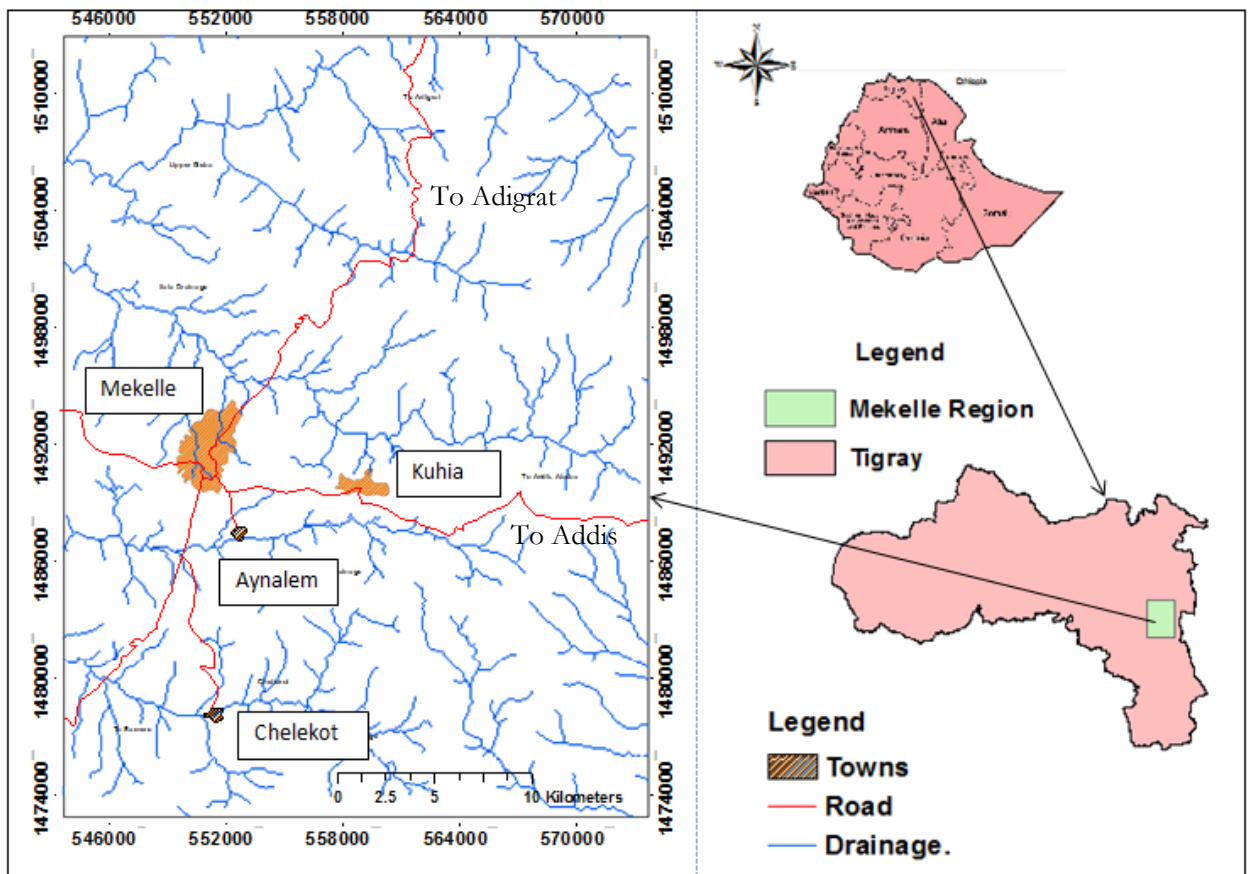


Figure 3: Location map of the study area

3.2. Physiography

The area can be grouped into two major physiographic regions separated by a nearly east-west running sub-basin in the study area. The western, central and eastern regions belong to the Tekeze drainage system while the south-eastern and north-eastern regions drain to the Danakil Depression. Elevations range between 1745-2759 m gently declining to the west, characterized by gentle rolling topography bounded by several steep cliffs.

3.3. Climate

Climatically, the area has a semi-arid climate with little variation within the area. Monthly mean minimum temperature is 15°C and maximum monthly temperature may go as high as 28°C (Kahsay, 2008). The mean annual temperature ranges from 14 to 26°C over the central part of the study area (Tewolde, 2012). In general, two distinct seasons can be recognized in Mekelle region. The first is the main rainy monsoon season which lasts from June to September (locally called Kiremti), where most of the annual rainfall occurs, the second is the dry winter season from March to April. The mean annual rainfall is estimated to be 670 mm (Kahsay, 2008).

3.4. Vegetation

The area generally falls in the little or no vegetation class. It has historically been largely deforested as the study region is highly populated (Tewolde, 2012). As a result of the historical deforestation, large indigenous trees such as olive trees (*Acacia Albiro* etc.) are non-existent except in areas which are around churches and some closed areas.

3.5. Land-use

According to Tahir et al. (2013), land-use is a dynamic phenomenon that changes with time and space due to anthropogenic pressure and development. Up-to-date and accurate land-use/land-cover information is important for water resources monitoring, management and planning (Tewolde, 2012). Hence, a land-use/land-cover map for the study area was produced from <http://glovis.usgs.gov/> (USGS Global Visualization Viewer) cloud free Landsat 5 TM satellite images of September 23 (path 168, row 051) 2011 with spatial resolution of 30 m. The standard ILWIS supervised image classification procedure was employed for this purpose.

Ground observation points (GPS points), Google Earth images interpretation, and own knowledge of the study area land-use characteristics was used as an input for image classification. Initially, 6 classes were identified. But the water body and sparse forest land-uses types cover a very small percentage of the area. Accordingly, four land-use/land-cover classes were finally produced for Mekelle region using ILWIS and Arc GIS as it is provided in Figure 5. The land-use/land-cover map showed that, nearly 86% of the land is covered by bare land and crops (irrigated + rainfed) land, while forest and urban lands cover about 14% (Figure 4).

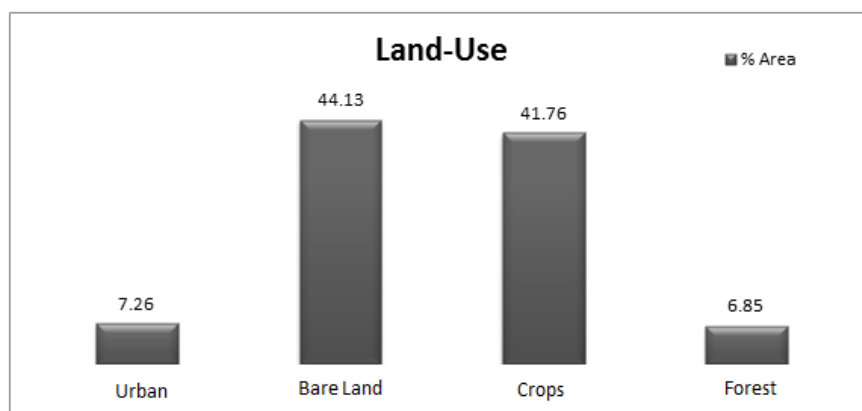


Figure 4: Percentage of land-use/land-cover area of the region

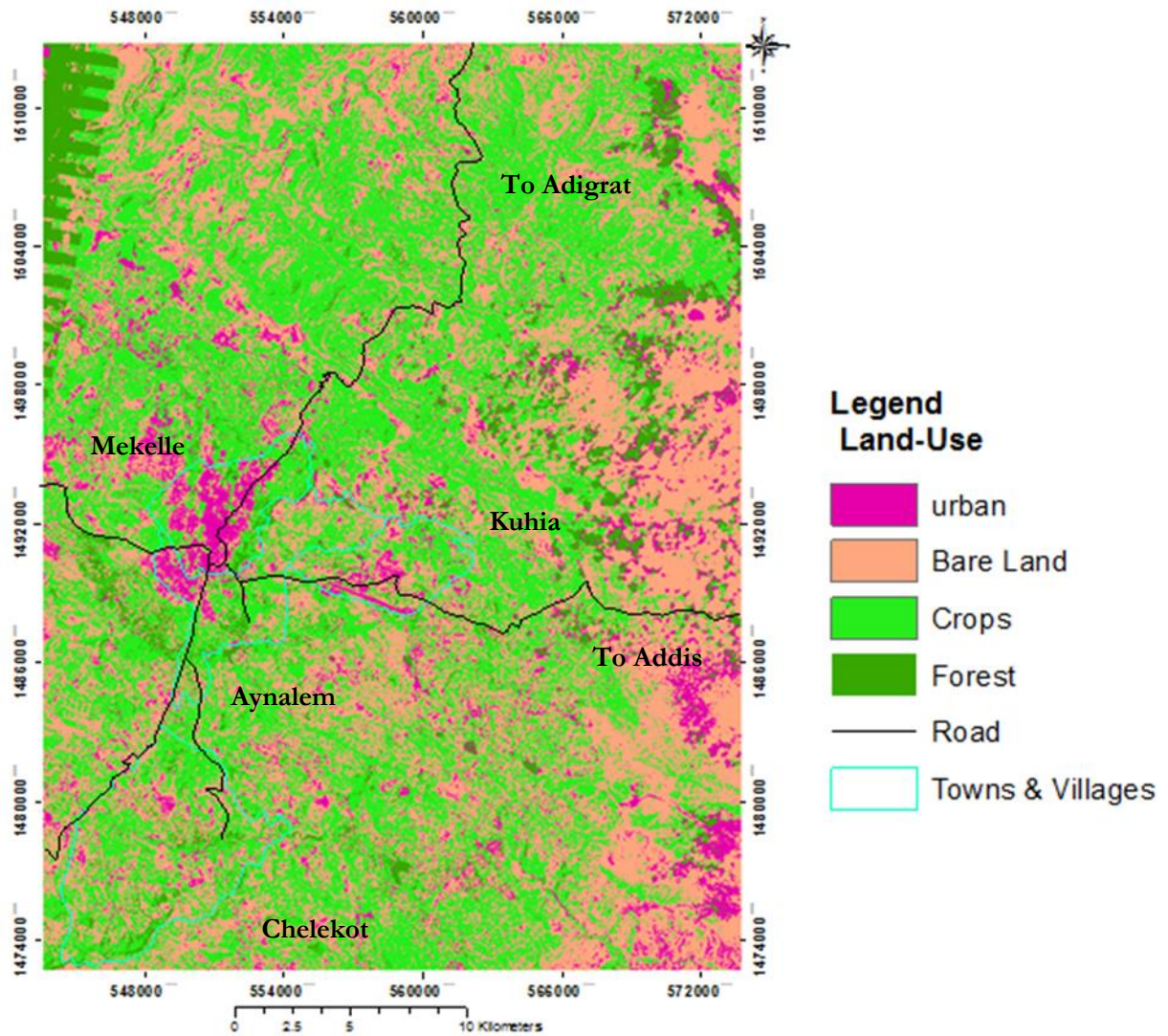


Figure 5: Land-use/ Land-cover map of Mekelle region

Moreover, the output land-use classes were assessed their accuracy of classification based on ground truth data collected during the fieldwork. More than 115 ground truth data for land-use were collected during field visits to be used for the verification of the classified image using ArcGIS and Excel. The relation between ground truths and their respective land-use classes on the map was also verified using confusion matrix in ILWIS. The results are shown in Table 1. The result for the average accuracy, average reliability, and overall accuracy was found to be 66.58%, 74.74%, and 72.65% respectively. Hence, the land-use/land-cover map produced is acceptable.

Table 1: Land-use classification accuracy analysis results

	Ground truth	Bare Land	Crop	Forest	Sparse Forest	Urban	Water	Unclassified	Accuracy
Bare Land	27	23	0	0	0	4	0	0	0.85
Crop	20	0	20	0	0	0	0	0	1.00
Forest	30	8	7	10	0	5	0	0	0.33
Sparse Forest	4	4	0	0	0	0	0	0	0.00
Urban	15	0	0	0	0	15	0	0	1.00
Water	21	0	0	4	0	0	17	0	0.81
Reliability		0.66	0.74	0.71	-	0.63	1.00		
Total	117								

Average Accuracy = 66.58 %; Average Reliability = 74.74 %; and Overall Accuracy = 72.65 %

3.6. Stratigraphy of the study area

Based on different geological studies conducted on the Mesozoic sedimentary successions of the eastern, north-eastern and northern Ethiopia, various transgression-regression cycles were occurred with shallow marine transgressions starting from the early Jurassic or late Triassic up to late cretaceous (Kazmin, 1975; Bossellini et al., 1997; Mengesha et al., 1996) as cited in (Kahsay, 2008). Hence, the stratigraphy of the study area contains from bottom to top; Adigrat sandstone, Antalo formation, Agula formation and Ambaradom formation (Worash & Valera, 2002).

3.6.1. Geology of the study area

The carbonate dominated Antalo supersequence is a thick succession of limestone, shale and marl (Gebreyohannes et al., 2010; Worash & Valera, 2002). The Agula Shale represents the top most part of the Supersequence and is composed of a number of faces cycles, which have a thickness of 10 to 50 m (Gebreyohannes et al., 2010). The Agula Shale is composed of finely laminated black shale, marl, limestone, and local evaporite units mainly composed of Gypsum (Worash & Valera, 2002). Moreover, Dolerite dykes/sills are observed throughout the study area. The presence of Dolerite dykes in the area plays a double role in creating a conductive environment for the presence and circulation of groundwater. The Dolerite cannot be a good aquifer unless it is fractured and deeply weathered (Water Works Design and Supervision Enterprise, 2007) as cited in (Kahsay, 2008). The main geology observed in the study area includes Agulae shale, Limestone + Marl, Limestone + Shale, Shale + Marl + Limestone, Marl + Limestone and Dolerite. Moreover, the fine to medium grained Adigrat Sandstone which cemented with iron is found as pinch out in the north-western of the study area. It is good aquifer and yields up to 50 l/s and has up to 30 m thickness in the pinch out area (Figure 6).

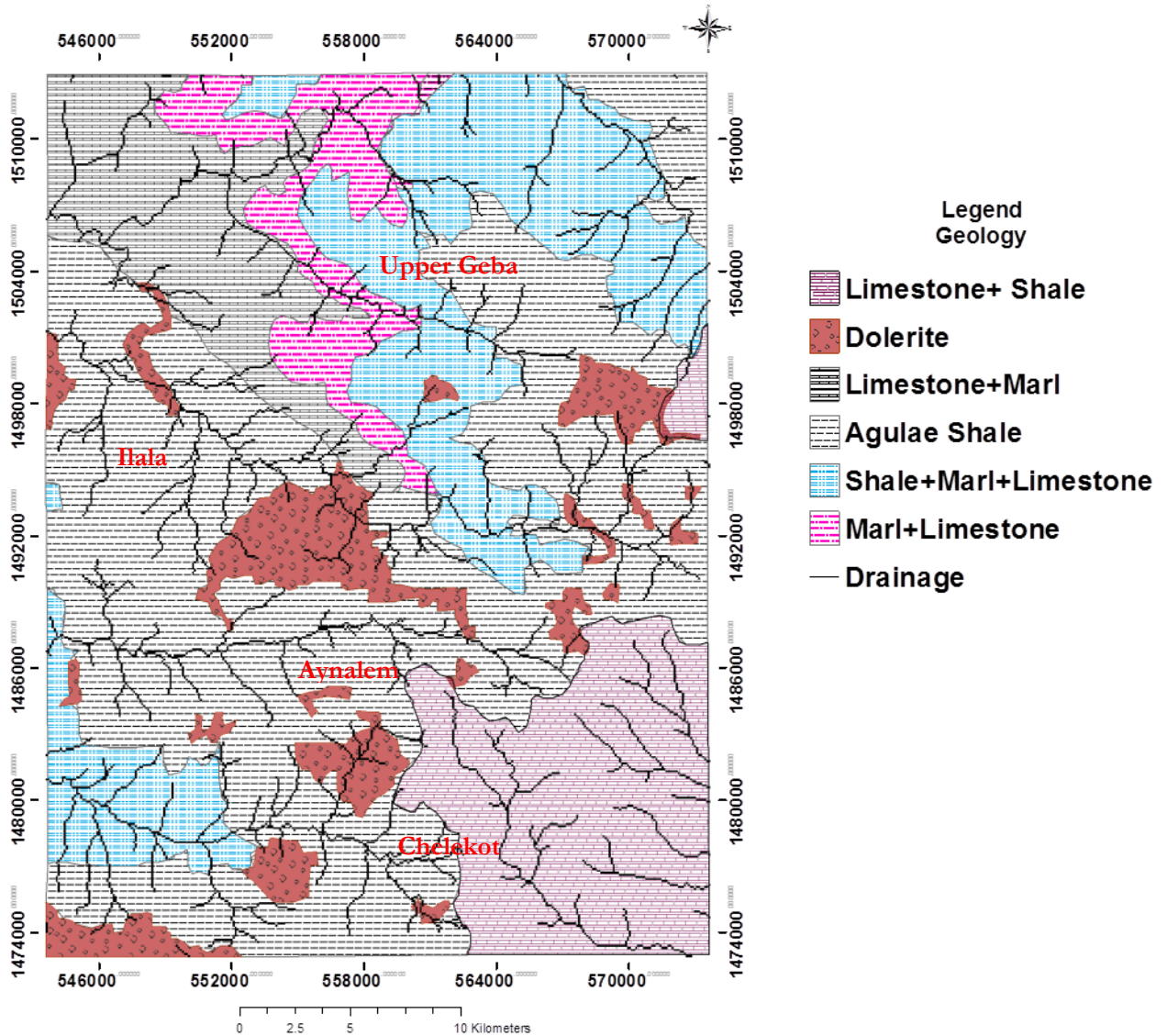


Figure 6: Geological map of the study area

3.7. Hydrogeological Setting

Geology, topography and climatic factors greatly influence the occurrence of groundwater in Aynalem area (Kahsay, 2008). By the same fact, geology and geological structures (faults, fractures and lithological contacts) play a great role in the movement and occurrence of groundwater in Geba basin area (Gebregziabher, 2003; Kahsay, 2008). The groundwater piezometric level map was constructed from ninety (90) water points indicates the flow direction of the water is towards the low altitude areas (Figure 7 A). Similarly Tewolde (2012), the potentiometric maps of all water bearing layers and particle tracking path lines show that groundwater flow in the Geba basin converges towards the major river valleys.

3.8. Hydrographic Setting

For water resources evaluation in the Mekelle Region, four sub-basins are considered i.e., the Aynalem, Ilala, Chelekot and Agulae (upper Geba) sub-basins, which are draining to the Geba Basin. In addition, there are two small catchments that drain to the Danakil depression as shown on Figure 7 B.

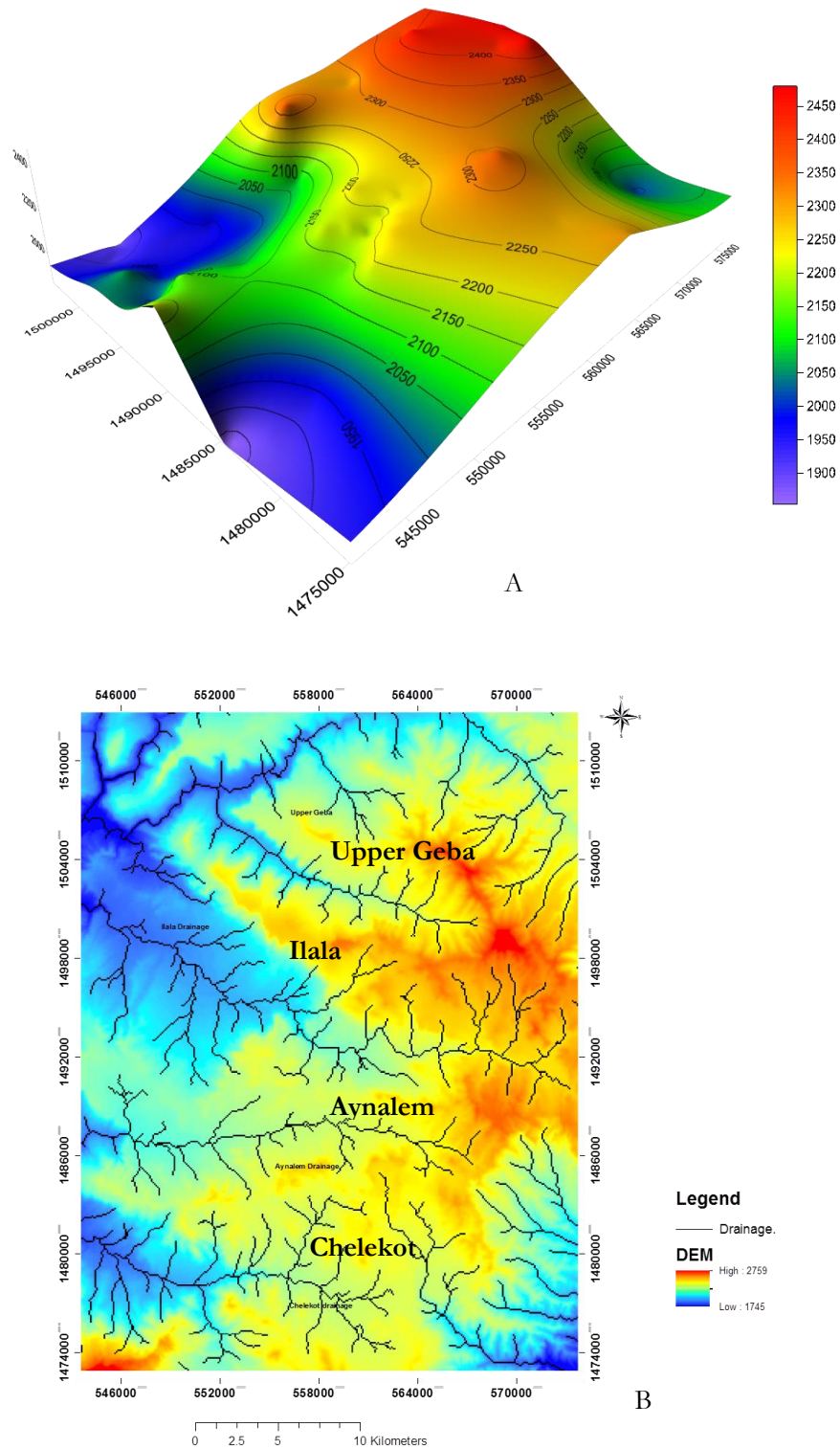


Figure 7: Topography and Groundwater Contour Map (A) and Drainage map (B) of the study area

4. DATA COLLECTION

4.1. Field Data Collection

The basic objective of the field data collection was to create a water quality database of geological, hydrogeological, isotopes and hydrogeochemical information, and to obtain as much detail as possible the necessary data for the isotopes fractionation, Aquachem and PHREEQC hydrogeochemical models. The flow chart for field data collection procedure is given in Figure 10.

4.1.1. Secondary Data

Secondary data collection was carried out in the Mekelle region northern Ethiopia. Geological map, water quality, isotopes, hydrogeological and log data of hand-dug wells, shallow boreholes, deep boreholes, springs, and streams were collected from different organisations such as Tigray region water resource development bureau, Tigray water supply service, and Ministry of water resource and energy. Moreover, isotopes of monthly mean precipitation of the year 2002 for KOBO station is collected from International Atomic Energy Agency (IAEA). The type of the data collected in the field is summarized in Table 2, 3, 4 and 5 and, their distribution is shown in Figure 8.

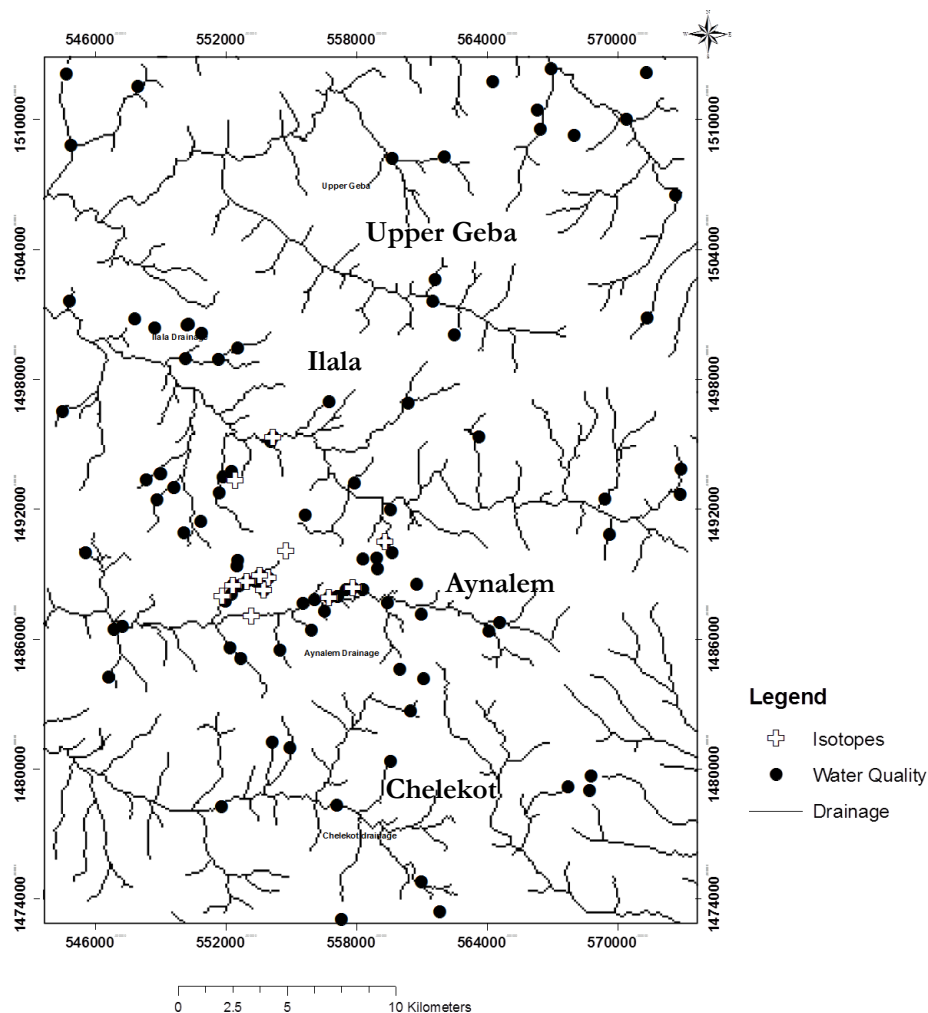


Figure 8: Location and distribution of water points having secondary data

Table 2: Description of water points having secondary data

No	Type of water point	Total number	Remark
1	Deep borehole	74	
2	Hand-dug Well	17	
3	Spring	35	
4	River	3	
Total		129	

Table 3: Summary statistics of cations and anions of water resource constituents from 103 secondary data (Appendix-11)

Parameters	Maximum	Minimum	Mean
EC $\mu\text{S}/\text{cm}$	5300.00	542.00	1237.85
TDS (mg/l)	3454	330	894.23
Tot Hardness (mg/l)	2041	210	678.78
pH	8.5	6.81	7.54
Ca^{2+} (mg/l)	631.8	53.8	211.34
Mg^{2+} (mg/l)	120	1.9	23.69
Na^{+} (mg/l)	260	6.6	43.29
K^{+} (mg/l)	9	0.3	2.47
HCO_3^{-} (mg/l)	691.1	14.64	330.13
Cl^{-} (mg/l)	298	5.76	43.37
SO_4^{2-} (mg/l)	1607	11.6	319.60
NO_3^{-} (mg/l)	336.1	0.21	32.65
F^{-} (mg/l)	1.92	0.04	0.49
PO_4^{3-} (mg/l)	0.583	0.02	0.31

Table 4: Summary statistics of the isotopes of water resources 2002 secondary data for the study area

S.No	Sample Code	Local ID	Water body	Longitude	Latitude	Elevation	$\delta^{18}\text{O}$	$\delta^2\text{H}$
1	MKB 01/GWB	PW-2	Borehole	556722	1487915	2227	-2.21	-4.7
2	MKB 02/GWB	PW-3	Borehole	553941	1488821	2214	-2.12	-4.7
3	MKB 03/GWB	PW-4	Borehole	553706	1488251	2210	-1.84	-4.2
4	MKB 04/GWB	PW-8	Borehole	557809	1488359	2237	-2	-4.2
5	MKB 05/GWB	PW-12	Borehole	553549	1488948	2208	-2.01	-2.5
6	MKB 06/GWB	TW-3	Borehole	552945	1488663	2202	-2.09	-3.6
7	MKB 07/GWB	Mai Shibti	Borehole	554730	1490057	2243	-2.43	-5.8
8	MKB 08/GWB	Enda Tarekgn	Borehole	552313	1488491	2195	-2.28	-4.6
9	MKB 09/GWB	Lachi	Borehole	554141	1495331	2016	-1.87	-4.9
10	MKB 010/GWS	Quiha spring	Spring	559285	1490499	2227	-1.57	-4.3
		Aynalem		551805	1487990	2176	-1.14	0.2
11	MKB 011/GWS	spring	Spring					
12	MKB 012/SRE	Aynalem river	River	553164	1487065	2174	0.03	4.3
13	MKB 013/SRE	Ellala river	River	552396	1493321	1978	-0.34	4.1

NB. The unit for Deuterium is δD_{V-SMOW} (‰) and Oxygen-18 is $\delta^{18}O_{V-SMOW}$ (‰).
 Table 5: Isotopes of precipitation for KOBO area (2002) from IAEA

Project- No	Site Name	Country	WMO Code	Latitude	Longitude	Altitude	Sample Date	Sample Types	δ^2H	$\delta^{18}O$
GNIP	KOBO	ET	6333304	12.144	39.640	1518	2002-05-15	Precipitation	24.5	2.91
GNIP	KOBO	ET	6333304	12.144	39.640	1518	2002-06-15	Precipitation	25.4	3.23
GNIP	KOBO	ET	6333304	12.144	39.640	1518	2002-07-15	Precipitation	23.5	1.88
GNIP	KOBO	ET	6333304	12.144	39.640	1518	2002-08-15	Precipitation	3.7	-1.15
GNIP	KOBO	ET	6333304	12.144	39.640	1518	2002-09-15	Precipitation	-3.3	-1.82
GNIP	KOBO	ET	6333304	12.144	39.640	1518	2002-10-15	Precipitation	0.0	-1.28
GNIP	KOBO	ET	6333304	12.144	39.640	1518	2002-12-15	Precipitation	10.6	-0.45

NB. The unit for Deuterium is δD_{V-SMOW} (‰) and Oxygen-18 is $\delta^{18}O_{V-SMOW}$ (‰).

4.1.2. In-situ Data

In-situ data were collected on the spot for water quality analysis from different water resources and data for land-use were also collected from different locations. The surveys were conducted in the Mekelle region, northern Ethiopia from September 9 to 27, 2013.

4.1.2.1. Water Quality on Spot Data Collection and Analysis

During the fieldwork, different on spot water quality data was collected from different water resource such as: - boreholes, hand-dug wells, springs and river. The data were include pH, EC, Temperature, Dissolved Oxygen, Alkalinity and Turbidity by using HQ40d18 series portable meters (pH, EC and OD probes), titration method and portable Turbidity meter model Hach 2100 respectively. The type of data that were collected on spot in the field is summarized in Table 6 and their distribution is also given in Figure 11.

Table 6: Summary statistics of on the spot data measurements

Parameters	pH	Temp °C	Cond uS/cm	O2 mg/l	Alkalinity mmol/l	Turbidity NTU
Maximum	9.15	28	3010	14.6	12	76.8
Minimum	6.74	19.8	221	0.58	1	0.35
Mean	7.38	23.22	1380.33	4.80	5.93	8.05

4.1.2.2. Land-use Ground Truth Data

Ground truth information's were collected from the study area using GPS and digital camera for land-use mapping and interpretation. The total number of observations collected were 117 and out of this 27 observations belongs to bare land, 20 for crops, 30 for forest, 4 for sparse forest, 15 for urban and 21 for water bodies Table 1.



Figure 9: Images for Land-use from the study area

4.2. Water Samples Collection

To assess the water chemistry, representative water samples collection was done parallel to the on spot measurements. Sampling points for water quality investigation were selected based on geomorphology, flow direction and geological formation obtained from secondary data. First, pumping was carried out for 5-10 minutes and about 113 water samples were collected from 41 different water points sampled from 5 water resources within the 4 sub-basins in the study area. The water samples were collected using 40 acid-washed polyethylene plastic bottles of 100 ml filtered and acidified with nitric acid for cation and anion. Besides, 40 plastic bottles 50 ml filtered and acidified with hydraulic acid for nitrate, 24 plastic bottles of 50 ml unfiltered for isotopes, 8 plastic bottles of 100 ml and 50 ml as duplicated and 1 plastic bottle of 50 ml acidified with nitric acid for chloride analysis were used to collect the water samples. The samples were collected following the standard methods of sampling protocol (Wilde, 2010), mainly filtered through a

0.45 μm cellulose acetate filter membrane, sample bottles were tightly capped, labelled and preserved in the refrigerator. Their detail descriptions are summarized in Table 7 and their location and distribution can be seen from Figure 11.

Table 7: Description of the type of water points for water sample collection

No	Sub-basins	Type of water points						Total
		Borehole	Hand-dug Well	Spring	River	Tap Water	Rain Water	
1	Chelekot	3	1	1	2	0	1	7
2	Aynalem	4	3	2	2	1		12
3	Ilala	6	2	2	2	2		14
4	Agulae (upper Geba)	2	2	1	2	0		7
	Total	15	8	6	8	3	1	41

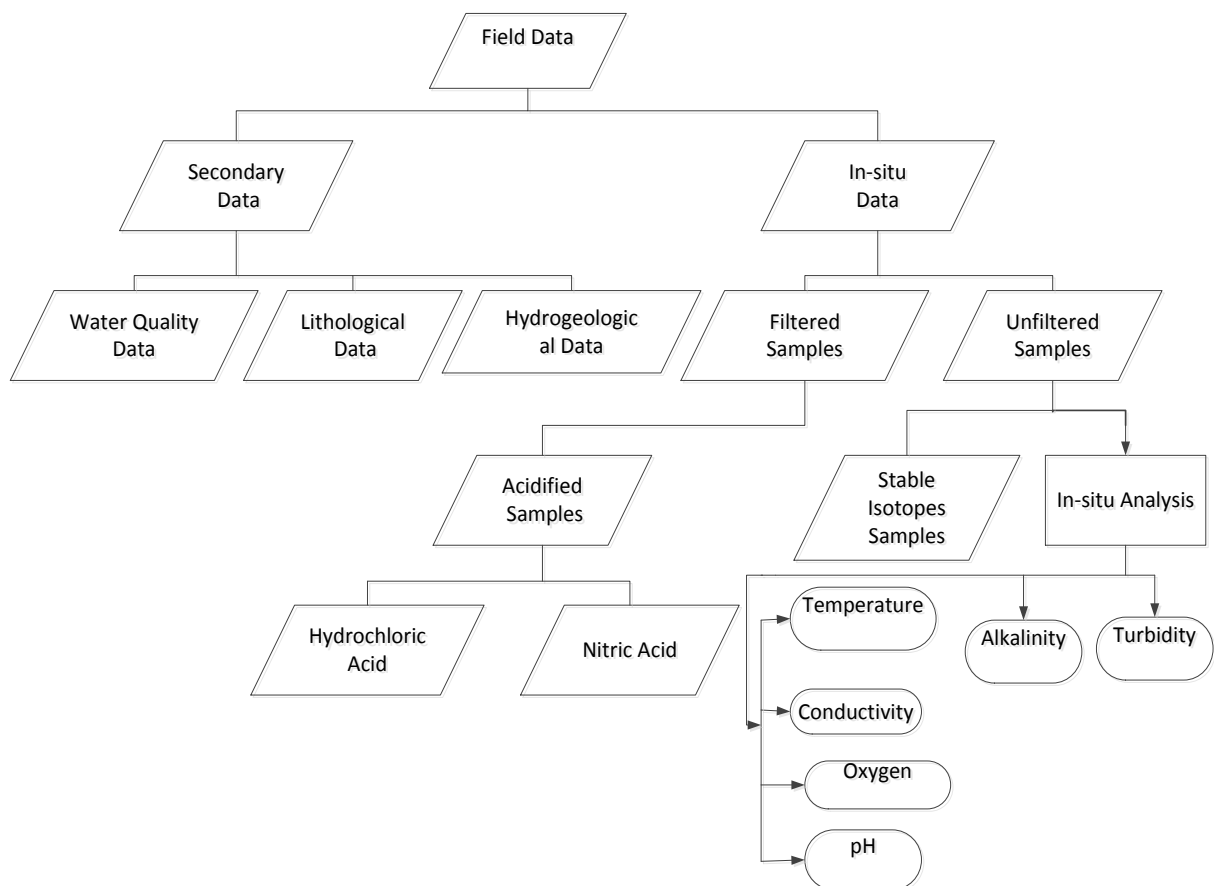


Figure 10: Field data collection flow chart

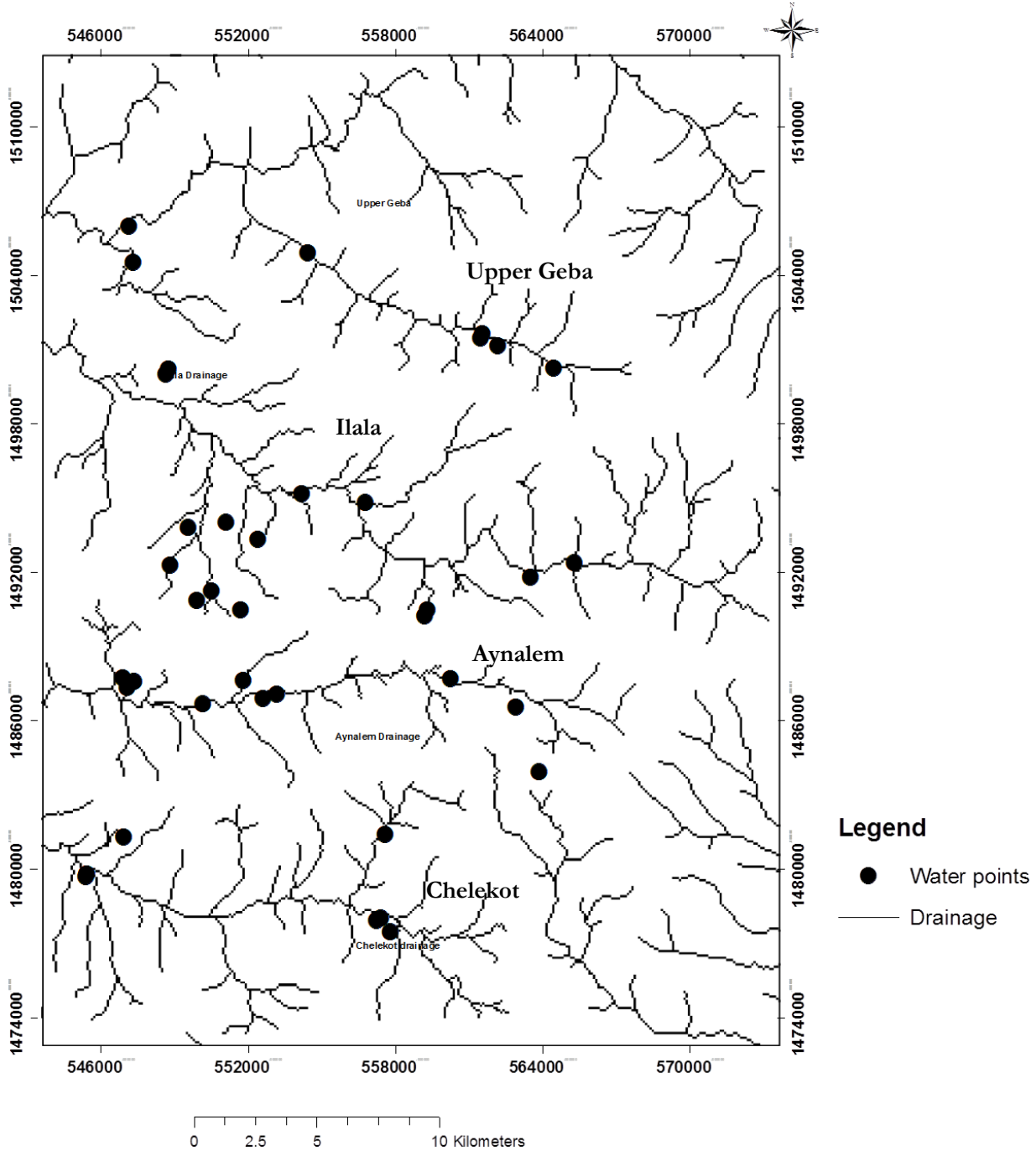


Figure 11: Location and distribution of water points from which water samples were collected in Sep, 2013

4.3. Remote Sensing Data

The remote sensing data includes satellite image downloaded from <http://glovis.usgs.gov/> (USGS Global Visualization Viewer) cloud free Landsat 5 TM of September 23, 2011 with spatial resolution of 30 m. Furthermore, SRTM data version 4.1 in ARC GRID, ARC ASCII and Geo Tiff format of decimal degrees and datum WGS84 which is derived from the USGS/NASA SRTM data. The satellite image and SRTM was then used for land-use classification and to derive the topography and drainage map of the study area respectively.

5. METHODS

The methods followed in the research process are based on the objectives formulated in section 1.3. The methodology designed for the research work consists of eight major phases: field survey, laboratory analysis, result checking, hierarchical clustering analysis, Source-rock deduction, modelling, isotopes fractionation, and water quality assessment for domestic, irrigation and engineering works. Brief descriptions of the methods employed in this study are discussed below. The field surveys were describe in chapter four.

5.1. Laboratory Analysis

The representative water samples from boreholes, springs, hand-dug wells, rivers, tap and rainfall water were collected from Aynalem, Ilala, Chelekot and Agulae (upper Geba) sub-basins for the analysis of major anions and cations, and stable isotopes of oxygen and hydrogen. The Standard Method procedure was followed for analysis (APHA et al., 1992). The major cations were analysed using Inductively Coupled Plasma Atomic Emission Spectrometry (ICP-AES) and anions of Chloride and Sulphate were analysed using HACH Spectrometry. Nitrate, Ammonia and Phosphate were analysed using a SEAL AQ-1 Discrete Multi-Chemistry Analyzer with different methods and chemicals in ITC Geo-water science laboratory. The stable isotopes were analysed at ISO ANALYTICAL in UK (England). Moreover, parameters of pH, EC, Alkalinity, Dissolved Oxygen, Temperature and Turbidity were measured on the spot during sampling of the water resources. The analysed water chemistry data were used to determine the water quality variables within the study area, and to correlate the water resources chemistry variation with geology, agricultural inputs, industrial or anthropogenic sources. Furthermore, it was used to prepare data input for hydrogeochemical model analyses, and isotopes fractionation determination.

In this study, the most important phase was to achieve quality management (quality control and assessment) of laboratory analysis techniques by checking sample containers and reagents, using blank samples, duplicate samples and standards materials. For this purpose, duplicated water samples from boreholes that are representative of Aynalem sub-basin (BHA4), Ilala sub-basin (BHIL5) and upper Geba sub-basin (BHMM2) and control samples were analysed. The results from both water samples and controls were compared, see Appendix 1. Most of the samples analysis result showed comparable constituents and the overall precision of the analysis from the control samples range from 3% to 8%. But the analysis results for chloride, sulphate and nitrate content showed differences between the samples and duplicates. The maximum, minimum and mean of the major inorganic constituents of water samples from different water resources and sub-basins of the study area are summarised in Table 8.

The stable isotopes of hydrogen and oxygen analysis were performed by triplicate equilibration technique and analysis was undertaken by continuous-flow isotope ratio mass spectrometry using a Europa Scientific ANCA-GSL and GEO 20-20 IRMS. The samples were measured against three reference standards. The standards used for Deuterium are IA-R054 with $\delta^2\text{H}_{\text{V-SMOW}} = +4.93 \text{ ‰}$, IA-R052 with $\delta^2\text{H}_{\text{V-SMOW}} = -157.12 \text{ ‰}$ and IA-R053 with $\delta^2\text{H}_{\text{V-SMOW}} = -61.97 \text{ ‰}$ and for Oxygen-18 are IA-R054 with $\delta^{18}\text{O}_{\text{V-SMOW}} = +0.56 \text{ ‰}$, IA-R052 with $\delta^{18}\text{O}_{\text{V-SMOW}} = -19.64 \text{ ‰}$ and IA-R053 with $\delta^{18}\text{O}_{\text{V-SMOW}} = -10.18 \text{ ‰}$. The reproducibility of laboratory measurements can be checked from the control samples standard deviation. Based on this the laboratory precision of deuterium and oxygen-18 analysis of natural water standards by the equilibration-IRMS method, has a 1sd of $<3 \text{ ‰}$ for $\delta^2\text{H}$ and $<0.2 \text{ ‰}$ for $\delta^{18}\text{O}$.

5.2. Hydrochemical Data Reliability Check

The water quality variables data, which were collected from the different sources during the fieldwork and/or obtained from laboratory analysis, were checked for their accuracy using anion-cation balance. A solution must be electrically neutral i.e. the sum of cations in meq/l should equal the sum of the anions in meq/l (Hounslow, 1995).

$$\text{Electro neutrality (\%)} = \frac{\sum \text{Cations} - \sum \text{Anions}}{\sum \text{Cations} + \sum \text{Anions}} * 100 \quad \text{Equation 1}$$

According to Hounslow (1995), if the electrical balance calculated is less than 5% then the analysis is assumed to be good and if it is greater than 5% the analysis is supposed to be poor, or some missed constituents are not include in the calculation or the water is very acid. But sometimes up to 10% is acceptable in dilute and saline water due to some errors during measurement (Fetter, 2001). The hydrogeochemical data from the laboratory analysis work were almost less than 10%. But for the secondary data collected from different resources only 103 out of 129 water quality data fulfilled the acceptable requirement of < 10% (Appendix-11).

Table 8: Summarized result of hydrogeochemical analysis in the laboratory and calculated Parameters for 40 water samples (Appendix-10)

Parameters	Units	Maximum	Minimum	Average
Temp	°C	28	19.8	23.22
pH		9.15	6.74	7.38
Cond	µS/cm	3010	221	1380.33
TDS	mg/l	2627.72	289.05	1249.84
Hardness	mg/l	1858.71	111.93	780.99
Alkalinity	meq/l [CaCO ₃]	24	2	11.87
Ca ²⁺	mg/l	610.65	37.54	253.61
Mg ²⁺	mg/l	107.22	4.34	35.27
Na ⁺	mg/l	174.58	5.39	47.05
K ⁺	mg/l	23.12	1.02	4.64
Al ³⁺	mg/l	5.23	0.01	0.27
Mn ²⁺	mg/l	0.36	-0.08	0.02
Fe ²⁺	mg/l	9.87	-0.11	0.59
Cl ⁻	mg/l	557.50	1.70	51.28
CO ₃ ²⁻	mg/l	720	60	356.03
HCO ₃ ⁻	mg/l	585.22	48.77	289.38
SO ₄ ²⁻	mg/l	1425	78	440.8
NH ₄ ⁺	mg/l	10.08	-0.05	0.49
NO ₃ ⁻	mg/l	407.85	0.65	59.75
PO ₄ ³⁻	mg/l	0.36	0.02	0.04

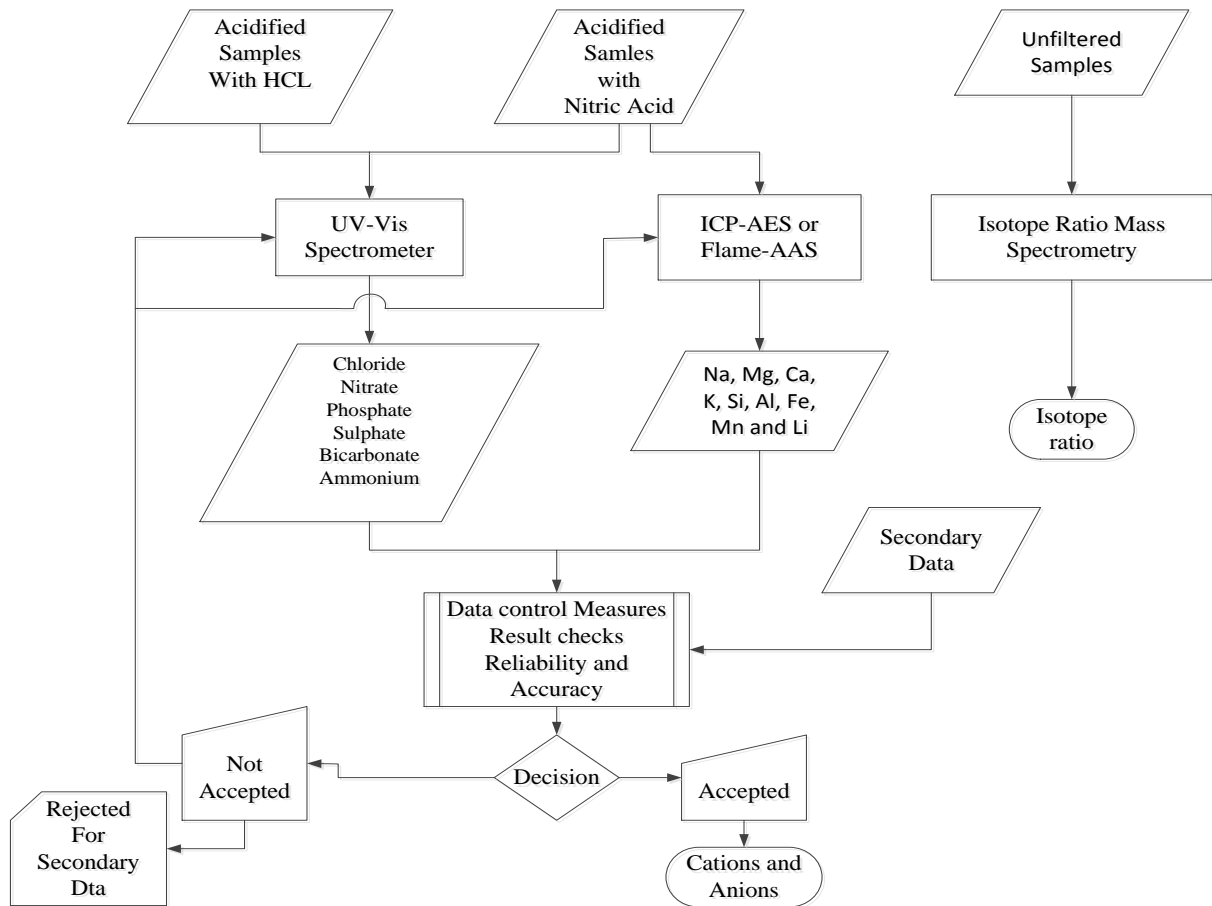


Figure 12: Laboratory Analysis, Data Control and Result Checks Flowchart

5.3. Hierarchical Cluster Analysis (HCA)

Hierarchical Cluster Analysis (HCA) is a multivariate statistical analysis and powerful classification method to divide water chemistry samples into similar groups and useful for data reduction and to check the overlap/continuity of clusters or similarities within the water chemistry data (Güler et al., 2002). Moreover, it is independent and quantitative method allowing groundwater classification into coherent groups that may be identified based on aquifer lithology, storage time or human impact and correlation with water quality parameters (Cloutier et al., 2008; Kebede et al., 2005). Research studies such as Yidana (2010), Addisu (2012), Yitbarek et al. (2012), Kebede et al. (2005) and Cloutier et al. (2008) used multivariate statistical analysis for classification of water chemistry samples. HCA provides complete analysis information in organized format and uses for interpretation of hydrogeochemical processes by formulating hypothesis (Addisu, 2012). However, the method does not provide cause-and-effect relationships of water chemistry (Güler et al., 2002; Yidana, 2010). HCA is used to figure out the water chemistry evolution and to conduct geochemical modelling among different groups and subgroups (Kebede et al., 2005).

The main objective of this classification approach is to determine the chemical relationships and associated chemical processes between water samples. Moreover, samples with similar chemical behaviour can be define in terms similar geologic, climate, resident time, infiltration, recharge area, flow and infiltration path and hydrogeochemical processes history (Addisu, 2012; Güler et al., 2002; Kebede et al., 2005). In HCA classification, data log-transformation and standardization is required for equal weighting

because parameters with higher or smaller variance during their distribution affects the Euclidean distance calculation (Addisu, 2012; Kebede et al., 2005; Yidana, 2010). In this study, HCA version XLSTAT 2013, an add-in of Microsoft EXCEL, was used to cluster water samples in to different groups and to carry out hydrogeochemical modeling among different groups.

5.4. Source-rock Deduction

This technique is used to get insight into the possible origin of the water samples analysis (Hounslow, 1995). Even though the initial composition of groundwater originates from rainfall, it is altered by rock weathering, evaporation (Gibbs, 1970) as cited in (Hounslow, 1995). During weathering processes, ions of Ca^{2+} , Mg^{2+} , SO_4^{2-} , HCO_3^- and SiO_2 are added to the water and the amount depend on the rock mineralogy (Hounslow, 1995). According Hounslow (1995), the source-rock for the water composition can be determined using ionic comparison, i.e. the pH should be > 6 , and the concentration of the ions should be changed to meq/l and SiO_2 in mmol/l.

5.5. Hydrogeochemical Modeling

Different hydrogeochemical processes affecting water chemistry can be identified by hydrogeochemical models which use the physical and chemical parameters of the water quality (Appelo & Postma, 1993). Moreover, it is used for classification of the water chemistry data into different water type groups (Schlumberger, 2006). It is also employed for speciation and to determine solid phase equilibrium saturation indices, to calculate the amount of mole transfer, and to identify the type of hydrogeochemical evolution along the flow direction of the water on its course (Hounslow, 1995; Kebede et al., 2005; B. Zhu et al., 2011). The main parameters including major cations (Ca^{2+} , Mg^{2+} , Na^+ , K^+) and major anions (HCO_3^- , SO_4^{2-} , Cl^-) are most widely used for modelling and understanding of hydrogeochemical process and evolution in ground water.

5.5.1. Aquachem 2012.1

Aquachem is used as a water quality database with functionality for numerical analysis, graphical presentation and modeling of water quality data. In addition, it has a built-in link to the geochemical modeling program PHREEQC for calculating equilibrium concentration or activities of chemical species and saturation indices of phases in a solution (Schlumberger, 2006). Moreover, it is used to cluster the hydrogeochemical data into distinct groups of water types and source rock deduction by plotting using piper and stiff diagram.

5.5.2. PHREEQC-2

According to Parkhurst and Appelo (1999), PHREEQC version-2 performs a wide variety of low-temperature aqueous geochemical calculations and simulates a variety of reactions and processes in natural waters or laboratory experiments. Moreover, the model provides an information about speciation, saturation and oxidation/reduction of a solution which is the first step in interpreting water chemistry using thermodynamic approach (Hounslow, 1995). PHREEQC interactive for Windows uses Aquachem samples as input solutions for modeling (Schlumberger, 2006).

Speciation is a relative amount of different species in water solution (Bricker, 1999; Hounslow, 1995) and saturation is an information of specific mineral in a solution whether or not saturated or in equilibrium with specified phase (Bricker, 1999). Saturation index was used to determine the potential of mineral phases for chemical reaction by determining the chemical equilibrium of the water with the phases (A. Singh et al., 2012). The hydrogeochemical equilibrium conditions of groundwater samples with solid mineral phases within an aquifer using a thermodynamic calculation can be determined using saturation

index (SI). Saturation index compares the equilibrium constant (K_{sat}) for the solubility of the mineral with the product of the activities of the ions (IAP) in a solution (Hounslow, 1995).

$$SI = \log \frac{IAP}{K_{sat}} \quad \text{Equation 2}$$

5.5.3. Inverse Modeling

Inverse modeling is used to determine the geochemical reactions controlling ground water chemistry and change in chemical compositions of water along a flow path (Federico et al., 2008; Hounslow, 1995). In addition, it is used to understand the nature and dimension of chemical reaction and to recover the chemical reactions that led to a given water quality in hydrologic system (Appelo & Postma, 1993; Parkhurst & Appelo, 1999). Hence, the amount and type of solid phase (minerals) that transfers during the chemical reaction or processes (precipitation/ dissolution) between two points along the flow path can be determined using inverse modelling (Hounslow, 1995; Kebede et al., 2005; C. Zhu, 2002). However, inverse modeling does not consider the thermodynamics and equilibrium conditions, it only employs the mass balance principles (C. Zhu, 2002). If hydrogeological data of the study area are available, the flow direction can be chosen based on hydrogeological knowledge (Addisu, 2012; Kebede et al., 2005). According Hidalgo and Cruz-Sanjulián (2001), end members for inverse modeling can be selected by considering the location and hydraulic head of the points and the observed changes in hydrochemical composition of the water in the system.

5.6. Relation and Fractionation of Stable Isotopes of Water (Oxygen and Hydrogen)

Environmental isotopes are commonly used for understanding of groundwater chemistry and evolution, rock-water interaction, water resources origin and mixing, source of salinity and contaminants (Mazor, 1991; Mook, 2000).

5.6.1. Stable Isotopes Ratio

The isotopic composition of water can be determined by mass spectrometry and compared to the isotopic composition of ocean water (SMOW) and expressed in per mil ($‰$) deviations from the SMOW standards (Mazor, 1991; Mook, 2000). The standard material, VSMOW, prepared by H. Craig has been decided by an IAEA panel in 1976 to replace the original SMOW in fixing the zero point of the $^{18}\delta$ scale. All water samples are to be referred to this standard (Mook, 2000).

$$\delta = \frac{R_{\text{sample}} - R_{\text{reference}}}{R_{\text{reference}}} * 1000 \text{ [in } \text{‰} \text{]} \quad \text{Equation 3}$$

5.6.2. Isotopic Fractionation

The tiny difference in chemical and physical behaviour between isotopes is called isotopic fractionation (Mook, 2000). Isotopic fractionation or separation occurred due to physical process in which energy-loaded water molecules move from the water phase into the vapour phase (evaporation) (Mazor, 1991; Mook, 2000). Isotopically light water molecules evaporate more efficiently than heavy ones because heavier isotopes have a lower velocity and higher binding energies (Mazor, 1991; Mook, 2000), as a result vapour has light molecules of water (negative δD and $\delta^{18}O$). In contrast, the residual water phase becomes relatively enriched in the heavy isotopes (positive δD and $\delta^{18}O$) (Mazor, 1991). According to Mook (2000), we have to consider two main processes such as evaporation of surface ocean water and the progressive raining out of vapour masses as they moves towards of lower temperature regions in order to better understand the variation in δD and $\delta^{18}O$.

5.6.3. The Meteoric Water Line

The relation between natural variations of $^{18}\delta$ and $^2\delta$ ocean water, atmospheric vapor and precipitation has become known as the Meteoric Water Line (MWL). MWL characterized by a slope of 8 and a certain intercept with the ^2H axis (= the $^2\delta$ value at $^{18}\delta = 0\text{‰}$) is Global Meteoric Water Line (GMWL) (Mook, 2000). MWL is used as convenient reference line for understanding and tracing of local groundwater origins and movements. Hence, a local meteoric line has to be established for hydrogeochemical investigations from individual rain events or monthly means of precipitation (Mazor, 1991).

$$^2\delta = 8 * ^{18}\delta + 10 \text{‰} \tag{Equation 4}$$

The general relation of the MWL is:

$$^2\delta = s * ^{18}\delta + d \tag{Equation 5}$$

Where s is slope and d is referred to as the deuterium excess (d-excess) or intercept.

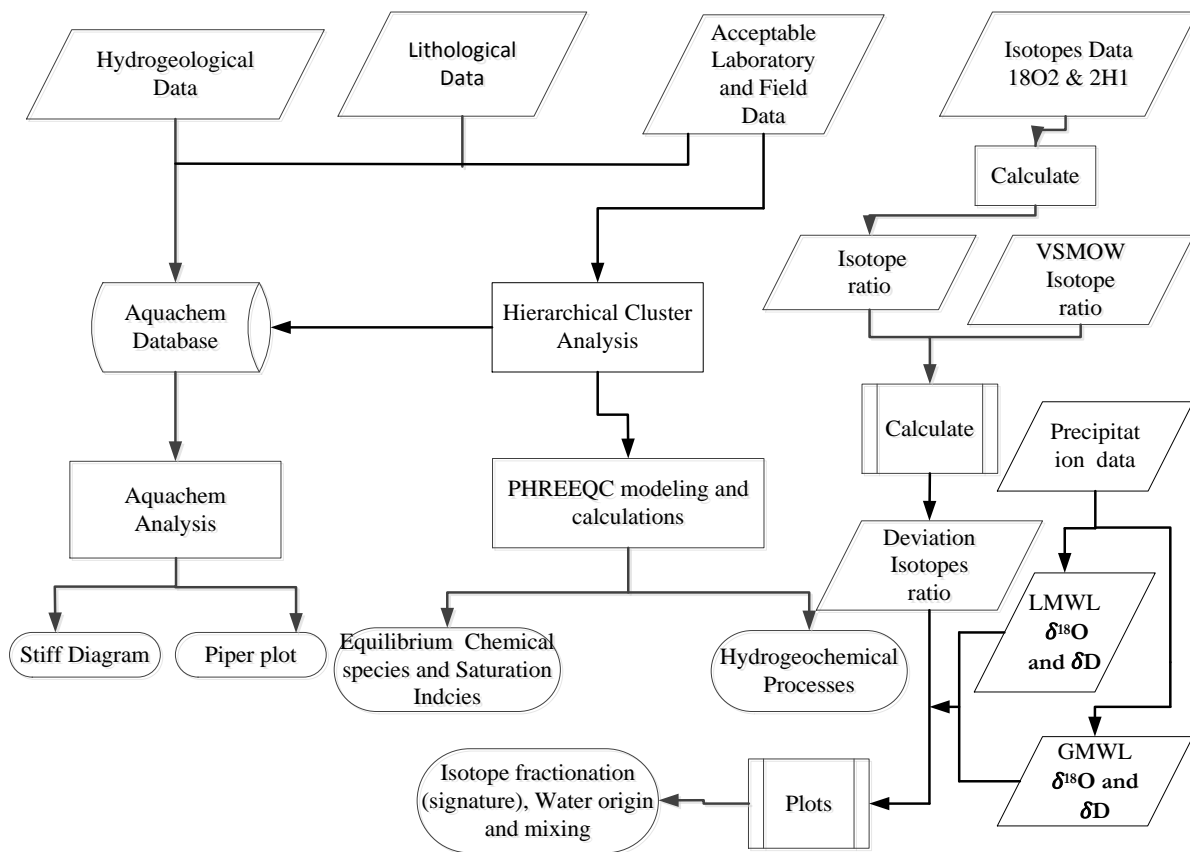


Figure 13: Aquachem Analysis, Geochemical Modeling and Isotope Fractionation Flow Chart

5.7. Water Quality Assessment

5.7.1. Domestic Use

The water quality parameters analysed in laboratory and in the field for water samples collected from the study area are compared to WHO and Ethiopia standards.

5.7.2. Irrigation Use

The quality of water for irrigation use depends on its composition and concentration of the dissolved constituents. In addition, consideration for increasing of salinity and alkalinity might be needed in irrigated area (Allison et al., 1954). SAR measures the tendency for sodium cations in irrigation water to be replaced the adsorbed Ca^{2+} and Mg^{2+} in soil clays and thus damages the soil structure (Hounslow, 1995). The characteristics of water quality for irrigation include electrical conductivity and sodium–adsorption–ratio that can be classified by plotting using Wilcox diagram. According to Allison et al. (1954) and Hounslow (1995), irrigation water can be classified into four categories based on conductivity (salinity hazard): low salinity water ($C1 \leq 250 \mu\text{s}/\text{cm}$) that can be used for irrigation with most crops; medium salinity ($250 < C2 \leq 750 \mu\text{s}/\text{cm}$) used if moderate leaching is occurring; high salinity water ($750 < C3 \leq 2230 \mu\text{s}/\text{cm}$) which cannot be used in soils with restricted drainage; and very high salinity water ($C4 > 2230 \mu\text{s}/\text{cm}$) that is not suitable for irrigation. Similarly, the classification based on sodium (alkalinity) hazard is a function of both sodium adsorption ratio and salinity (Equation -6, 7 and 8) such as low sodium water ($S1 \leq 10$) that can be used for irrigation almost in all types of soil, medium sodium water ($10 < S2 \leq 18$) present an appreciable sodium hazard in fine texture soil, high sodium water ($18 < S3 \leq 27$) may produce harmful level of exchangeable sodium in most soil, very high sodium water ($S4 > 27$) generally unsatisfactory for irrigation.

The three dividing lines for sodium hazard are:-

$$S = 18.87 - 4.44 \log EC \quad \text{Equation 6}$$

$$S = 31.31 - 6.66 \log EC \quad \text{Equation 7}$$

$$S = 43.85 - 8.87 \log EC \quad \text{Equation 8}$$

Where S is the SAR and EC is the conductivity

5.7.3. Larson and Langelier Index

Corrosion is destruction of metals by inter related influence of chloride, sulphate, calcium, alkalinity and pH, and results in complicated and costly problems in drinking and groundwater utilities (Larson, 1975; Larson & Skold, 1957; McNeill & Edwards, 2001). The Larson Index and Langelier Index are methods used to determine the corrosiveness of water in pipe lines and construction materials. Larson Index is the ratio of chloride and sulphate to bicarbonate (Larson, 1975; Larson & Skold, 1958; McNeill & Edwards, 2001).

$$\text{Larson Index} = \frac{2[\text{SO}_4] + [\text{Cl}]}{[\text{HCO}_3]} \quad \text{Equation 9}$$

The Langelier Index, which is the saturation index of calcite (Hounslow, 1995) is given by the equation

$$\text{Aggressive Index (LSI)} = \text{pH}_a - \text{pH}_s \quad \text{Equation 10}$$

Where pH_a is actual pH of a solution and pH_s is the pH of the same solution that would be at saturation with calcite or at equilibrium with calcite.

6. RESULTS AND DISCUSSION

6.1. General hydrogeochemistry

In the field of hydrogeochemical study, hydrochemistry is a scientific approach used to understand the hydrogeochemical process, evolution of water quality, to examine human impacts against natural conditions and to take a look at how the protection and management of water resources can be achieved (Freeze & Cherry, 1980; Hem, 1985; Krishnaraj et al., 2011; Prasanna et al., 2011). The water chemistry of different water resources result from solution of solid minerals, precipitation of solids, solution or evolution of gases, and sorption/ion exchange (Hounslow, 1995). The water samples from different water resources of the study area indicates that the dominant dissolved ions are Ca^{2+} , SO_4^{2-} and HCO_3^- followed by Na^+ , Mg^{2+} , Cl^- , NO_3^- , SiO_2 and with lower levels of K^+ , Al^{3+} , Mn^{2+} , Fe^{2+} and PO_4^{3-} . The summarized and detailed hydrochemical results of different water resources of Mekelle region from the secondary and primary data are listed in Table 9. However, the data doesn't contain bacteriological quality of the water resources.

The water temperature measured from the different water samples collected ranges between 19.8 and 27°C. The mean temperature of the water was 23.2°C, which is similar to the local annual surface temperature, indicating a shallow active water cycle or circulation being limited to 100 or rarely 200 m (Mazor, 1991). The pH from the water sample analyzed ranges from 6.74 to 9.15. The highest alkalinity was observed from the river at Aynalem sub-basin (RIA1), which is specifically located on Basalt and at irrigated land (crops) but the river flows from Limestone + Marl through Shale to Shale + Limestone + Marl lithology. The higher acidity is from boreholes (BHCH1) at Chelekot sub-basin located at Shale + Limestone + Marl lithology and irrigated land. The study area is mainly covered by alkalinity except the lower part of Chelekot and Ilala sub basins (Figure 14 and Appendix-2 A). The EC (salinity) and total dissolved solids (TDS) ranged between 221 to 5,300 $\mu\text{S}/\text{cm}$ and 289 to 3454 mg/l, respectively. The highest values for EC and TDS were observed from hand-dug well Jibruk-2001, which is located at Ilala sub-basin within urban land-use and lithology of Shale-Gypsum intercalation. However, the lowest value for EC is from hand-dug well (HDWCH1) located in Chelekot sub-basin on Dolerite formations, while the lowest TDS value is from river (RIA1) at Aynalem sub basin, located at basaltic formations within irrigated land in the study area (Figure 16 and 17 A and B).

The result for the TDS and EC values show increasing along groundwater flow direction from the upper part of the sub-basins to the lower parts of the sub-basins, except for Aynalem sub-basin that shows almost uniform TDS and the lower part of Ilala sub-basin which shows lower EC and TDS values (Appendex-2 B and C). Similarly, at the central part and along the flow direction of each sub-basin relatively higher TDS values and at the central part of Ilala, upper Geba and lower part of Chelekot sub-basins high EC values were observed. This is strongly related to the lithology, industrial discharge and urban sewage disposals in the area (Figure 16, 17 and Appendix-2 B and C). Similarly, the study by Berhane (2010) for Mekelle town showed that areas controlled by geological structures of fault and dyke causes sluggish groundwater flow downstream and high resident time results in higher dissolution of ions in the central basin.

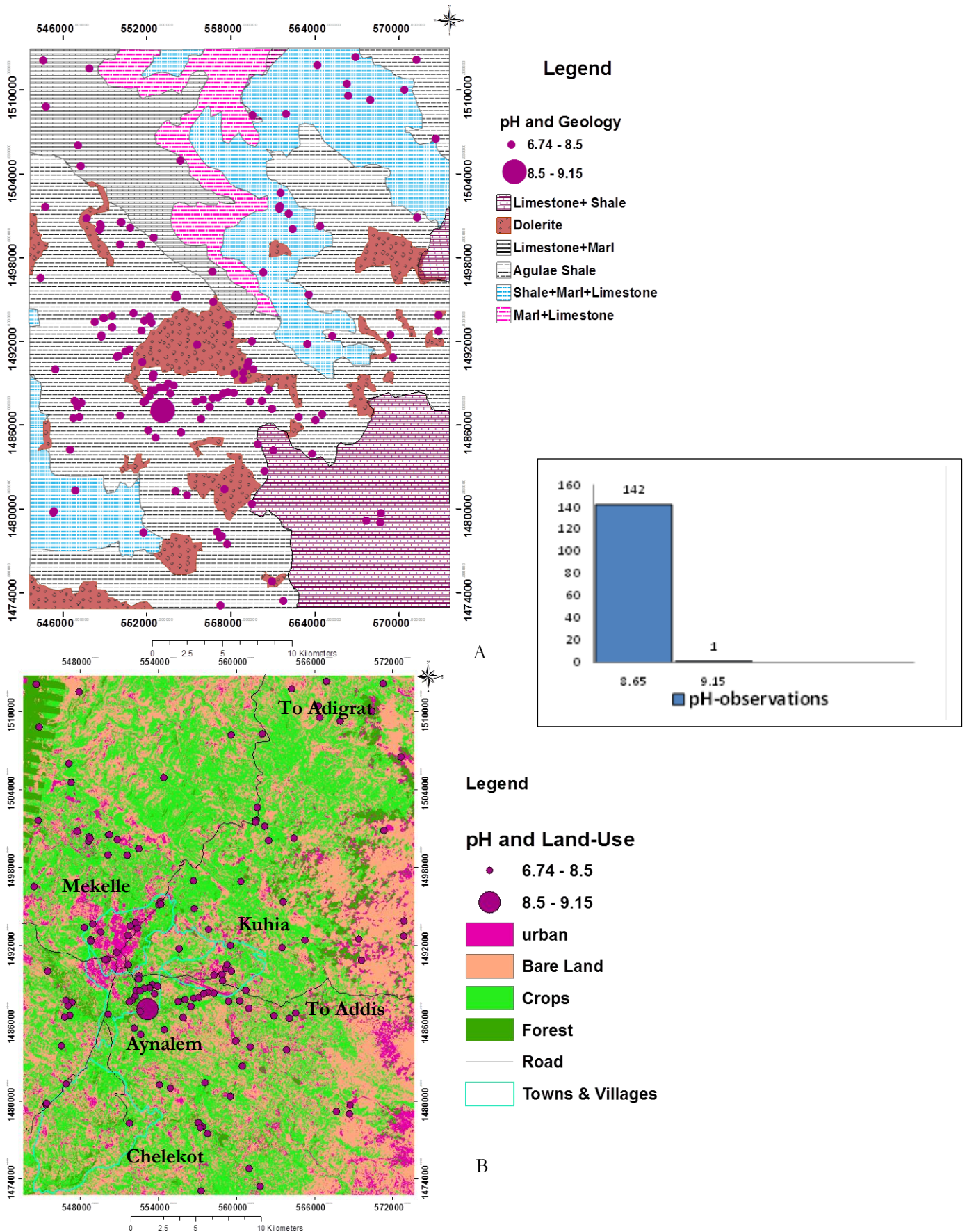


Figure 14: The distribution of pH with Geology (A) and Land-use (B) in Mekelle region

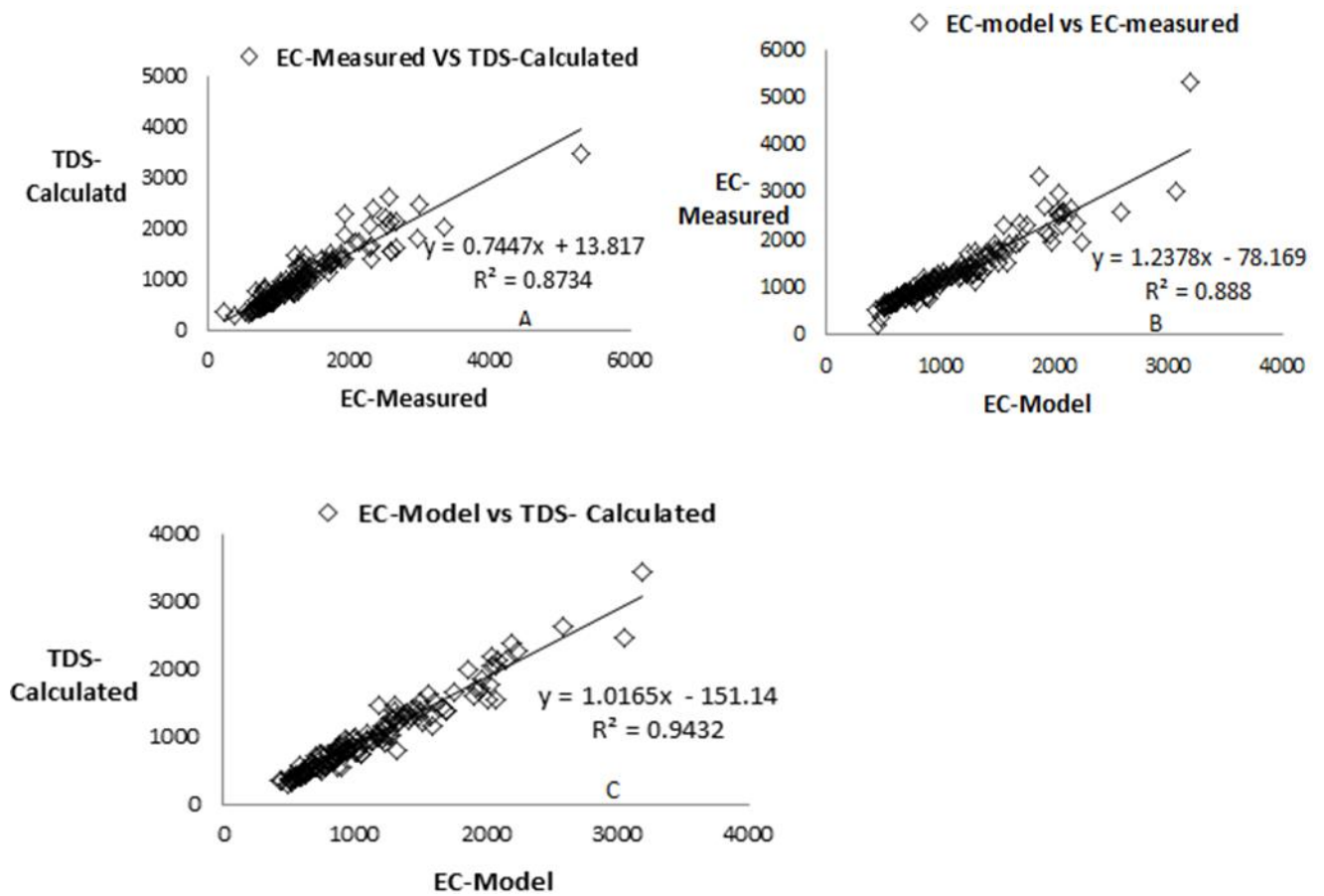


Figure 15: Graphs of correlation between measured, laboratory and model TDS and EC values

Furthermore, a good correlation between TDS calculated and EC measured, EC measured and EC model, and TDS calculated and EC model were observed (Figure 15). According to the WHO (2011) standards, out of the 143 samples from both primary and secondary data about 90 or 62.9% of them fall within the range of WHO allowable TDS concentration (< 1000 mg/l) and is classified as fresh water. The remaining 53 or 37.1% are above the TDS concentration of WHO standards (> 1000 mg/l), which is classified as brackish water type.

Table 9: Maximum, Minimum and Mean value of water quality parameters for 143 primary and secondary data (Appendix- 10 and 11)

Parameters	Maximum	Minimum	Mean
Temperature	28	19.8	23.22
pH	9.15	6.74	7.5
EC	5300	221	1283
TDS	3454	289	1001.6
Alkalinity	24	2	11.87
Hardness	2050	111.93	671.92
Ca ²⁺	631.8	37.54	225.52
Mg ²⁺	120	1.9	25.95
Na ⁺	260	5.39	42.73
K ⁺	23.12	0.4	3
SiO ₂	30.4	1.1	13
Al ³⁺	5.23	0.01	0.27
Mn ²⁺	0.36	-0.08	0.02
Fe ²⁺	9.87	-0.11	0.59
Cl ⁻	557.5	1.7	44.74
HCO ₃ ⁻	691.1	14.64	316
SO ₄ ²⁻	1607	11.6	352.6
F ⁻	1.27	0.04	0.42
NH ₄ ⁺	10	-0.05	0.49
NO ₃ ⁻	407.85	0.21	43.78
PO ₄ ³⁻	0.58	0.02	0.21

EC in $\mu\text{s}/\text{cm}$, Temperature in $^{\circ}\text{C}$, Alkalinity meq/l [CaCO₃] and the remain parameters are in mg/l

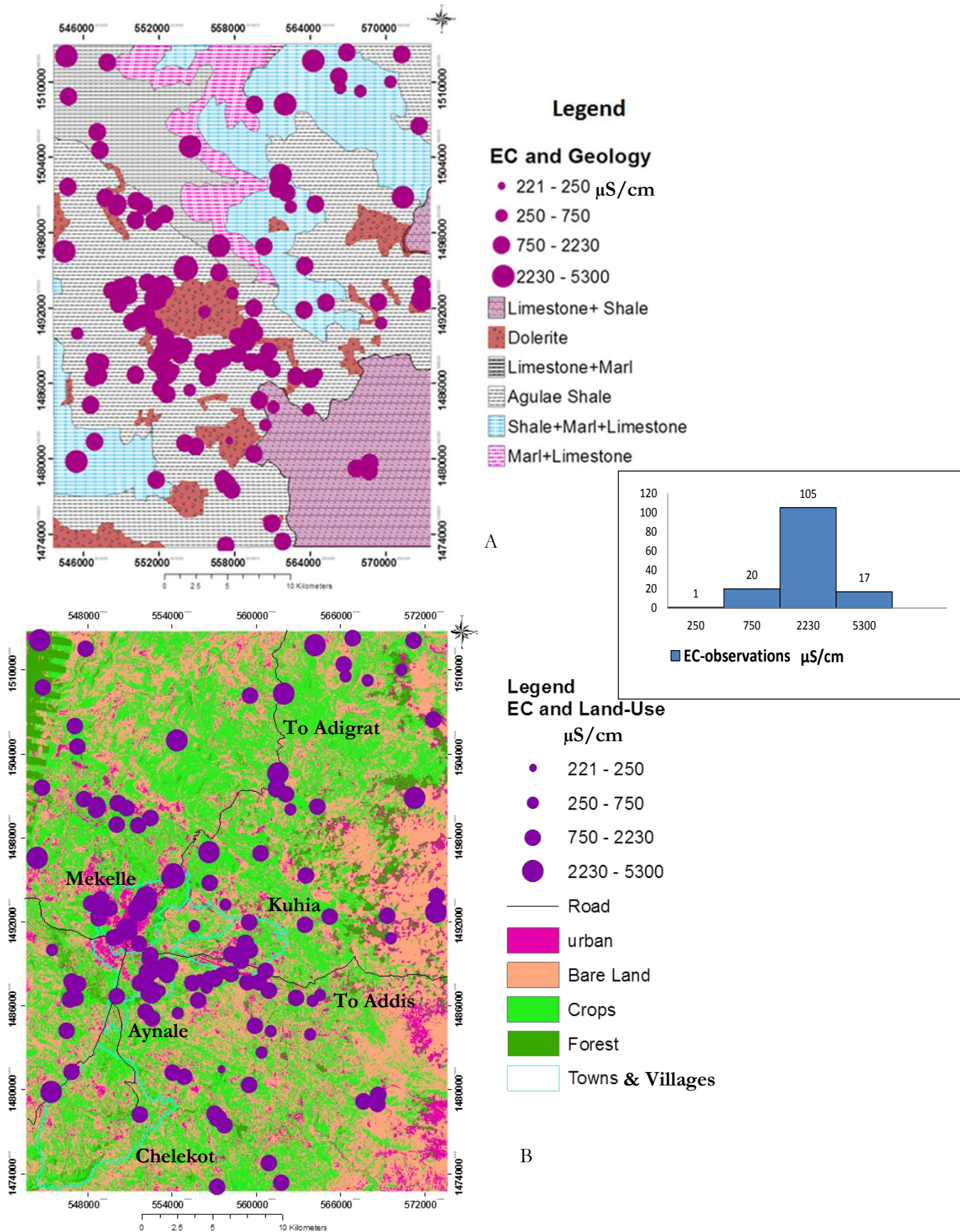
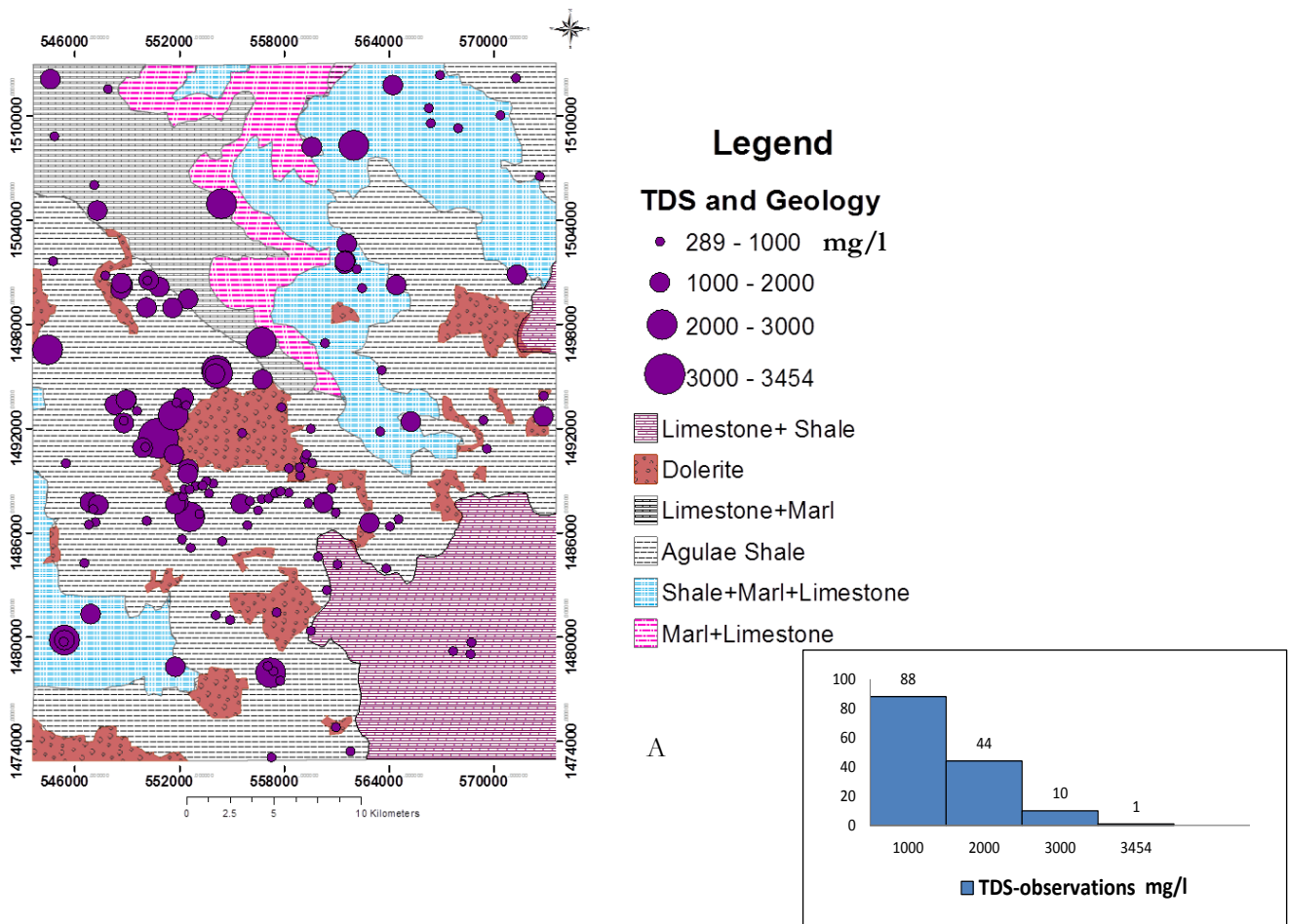


Figure 16: Spatial Variation of Electrical Conductivity (Salinity Hazard) with Geology (A) and Land-use (B) in the study area

The result indicated that the dominant anions in the water samples are SO_4^{2-} , HCO_3^- and Cl^- . The concentration of sulphate (SO_4^{2-}) varies between 11.6 and 1607mg/l (average 352.61 mg/l). The higher and the lower concentrations were observed at Ilala and Aynalem sub-basin from hand-dug well (Jibruk-2001) and borehole (BH-59) due to dissolution of Gypsum evaporite and reduction of sulphate respectively. Similarly, the concentration of bicarbonate ranges within 14.64 and 691.10 mg/l (average 316.06 mg/l) and the higher concentration is from hand-dug well (MWQ63) at Ilala sub-basin. High bicarbonate was observed from many hand dug-wells and springs in the study area, while lower concentration was observed from borehole (BH-89). According to A. K. Singh et al. (2011), bicarbonate is mainly derived from neutralization of $CO_2(g)$, by adsorption from atmosphere or organic matter decomposition in the recharge area and may release by reaction of carbonate and/or silicate minerals with carbonic acid. The result show that the chloride concentration of the study area ranges between 1.7 and 557.5 mg/l with an average 44.7 mg/l. It was observed that hand-dug wells of (HDWMM2 and HDWCH1) located at Agulae (upper Geba) and Chelekot sub-basins have higher and lower chloride concentrations respectively. In contrast, the result from the laboratory analysis indicated that the concentration of chloride in the rainfall is very low (0.3mg/l). Kahsay (2008) found similar result for rainfall chloride concentration is 0.8 mg/l. The abnormal concentration of chloride in the study area could be due to agricultural practice and industrial waste, which is a common in the study area for which the sample was taken. The major cations are calcium, magnesium, sodium and potassium but the most abundant cation is calcium. It has a concentration that ranges from 37.54 to 631.8 mg/l. Its abundance is 75.76 % of the total cations, which is followed by (14.46%) sodium, (8.74 %) magnesium and (1%) potassium, in the order of $Ca > Na > Mg > K$ (Table 9).



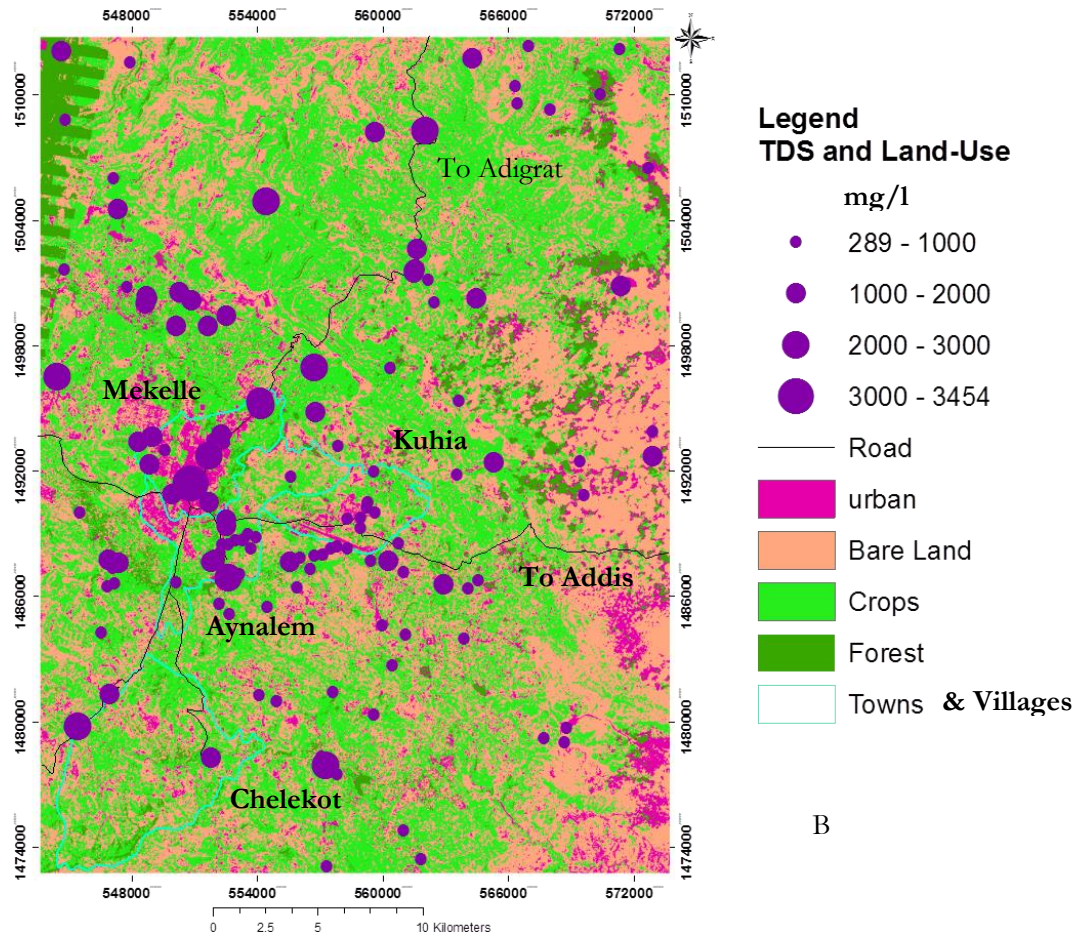


Figure 17: Spatial Variation of Total Dissolved Solids with Geology (A) and Land-use (B) in the study area

6.2. Correlation of Total Dissolved Solids and Major Elements (Ions)

The relation between the major ions and TDS is illustrated in Figure 18 and Table 10 using the water quality parameters (Ca^{2+} , Mg^{2+} , Na^+ , Cl^- , HCO_3^- and SO_4^{2-}) against TDS. Both Ca^{2+} ($R = 0.92$) and SO_4^{2-} ($R = 0.88$) have found to be linearly correlated with TDS values indicating primary salinity contributors for groundwater (Mazor, 1991). This is due to dissolution of evaporite Gypsum by the movement and circulation of ground water in the study area. The correlation between TDS and Na ($R = 0.71$) is found to be moderate (Figure 18 C and Table 10) and might be contributed from marl dissolution and anthropogenic process. Similarly, the correlation between Mg^{2+} and TDS is moderate ($R = 0.76$), and this is due to dissolution of dolomite or fertilizer inputs, while the correlation between TDS and HCO_3^- ($R = 0.17$) concentrations was found to be weak (Figure 18 E and Table 10). The weak correlation between bicarbonate concentrations and TDS is mainly due to calcite precipitation in the water. The remaining ions having a correlation coefficient of Cl ($R = 0.33$) and K ($R = 0.46$), with TDS are low (Table 10), showing proportionately a lesser contribution towards ground water salinity.

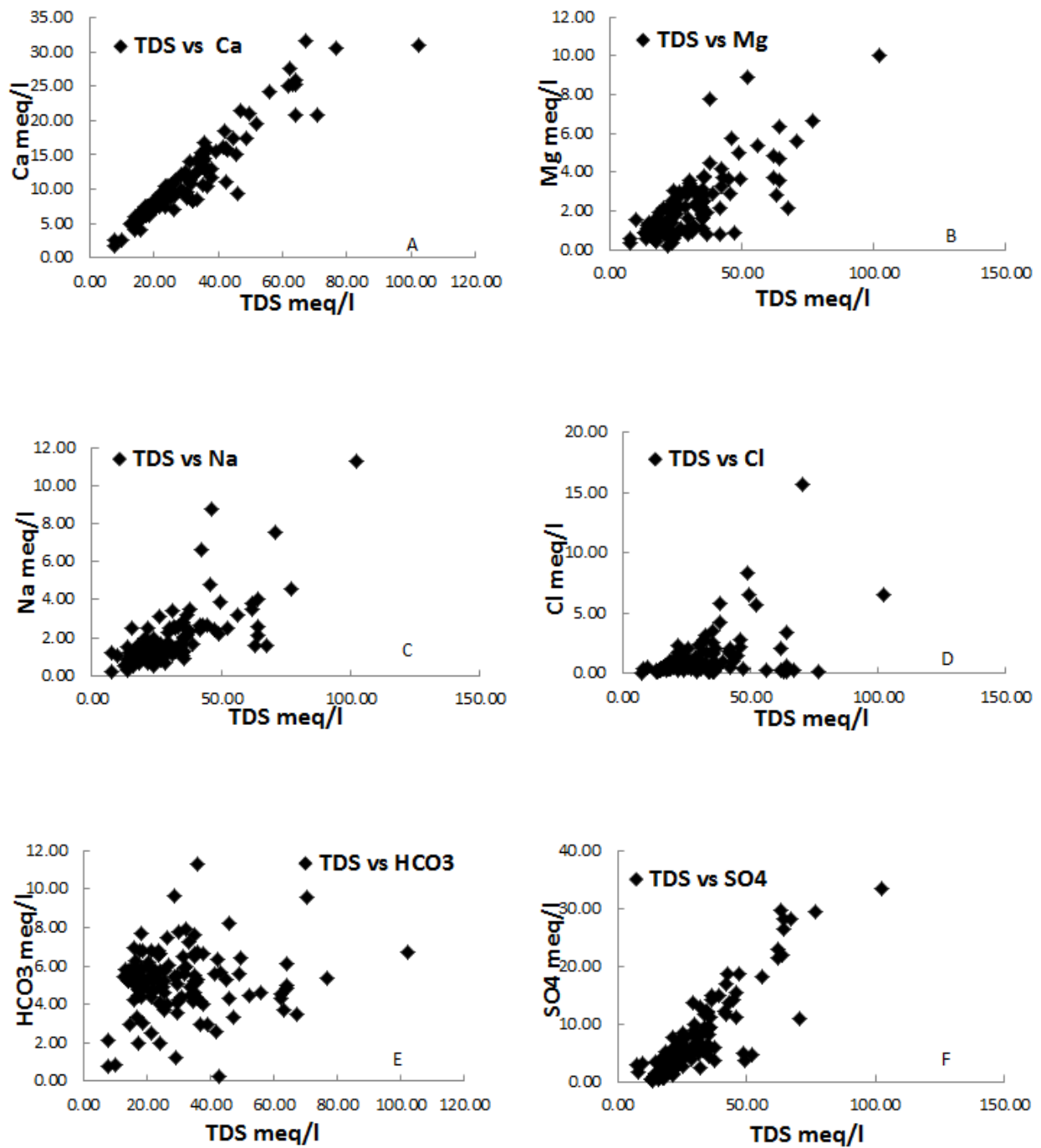


Figure 18: Relationship between major ions concentration and TDS values of the water resources

Table 10: Correlation matrix of dissolved constituents (n = 143)

	<i>pH</i>	<i>EC</i>	<i>TDS</i>	<i>Ca</i>	<i>Mg</i>	<i>Na</i>	<i>K</i>	<i>Cl</i>	<i>HCO₃</i>	<i>SO₄</i>
pH-	1.00									
EC	-0.33	1.00								
TDS	-0.39	0.95	1.00							
Ca	-0.37	0.88	0.92	1.00						
Mg	-0.29	0.76	0.76	0.65	1.00					
Na	-0.26	0.79	0.71	0.54	0.68	1.00				
K	-0.05	0.26	0.33	0.24	0.26	0.35	1.00			
Cl	-0.11	0.55	0.46	0.33	0.53	0.57	0.28	1.00		
HCO ₃	-0.27	0.18	0.17	0.07	0.25	0.22	0.06	0.36	1.00	
SO ₄	-0.25	0.81	0.88	0.87	0.55	0.56	0.23	0.09	-0.13	1.00

6.3. Hydrogeochemical Water Classification using Piper Diagram and Mapping

Hydrogeochemical water classification was done using the major anions and cations having charge balance error less than 10% and by plotting on piper diagram using Aquachem version 2012.1. Eight variables (Ca^{2+} , Mg^{2+} , Na^+ , K^+ , HCO_3^- , Cl^- , SO_4^{2-} , and NO_3^-) were included in clustering of the 143 hydrochemical data. Based on anions, four groups and ten sub-groups of water types were identified as illustrated in Figure 19 and Appendix-3. These are G1 (Bicarbonate), G2 (Bicarbonate–Sulphate), G3 (Sulphate–Bicarbonate) and G4 (Sulphate) water types. Moreover, the groups that consist of the most dominant sub-groups are G1 consists SG1 (Ca-HCO₃), G2 consists of SG2 (Ca-HCO₃-SO₄), G3 consists of SG3 (Ca-SO₄-HCO₃) and G4 consists SG4 (Ca-SO₄). The result reveal that lower TDS value were observed at the upper part of the Chelekot and Ilala, lower part of Ilala and upper Geba, north-east of upper Geba and almost all part of Aynalem sub-basins. Low EC (Salinity) values were observed from the upper part of Aynalem, north-east and north-west upper Geba and small portions of Ilala and Chelekot, and north-east of upper Geba sub-basins. The low TDS and EC values mainly attributed to Ca–HCO₃ and Ca-HCO₃-SO₄ water types (Appendix-2 B, C and F). The water type of the central part of Ilala, upper Geba, Aynalem and lower and central part of Chelekot sub-basins are Ca–SO₄ and Ca–SO₄-HCO₃. The water samples collected from these areas have higher TDS and EC value. Moreover, the groundwater from the upper part of the sub-basins that are dominantly Ca–HCO₃ type evolves to Ca–SO₄ water type through Ca–HCO₃-SO₄ and Ca–SO₄-HCO₃ along the flow direction (Figure 20 and Appendi-2 F). Thus, it can be suggested that the hydrogeochemistry of the water resources are controlled by water-rock interaction and anthropogenic pollution. Accordingly, the evolution or spatial variability of the major ions composition in groundwater can be used to trace the aquifer type and the hydrogeochemical processes taking place in the area (Güler et al., 2002).

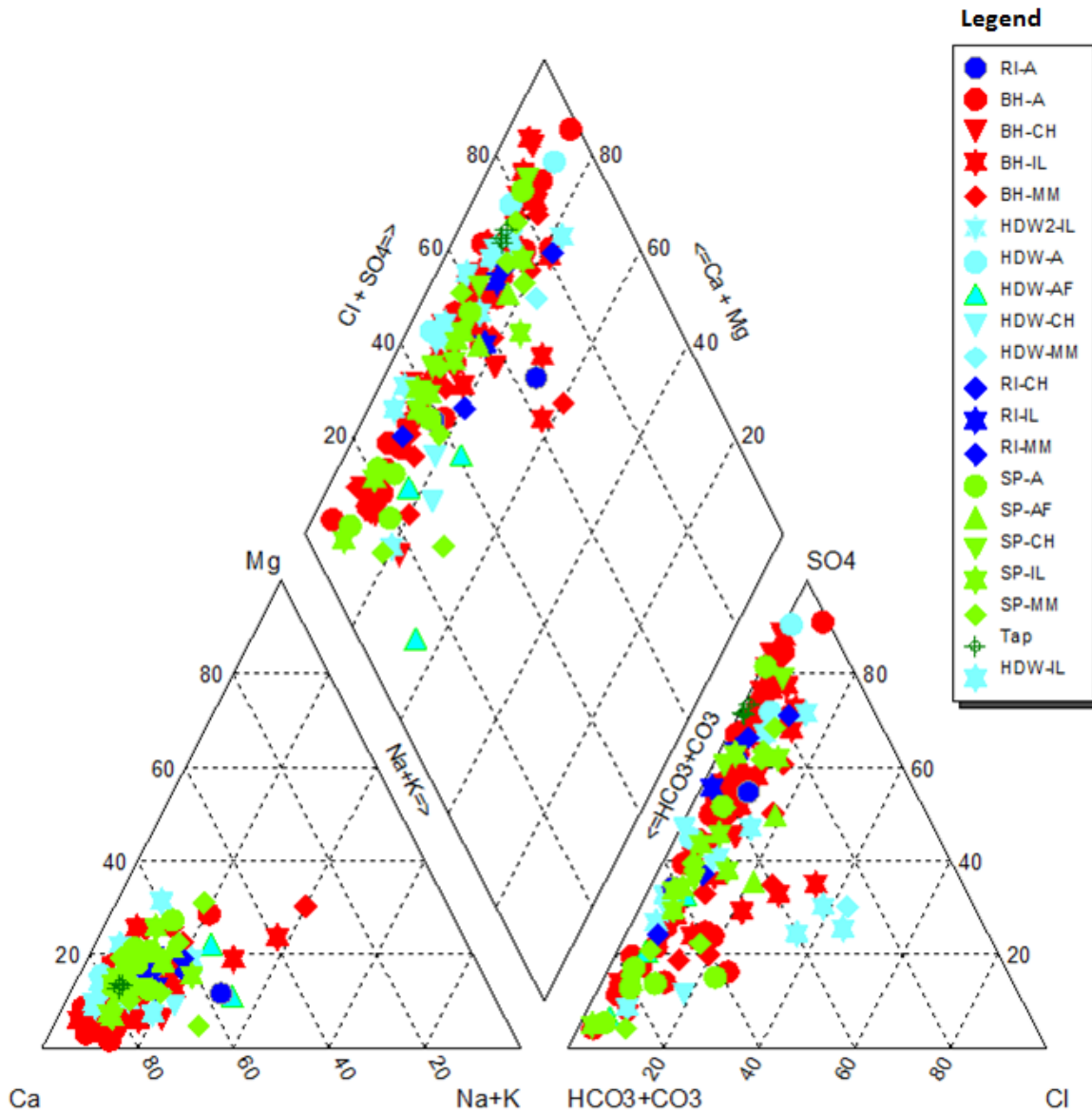


Figure 19: Water type classification of water samples from Mekelle region using piper plot

The water types for borehole (BH-52) and spring (SP-24) both from Ilala sub-basin are Bicarbonate-Nitrate-Sulphate-Chloride ($\text{Ca-HCO}_3\text{-NO}_3\text{-SO}_4\text{-Cl}$) and Chloride-Bicarbonate-Nitrate ($\text{Ca-Mg-Cl-HCO}_3\text{-NO}_3$). This is mainly due to contamination from the urban sewage, industrial disposal and agricultural activities in the sub basins. Similarly, Chloride-Bicarbonate-Nitrate ($\text{Ca-Mg-Cl-HCO}_3\text{-NO}_3$), Bicarbonate-Chloride ($\text{Ca-HCO}_3\text{-Cl}$), Bicarbonate-Sulphate-Chloride ($\text{Ca-Mg-HCO}_3\text{-SO}_4\text{-Cl}$), Bicarbonate-Nitrate-Sulphate-Chloride ($\text{Ca-HCO}_3\text{-NO}_3\text{-SO}_4\text{-Cl}$) water types are observed in BH-43, BH-52, BH-90 and SP-24 respectively, which is derived by anthropogenic sources. The hydrochemical water samples group and sub-group from different water resources are given in Appendix-3.

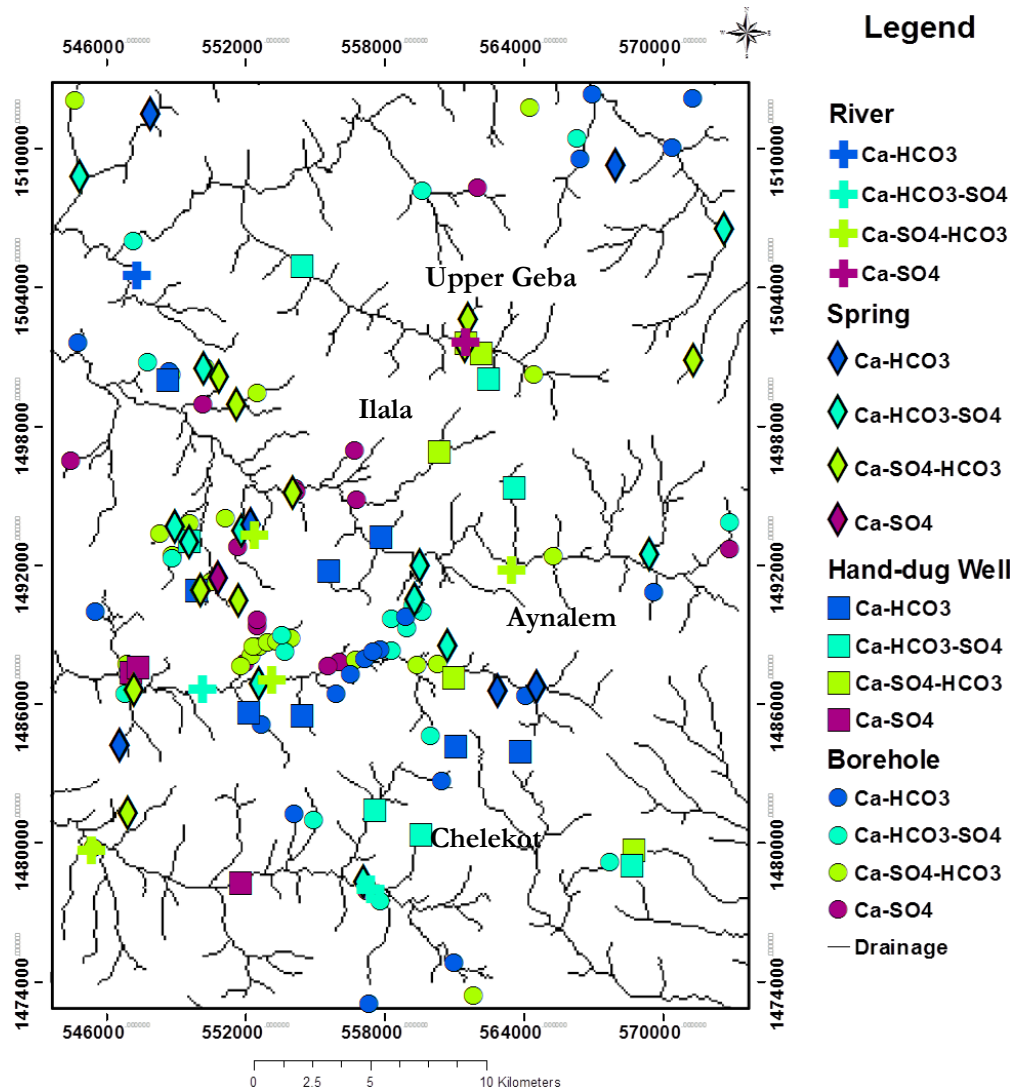


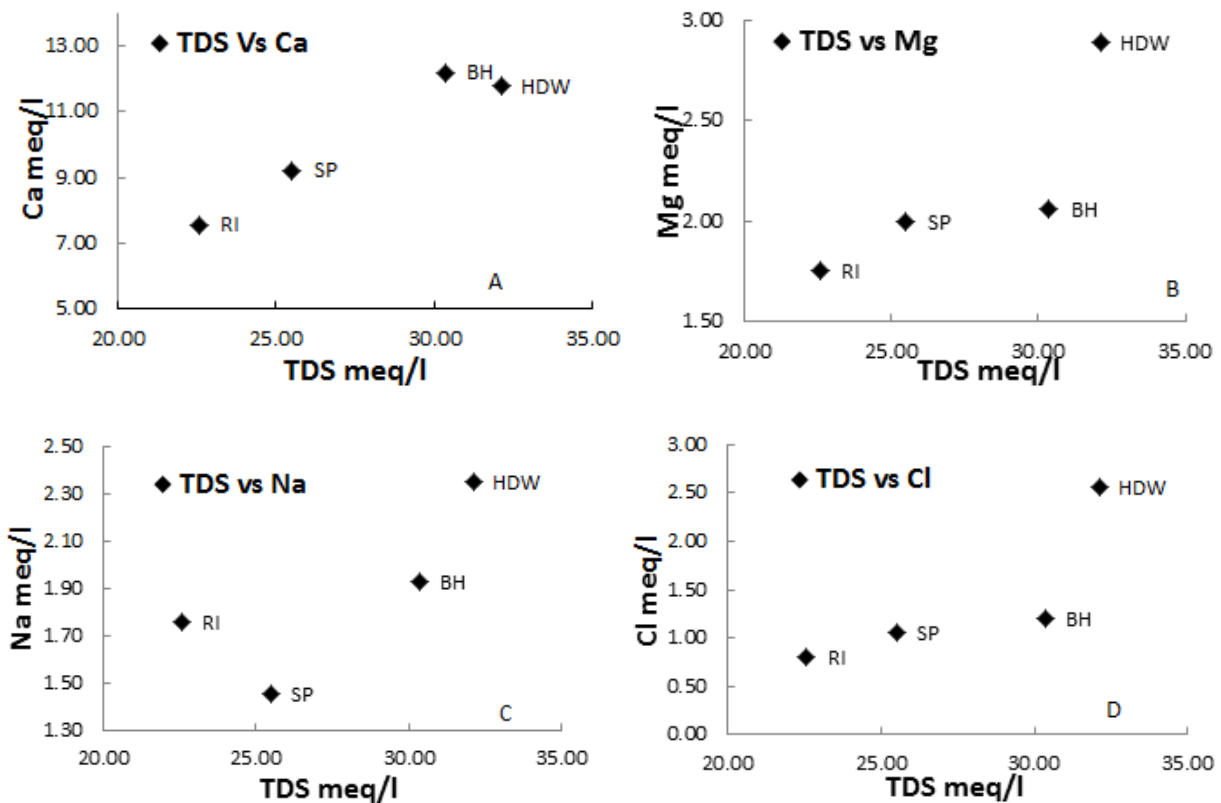
Figure 20: Spatial distribution hydrochemical water types as a function of water resource type (River, Spring, Hand-dug Well & Borehole)

6.4. Comparison of groundwater and surface water hydrogeochemistry

Both groundwater and surface water from boreholes, hand-dug wells, springs and rivers are characterized by four types of water including Ca-HCO₃, Ca-HCO₃-SO₄, Ca-SO₄-HCO₃ and Ca-SO₄ (Figure 20 and Appendix-3). The stable isotopes signature of $\delta^{18}\text{O}$ for groundwater and surface water is depleted except for rivers from Aynalem and hand-dug well from upper Geba sub-basin that show enrichment of $\delta^{18}\text{O}$ (Figure 22 and Appendix-7). The groundwater of boreholes was characterized by higher concentration of calcium, magnesium, sodium, chloride, sulphate ion and TDS as compared to springs and rivers (Figure 21). But boreholes have depleted in $\delta^{18}\text{O}$ at both higher and lower altitudes that ranges -3.9 to -1.48 ‰ (Figure 22 and Table 23) indicating a direct recharge from rainfall or less altitude effects (Mazor, 1991). The boreholes located at the central sub-basins of Ilala, Aynalem and upper Geba and upper parts of Ilala and Chelekot sub-basin show Ca-SO₄ and Ca-SO₄-HCO₃ water types, indicating a high water-rock interaction (Figure 20). The boreholes located at the central part of Aynalem, upper part of Chelekot and upper Geba sub-basins are characterized by Ca-HCO₃ and Ca-HCO₃-SO₄ water types indicating a shallow circulation of groundwater. Similarly, the hand-dug wells are characterized by higher magnesium, sodium, chloride, bicarbonate and TDS, while lower calcium and sulphate were observed as compared to boreholes implying low water-rock interaction, short flow path and high anthropogenic effects (Figure 21).

Moreover, it was observed that the hand-dug wells have a $\delta^{18}\text{O}$ that range between -2.47 ‰ and 0.04 ‰. The result indicated that the hand-dug wells show depletion of $\delta^{18}\text{O}$ with increase in altitude. However, it was exceptionally observed enrichment in $\delta^{18}\text{O}$ at an altitude of 2204 m (Figure 22). The hand-dug wells located at central part of upper Geba, Ilala and Chelekot sub-basins show Ca-SO_4 and $\text{Ca-SO}_4\text{-HCO}_3$ water types. Ca-HCO_3 , $\text{Ca-HCO}_3\text{-SO}_4$ water types are common in the hand-dug wells located at central Aynalem, upper Geba and Ilala sub-basins and upper part of Aynalem and Chelekot sub-basins (Figure 20).

The springs show relatively high calcium, magnesium, chloride and bicarbonate ions and lower sodium than rivers (Figure 21). It was also observed that the $\delta^{18}\text{O}$ values for springs ranges between -2.05 to -1.14 ‰ and it shows depletion in $\delta^{18}\text{O}$ at all altitudes similar to the groundwater from boreholes. In the springs, Ca-HCO_3 , $\text{Ca-HCO}_3\text{-SO}_4$ water types were dominantly found at all parts of Ilala and Aynalem sub-basins and lower and upper part of upper Geba. Similarly, Ca-SO_4 and $\text{Ca-SO}_4\text{-HCO}_3$ water types were mainly located at central part of Ilala and upper Geba and lower part of Aynalem and Chelekot sub-basins (Figure 20). However, the water samples from rivers are characterized by lower major cations and anions as compared to other water resources, while it shows higher sodium concentration as compared to spring water (Figure 21). The isotopes signature of $\delta^{18}\text{O}$ shows less depletion as altitude decreases. While for water samples from Aynalem River (RIA1 and MKB 012/SRE) show enrichment of $\delta^{18}\text{O}$ indicating fractionation effect due to secondary evaporation. The value for $\delta^{18}\text{O}$ of the water samples from river range from -1.74 to 1.92‰ (Table 23). It was also observed that the river water samples from the upper to the lower part of the sub-basins indicate Ca-SO_4 to Ca-HCO_3 at upper Geba, $\text{Ca-SO}_4\text{-HCO}_3$ to $\text{Ca-HCO}_3\text{-SO}_4$ at Aynalem, $\text{Ca-HCO}_3\text{-SO}_4$ to $\text{Ca-SO}_4\text{-HCO}_3$ at Chelekot and remains $\text{Ca-SO}_4\text{-HCO}_3$ at Ilala (Figure 20).



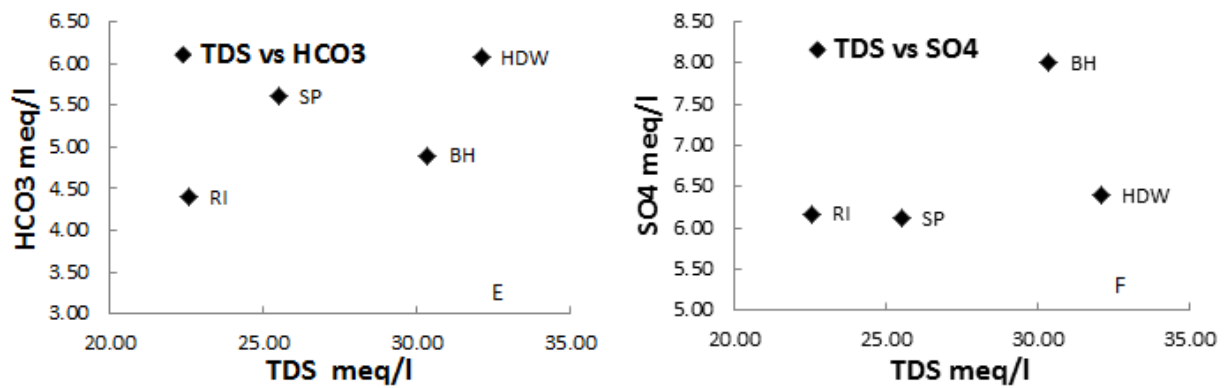


Figure 21: Average concentration of major ions comparison with TDS for different water resources

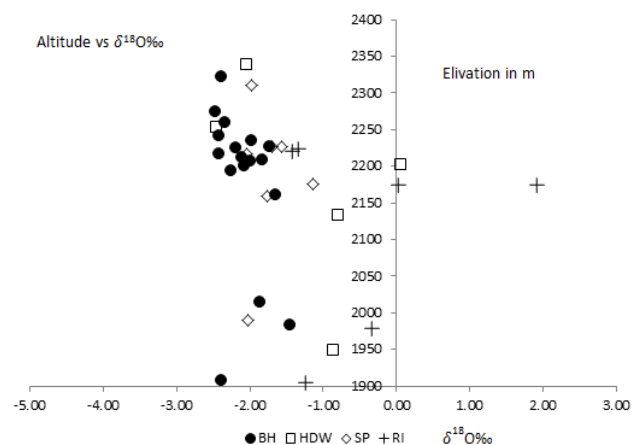


Figure 22: Altitude effects on stable isotopes of oxygen-18 of boreholes, hand-dug wells, springs and rivers

6.5. Hierarchical Cluster Analysis

Accordingly, HCA classification was conducted after all hydrochemical data were log-transformed and standardized to have equal weights. The classification was done based on the dissimilarity and Euclidean geometric distance among observations. In addition, water samples with similar quantitative values of variables/parameters were linked (agglomerated) using truncated of parallel lines and Ward's method. As a result, five sub-groups were chosen based on dissimilarity index line (phenol line) and visual inspection from the dendrogram (Figure 23) because they can clearly separate one from the other based on their hydrochemical properties.

A total of 132 out of 143 water samples were used to cluster into two major groups and five sub-groups based on eleven (11) parameters such as:- pH, EC, TDS, Ca, Mg, Na, K, Cl, HCO₃, SO₄ and NO₃ since the three water samples from tap water and eight water samples from river are not included in the classification (Appendix-4). Two major groups are distinguished by their distinct TDS values (Figure 23 and Table 11). The TDS of the water samples grouped as members of Group 1 ranges from 780-3454 mg/l and Group 2 ranges from 289-1136 mg/l. Both groups comprised five sub-groups in which sub-groups of 3 and 5 belong to Group 1 water samples and sub-groups of 1, 2 and 4 belong to Group 2 water samples. Based on Yitbarek et al. (2012), the sub-groups are distinct in recharge, residence time and degree of rock-water interactions. Moreover, the compositions of the water samples parameters were averaged and summarized in Table 11 and plotted in piper diagram (Figure 24). This helps to gain additional insight and easy understanding on the Physico-Chemical behaviour, hydrogeochemical

evolution along flow paths, to separate recharges from discharges water and to conduct inverse geochemical modeling (Addisu, 2012; Kebede et al., 2005).

The HCA also shows the chemical evolution history of the water samples, which are plotted near each other on piper diagram are not necessarily similar (Kebede et al., 2005). As a result of the piper plot (Figure 24) sub-groups SG4, SG2 and SG5 are plotted near each other that are chemically and statistically different (Table 11 and Figure 25). Generally, Group 1 water samples are distinct by their higher TDS and ions concentration than Group 2 water samples. The water samples are hydrogeochemically evolved from sub-group SG1 Ca-HCO₃ water type to sub-group of SG3 Ca-SO₄, sub-group of SG4 Ca-HCO₃-SO₄ and sub-groups of SG2 and SG5 Ca-SO₄-HCO₃ water types along the flow path (Figure 24 and 28). Detail description of each sub-groups based on geology, location in the sub-basins and degree of rock-water interactions are given in Table 12.

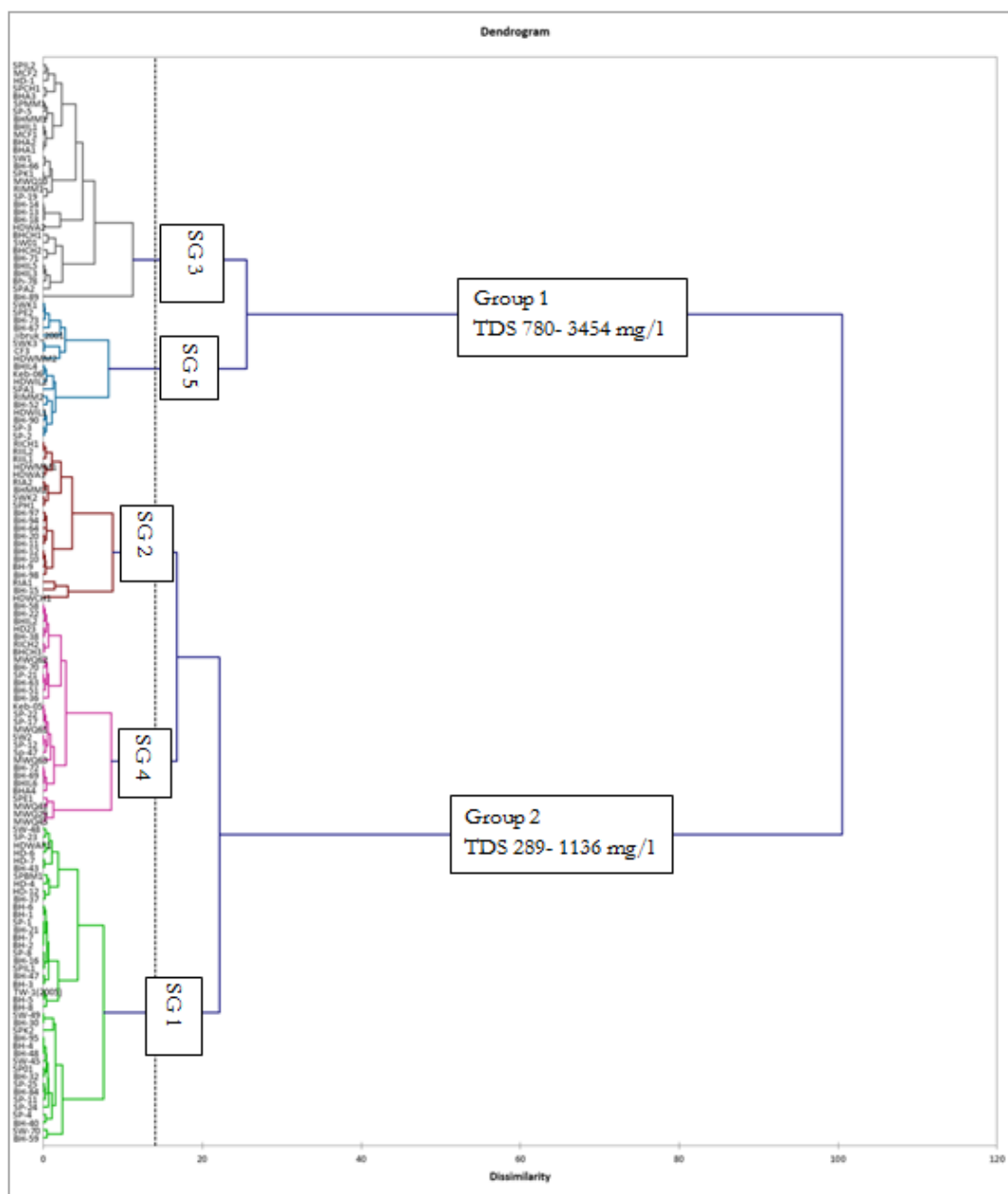


Figure 23: Dendrogram of the hierarchical cluster analysis for groundwater samples classified in to groups and sub-groups

Table 11: Mean hydrogeochemical composition of cluster sub-groups (except pH, EC ($\mu\text{S}/\text{cm}$), all others in mg/l)

Group	Sub-Group	pH	EC	TDS	Ca	Mg	Na	K	Cl	HCO ₃	SO ₄	NO ₃
G2	SG1	7.5	797.7	522.7	129.4	11.6	24.5	1.5	22.6	338.5	81.5	29.1
G2	SG2	7.8	874.9	675.3	150.4	16.0	30.7	4.5	20.0	213.7	255.0	18.9
G1	SG3	7.3	1936.6	1570.3	354.6	38.7	62.4	4.2	32.2	281.0	797.1	9.0
G2	SG4	7.6	1185.6	860.7	215.6	24.2	27.6	1.9	39.6	383.3	261.0	41.0
G1	SG5	7.4	2184.1	1610.4	310.7	58.1	103.0	4.8	169.6	383.8	484.7	154.9

Table 12: Description and interpretation of statistical sub-groups

Cluster	Description and Interpretation
Sub-group 1	This sub-group has three types of water resources such as springs, hand-dug wells, and boreholes. It is characterized by TDS that range from 330 to 785 mg/l , high bicarbonate and low sulphate ions and Ca-HCO ₃ water type indicating young groundwater with low resident time and minimum water-rock interaction (Figure 24). This sub-group is located at Ilala, Aynalem, Chelekot and upper Geba sub-basins on lithology of Shale, Shale + Marl + Limestone, Dolerite and Limestone + Shale and the source mineral is calcite (Figure 25 and 26).
Sub-group 2	All types of water resources belong to this sub-group with TDS ranging from 299-1005 mg/l . It has low bicarbonate and sulphate ions and characterized by Ca-SO ₄ -HCO ₃ water type. Located mainly at Ilala and Aynalem sub-basins and on lithology of Shale, Shale + Marl + Limestone and Dolerite in the study area, main source-rocks and minerals are Gypsum (Anhydrite) and Limestone (Calcite) Figure 25 and 26.
Sub-group 3	It contains water samples from boreholes, hand-dug wells and springs, which are located at all sub-basins of the study area. It distinguishes by high TDS range from 780-2627 mg/l , low bicarbonate and high sulphate ions. Moreover, it has characterized by Ca-SO ₄ water type. The source-rock is Gypsum (Anhydrite) intercalated with Shale, Limestone and Marl in the study area.
Sub-group 4	It can be distinguished by its moderate TDS values ranges from 543-1136 mg/l , high bicarbonate ion and it includes water resources from boreholes and spring, which are located mainly at the central part of Aynalem, Ilala and upper part of Chelekot sub-basins. It can be characterized by Ca-HCO ₃ -SO ₄ water type and low concentration of Cl ⁻ , NO ₃ ⁻ and SO ₄ ²⁺ indicated the absence of pollution. The source-rocks are Limestone (Calcite) and thin layers of Gypsum (Anhydrite) intercalated with Shale, Limestone and Marl in the study area.
Sub-group 5	It is characterized by higher TDS that ranges from 936-3454 mg/l , high bicarbonate, sulphate, chloride and nitrate ions with Ca-SO ₄ -HCO ₃ water type indicated high pollution from anthropogenic. It contains water samples from all water resource types and located mainly at Ilala and upper Geba sub-basins. Higher TDS value was observed from jbruk-2001 hand-dug well found at Ilala sub-basin of urban land-use, which is caused by contamination from urban sewage discharge in the area. The main lithologies are Shale, Limestone and marl, and the main source-rocks for the water samples are Limestone and Gypsum with minerals of Calcite and Anhydrite respectively.

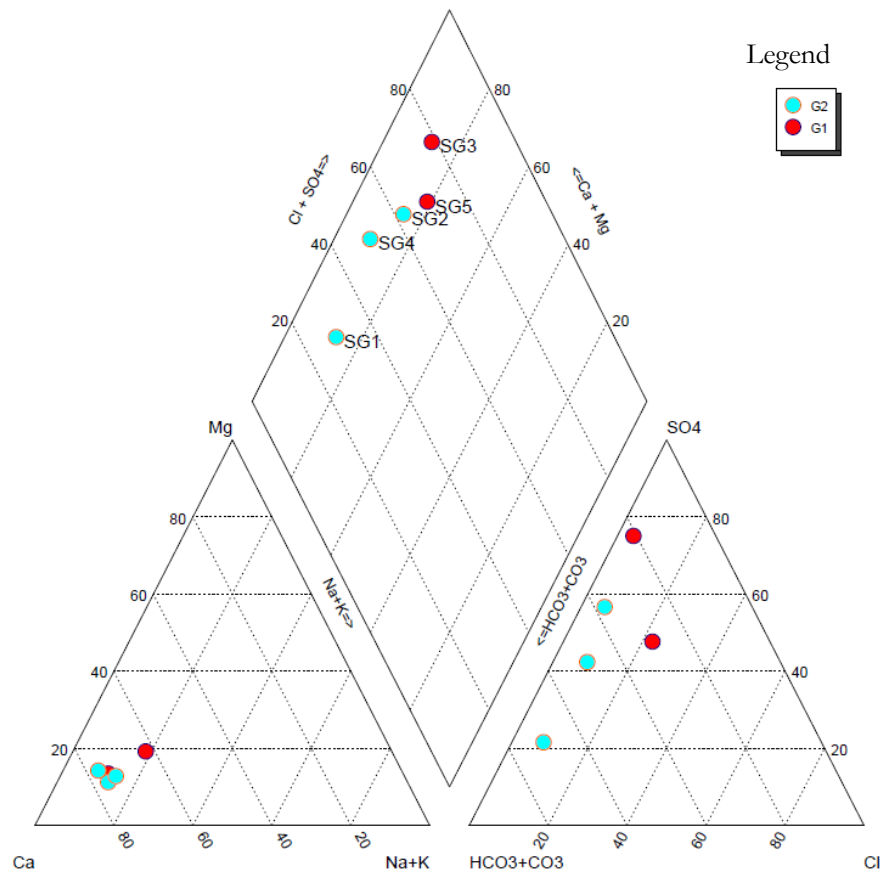


Figure 24: Water Type Classifications of the Sub-Groups using Piper Diagram

6.5.1. Source-rock Deduction and Chemical composition

As it is discussed in the methodology section 5.4, different ionic comparisons of Hounslow (1995) are given in Appendix-5. Based on this a summarized result of different ionic comparisons and their value for sub-groups is provided in Table 13. The result shows that the ratio between bicarbonate and silica is greater than ten for all sub-groups, indicating the source-rocks are carbonate weathering. The ratio between silica and sodium plus potassium and minus chloride is less than one for sub-groups 1, 2, 3 and 5 indicating cation exchange. However, it was observed that sub-group 5 have greater than one and less than one point two, indicating albite weathering. The ratio of sodium plus potassium and minus chloride to sodium plus potassium plus calcium and minus chloride is less than zero point two for all sub-groups, indicating plagioclase weathering unlikely. The ratio of sodium to sodium plus chloride is greater than zero point five for sub-groups 1 up to 4, while sub-group 5 has less than zero point five and TDS greater than five hundred (500), indicating sodium source rather than halite, albite and ion exchange, and revers softening. Similarly, the ratio of magnesium to calcium plus magnesium is less than zero point five, while the ratio of bicarbonate to silica is greater than ten, indicating Limestone-Dolomite weathering. The ratio of calcium to calcium plus sulphate was found to be greater than zero point five for sub-groups 1, 2, 4, 5 and equal to five for sub-group 3, showing calcium source other than gypsum, carbonate or silicate and gypsum dissolution respectively. Based on the discussion, Table 14, and stiff diagram in Figure 25, the main source-rocks for the composition of ion in the water resources in the study area are Limestone and Dolomite due to carbonate weathering, and dissolution of Gypsum, while anthropogenic processes also play a major role. Moreover, the lithology of Marl observed in the study area which contains Ca^{2+} , CO_3^{2-} and SiO_2 ions as major composition could be a source for the ions in the solution. However, the lithology

of shale is hydro aluminium silicate does not add salt to water but it contains nodules and veins of gypsum (Mazor, 1991).

Table 13: Source-rocks Deduction

Parameters	SG1	SG2	SG3	SG4	SG5
HCO ₃ ⁻ /SiO ₂	24.48	24.59	16.95	32.23	24.83
SiO ₂ /(Na ⁺ +K ⁺ -Cl)	0.48	0.16	0.14	1.46	-1.43
(Na ⁺ +K ⁺ -Cl)/(Na ⁺ +K ⁺ -Cl + Ca ²⁺)	0.07	0.11	0.10	0.01	-0.01
Na ⁺ /(Na ⁺ + Cl)	0.63	0.70	0.75	0.52	0.48
Mg ²⁺ /(Ca ²⁺ + Mg ²⁺)	0.13	0.15	0.15	0.16	0.24
Ca ²⁺ /(Ca ²⁺ SO ₄ ²⁻)	0.79	0.59	0.50	0.66	0.61

Table 14: Chemical Composition of Source-rocks (Source Mesebo Cement Factory)

Rock type	Chemical Composition in %												
	SiO ₂	Al ₂ O ₃	Fe ₂ O ₃	CaO	MgO	Na ₂ O	K ₂ O	CO ₃	SO ₃	Cl	MnO	TiO ₂	P ₂ O ₅
Limestone	7.43	3.02	1.35	46.35	1.26	0.17	0.23	38.68	0.37	0.01	0.09	0.16	0.07
Shale + Limestone	16.17	7.17	2.18	36.63	2.08	0.23	0.42	33.65	0.28	0.06	0.09	0.30	0.09
Marl	15.27	5.68	2.30	38.52	1.49	0.12	0.37	34.73	0.20	0.03	0.07	0.32	0.09

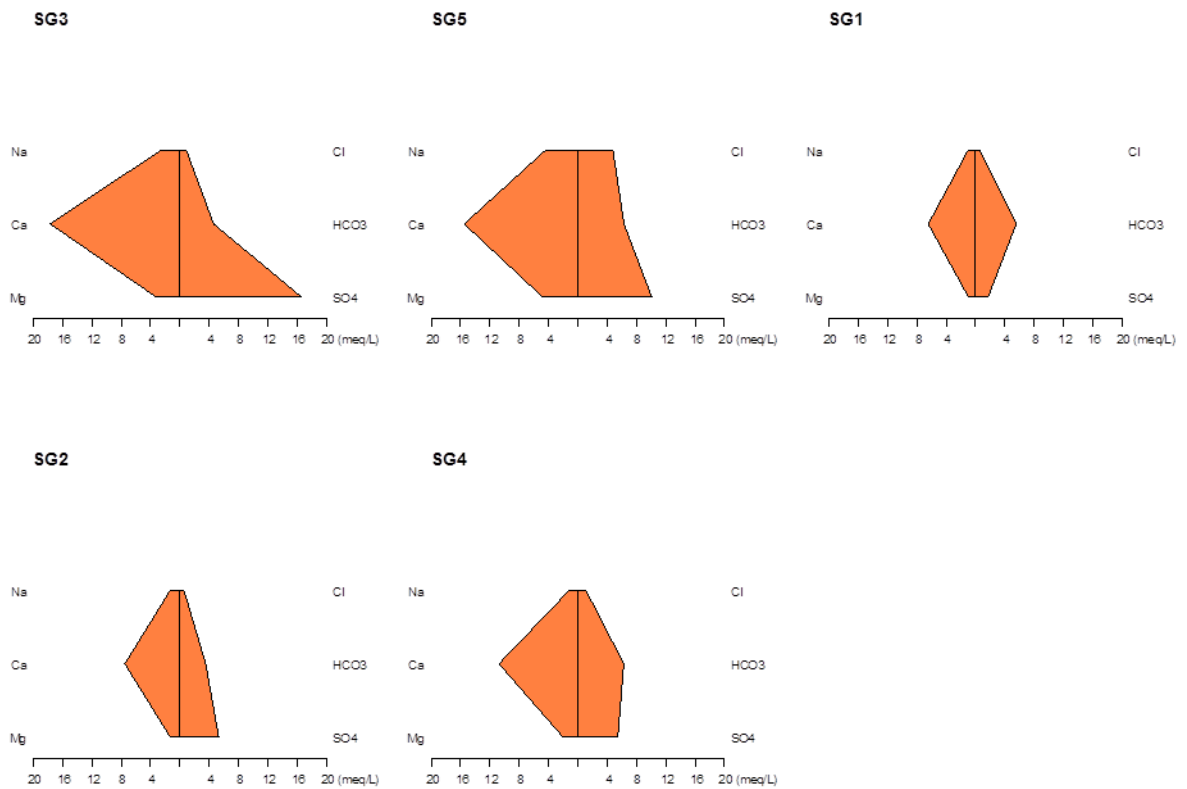


Figure 25: Stiff diagram shows Source-rocks of sub-groups in the study area

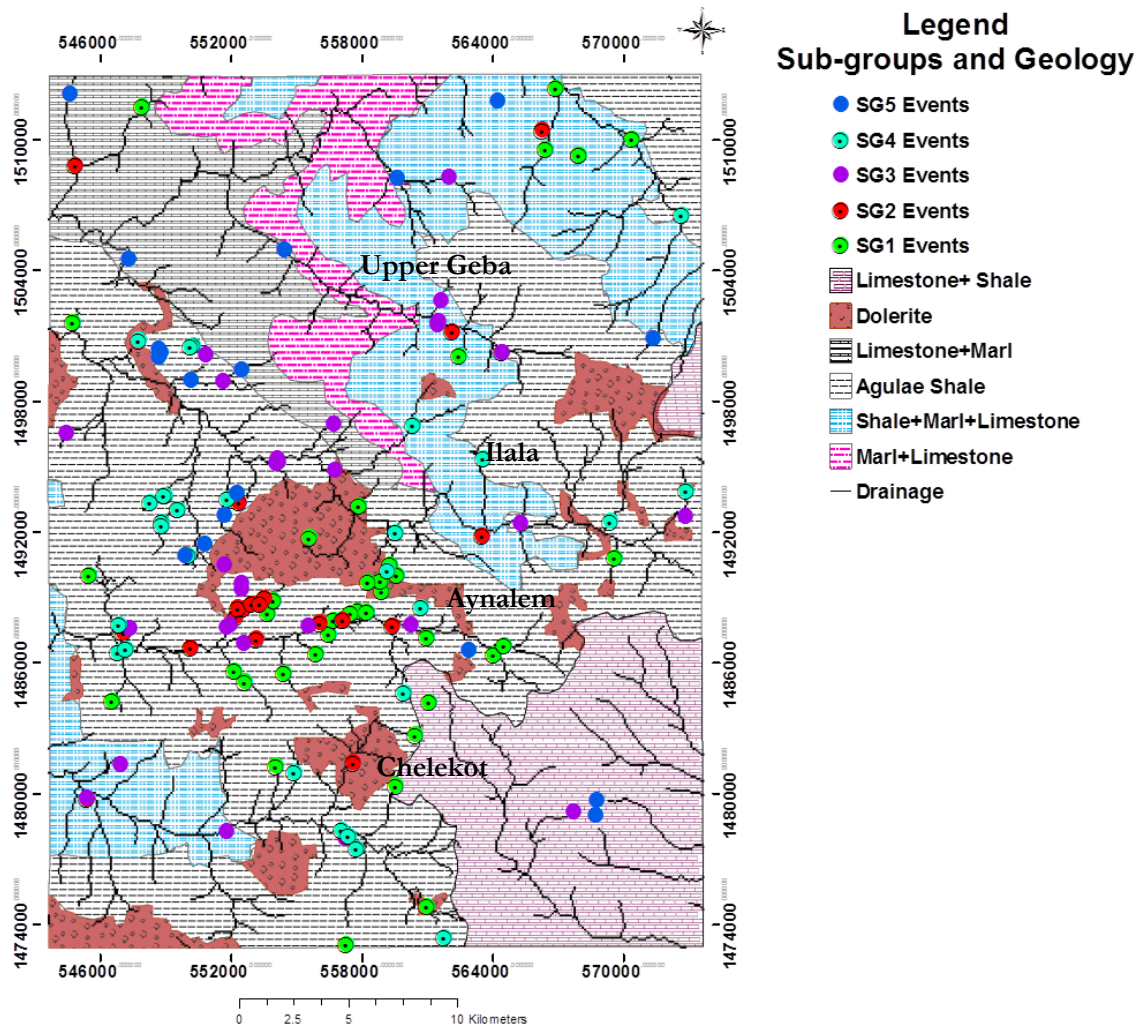


Figure 26: Spatial distribution map of sub-groups relative to the geology and drainage of the study area.

6.6. Hydrogeochemical Modeling

Geochemical modeling PHREEQC interactive version 2.12.5 and thermodynamic data base phreeqc.dat was used for speciation, saturation index and invers geochemical modeling.

6.6.1. Equilibrium Speciation and Saturation Indices of Mineral Phases in Solutions

The thermodynamic calculations of saturation indices for the water samples cluster in to sub-groups before equilibrium condition are given in Table 15. The result indicate that the solid mineral phases of the sub-groups such as Anhydrite, Gypsum, Halite and Sylvite were under saturated, implying more phases or solid minerals need to dissolve. Minerals of Aragonite, Calcite and Dolomite were over saturated, indicating more minerals need precipitation. The common mineral phases, which controlled the chemical composition of the water resources in study area, were carbonate minerals (Aragonite, Calcite and Dolomite) and sulphate minerals (Gypsum and Anhydrite) as it is provided in Figure 27. The saturation index of the carbonate mineral of Aragonite was over saturated and the over saturation has increased from sub-group SG1 to sub-groups of SG2, SG4 and SG5, while decreased in sub-group SG3 due to dissolution and precipitation process respectively. Similarly, carbonate minerals of Calcite and Dolomite were over saturated and the saturation has increased from sub-group SG1 to sub-groups of SG2, SG4 and SG5 but decreased in sub-group SG3. The sulphate minerals both Gypsum and Anhydrite were under saturated but the under saturation has decreased from sub-group SG1 to sub-groups of SG2, SG3, SG4

and SG5 due to dissolution process along the flow paths. The result further indicated that the carbonate (Aragonite, Calcite and Dolomite) minerals likely to precipitate and the sulphate (Gypsum and Anhydrite) minerals likely to dissolve during the hydrogeochemical processes.

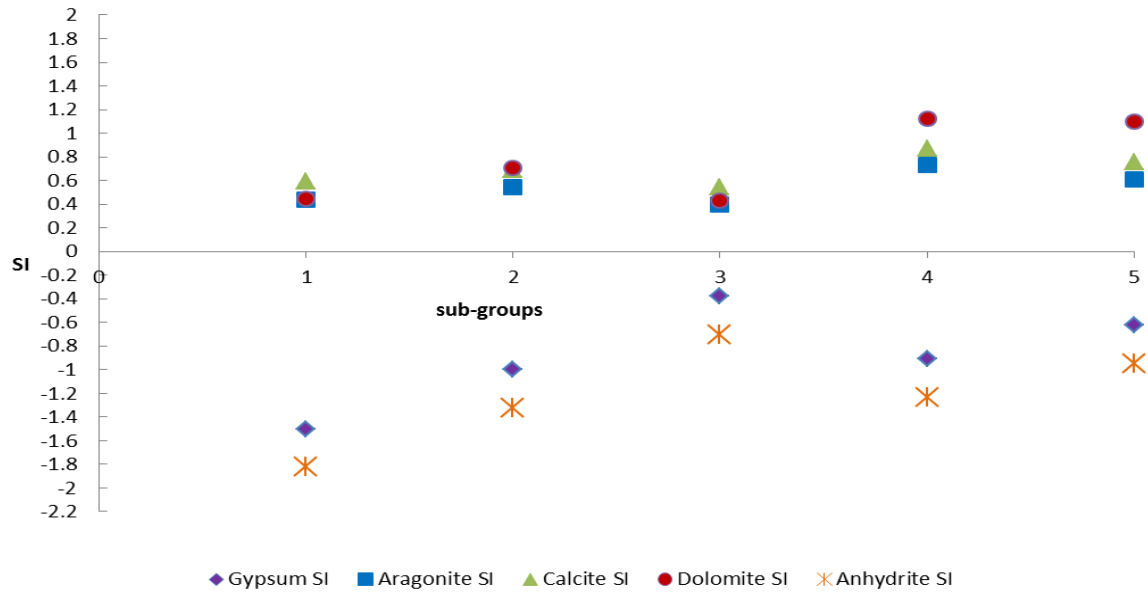


Figure 27: Saturation indices of common minerals in Mekelle region: carbonate (Aragonite, Calcite, and Dolomite) and sulphate (Gypsum and Anhydrite) in the water samples.

Table 15: Pure solid mineral phases and their Initial saturation indices of sub-groups of the study area

Phase	Mineral	SG1	SG2	SG3	SG4	SG5
		SI	SI	SI	SI	SI
Anhydrite	CaSO ₄	-1.82	-1.32	-0.70	-1.23	-0.95
Aragonite	CaCO ₃	0.44	0.55	0.40	0.73	0.61
Calcite	CaCO ₃	0.59	0.70	0.55	0.88	0.76
Dolomite	CaMg(CO ₃) ₂	0.46	0.74	0.44	1.12	1.10
Gypsum	CaSO ₄ ·2H ₂ O	-1.50	-1.00	-0.38	-0.91	-0.62
Halite	NaCl	-7.83	-7.80	-7.33	-7.56	-6.39
Sylvite	KCl	-8.59	-8.18	-8.05	-8.27	-7.26

Moreover, different species of water samples at equilibrium condition including elements of Carbon, Calcium, Chloride, Hydrogen, Potassium, Magnesium, Sodium, sulphur and Oxygen were observed. The concentration and activity of many species of the elements were very small except for species such as Ca²⁺, CaSO₄, CaHCO₃⁺, HCO₃⁻, CO_{2(g)}, Cl⁻, Mg²⁺, MgSO₄, MgHCO₃⁺, Na⁺, SO₄²⁻ and H₂O, which have relatively higher concentration (Appendix-6 A).

In addition, using the initial phases from Table 15, their initial concentration was determined using the initial saturation indices of the initial phases before equilibrium condition (Appendix-6 B). The equilibrium saturation indices and final concentration of the phases was determined using PHREEQC modeling (Table 16). The result indicate that the phases in Table 15 which were over saturated, only Calcite and Dolomite phases were reached equilibrium with the solution due to precipitation process. Moreover, the

under saturated Gypsum mineral phase reached equilibrium condition due to dissolution process. But the mineral phases including the over saturated phase Aragonite before equilibrium condition became under saturated at equilibrium condition. Similarly, the under saturated mineral phases such as Anhydrite, Halite and Sylvite before equilibrium condition remain under saturated at equilibrium condition.

Table 16: Equilibrium saturation indices and mineral phases of sub-groups

Phase	SG1			SG2			SG3			SG4			SG5		
	SI	Initial	Final												
Anhydrite	-0.32	0.02	0.00	-0.32	0.05	0.00	-0.32	0.20	0.00	-0.32	0.06	0.00	-0.32	0.11	0.00
Aragonite	-0.15	2.75	0.00	-0.15	3.55	0.00	-0.15	2.51	0.00	-0.15	5.37	0.00	-0.15	4.07	0.00
Calcite	0.00	3.89	6.66	0.00	5.01	8.58	0.00	3.55	6.08	0.00	7.59	12.98	0.00	5.75	9.84
Dolomite	0.00	2.88	2.87	0.00	5.50	5.49	0.00	2.75	2.74	0.00	13.18	13.17	0.00	12.59	12.58
Gypsum	0.00	0.03	0.03	0.00	0.10	0.13	0.00	0.42	0.61	0.00	0.12	0.16	0.00	0.24	0.33
Halite	-7.95	0.00	0.00	-7.89	0.00	0.00	-7.38	0.00	0.00	-7.65	0.00	0.00	-6.45	0.00	0.00
Sylvite	-8.71	0.00	0.00	-8.28	0.00	0.00	-8.11	0.00	0.00	-8.37	0.00	0.00	-7.33	0.00	0.00

NB. Where initial and final are phase concentrations in mole before and after equilibrium respectively.

6.6.2. Inverse Modeling with Removal or Dilution of Water

PHREEQC interactive version 2.12.5 and thermodynamic data base of phreeqc.dat was used to simulate the geochemical evolution and amount of mole transfer along the flow path between two solutions. According, Parkhurst and Appelo (1999) the most important concept in modeling evaporation is the water mole-balance equation and it is necessary to include a phase with the composition H_2O . The end members or solutions for inverse modeling were selected from different sub-groups based on the HCA assumptions in which water samples clustered in the same group or sub-group have similar geologic, climate, resident time, infiltration, recharge area, flow and infiltration path and hydrogeochemical processes history. Moreover, by taking into consideration the location of end members and a logical assumption that the final end member has higher TDS than the initial along the flow direction. In the study area, the low TDS value and $Ca-HCO_3$ solutions were considered as recharge area, and solutions with relatively high TDS values and $Ca-HCO_3-SO_4$, $Ca-SO_4-HCO_3$ and $Ca-SO_4$ water types were considered as discharge area. Some examples of flow directions from lower TDS values to higher TDS values of sub-groups are shown in Figure 28. Based on these assumptions, four flow paths were identified for inverse modelling in the study area such as, F1 from SG1 to SG4, F2 from SG1 to SG2, F3 from SG1 to SG5 and F4 from SG1 to SG3 (Table 17 and Figure 28). In addition, the mineral phases of the sub-groups which are outputs of PHREEQC (equilibrium speciation and saturation indices) determined in the Tables of 15 and 16 and the chemical composition of rocks in the area (Table 14) were used as initial inputs for inverse modeling.

Table 17: Hydrogeochemistry data inputs for inverse modeling

Model	Solution	Sub-group	pH	EC	TDS	Ca	Mg	Na	K	Cl	HCO ₃	SO ₄	NO ₃
1	Initial	SG1	7.5	797.7	522.7	129.4	11.6	24.5	1.5	22.6	338.5	81.5	29.1
	Final	SG4	7.6	1185.6	860.7	215.6	24.2	27.6	1.9	39.6	383.3	261.0	41.0
2	Initial	SG1	7.5	797.7	522.7	129.4	11.6	24.5	1.5	22.6	338.5	81.5	29.1
	Final	SG2	7.8	874.9	675.3	150.4	16.0	30.7	4.5	20.0	213.7	255.0	18.9
3	Initial	SG1	7.5	797.7	522.7	129.4	11.6	24.5	1.5	22.6	338.5	81.5	29.1
	Final	SG5	7.4	2184.1	1610.4	310.7	58.1	103.0	4.8	169.6	383.8	484.7	154.9
4	Initial	SG1	7.5	797.7	522.7	129.4	11.6	24.5	1.5	22.6	338.5	81.5	29.1
	Final	SG3	7.3	1936.6	1570.3	354.6	38.7	62.4	4.2	32.2	281.0	797.1	9.0

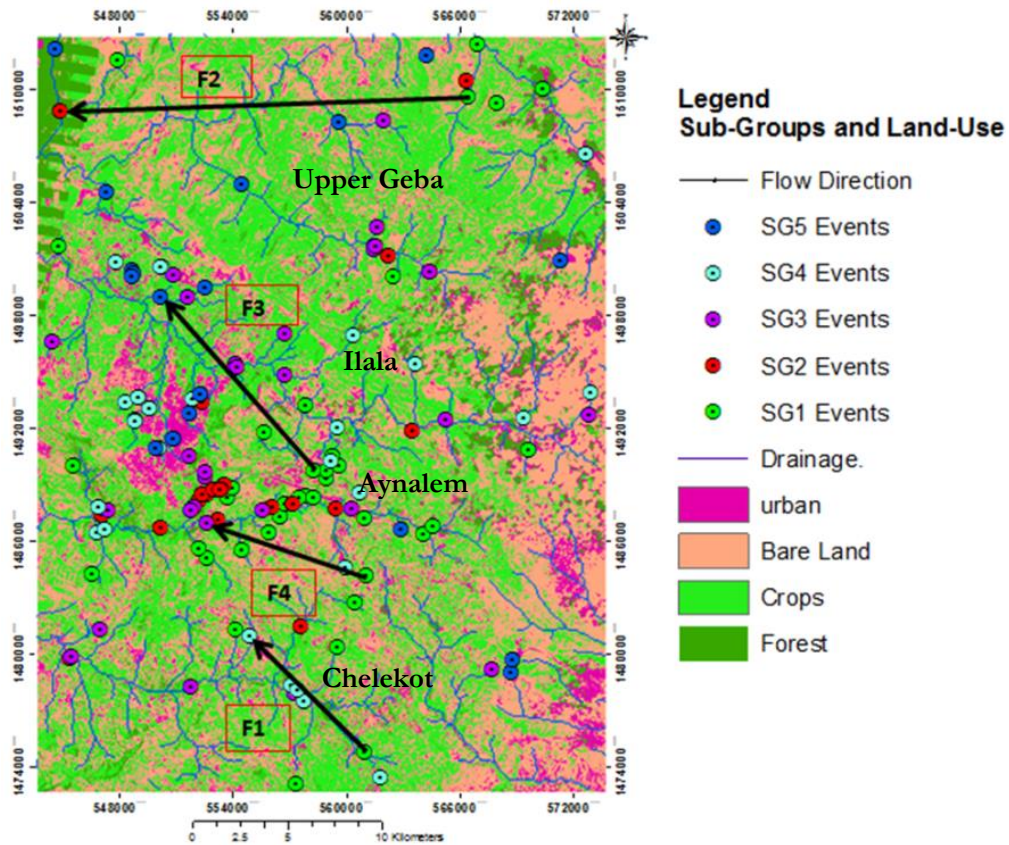


Figure 28: Example of sub-groups flow paths for inverse modeling from recharge to discharge areas

Model 1

Inverse geochemical modeling was conducted between SG1 and SG4 along the flow path 1 (F1). The low TDS value 522.7 mg/l and Ca-HCO₃ water type of sub-group SG1 with lithology of Shale, Shale + Marl + Limestone, Dolerite and Limestone + Shale were used as initial solution in the inverse modelling. While the relatively higher TDS 860.7 mg/l and Ca-HCO₃-SO₄ water type of sub-group SG4 with lithology Shale and, Limestone and Marl as final solution.

Table 18: Outputs of inverse modeling flow path 1

Phase	Mole Transfer	Minimum	Maximum	Molecular Formula
CO ₂ (g)	2.926e-03	1.878e-03	3.492e-03	CO ₂
H ₂ O	4.481e+01	2.778e+01	5.412e+01	H ₂ O
Calcite	9.308e-04	4.055e-04	1.358e-03	CaCO ₃
Dolomite	9.044e-04	6.961e-04	1.023e-03	CaMg(CO ₃) ₂
Gypsum	2.689e-03	2.410e-03	2.833e-03	CaSO ₄ ·2H ₂ O
Halite	9.539e-04	6.948e-04	1.114e-03	NaCl
Sylvite	4.124e-05	2.628e-05	4.983e-05	KCl

The inverse modeling result indicated that solution SG1 was concentrated by 0.1926 fold to produce solution SG4. Thus 0.1926 kg of water in SG1 is increase to 1 kg of water in SG4. The model shows 44.81 mol or 0.807 kg (419 % of solution SG1) water is added along the flow path. The main hydrogeochemical processes observed between the end members with uncertainty of 0.05 (5%) are dissolving of Carbon dioxide (0.0029 mol), dilution of water (recharge from surface and rain water and water release during

chemical reactions) and dissolution Calcite (0.00093 mol), Dolomite (0.0009 mol), Gypsum (0.0027 mol), Halite (0.00095 mol) and Sylvite (0.00004 mol) along the flow path, resulting in the increase of TDS, Ca^{2+} , Mg^{2+} , Na^+ , K^+ , HCO_3^- , SO_4^{2-} and Cl^- .

Model 2

Inverse geochemical modeling was conducted between SG1 and SG2 along the flow path 2 (F2). The low TDS value 522.7 mg/l and Ca- HCO_3 water type of sub-group SG1 with lithology of Shale, Shale + Marl + Limestone, Dolerite and Limestone + Shale was used as initial solution. The relatively higher TDS 675.3 mg/l and Ca- SO_4 - HCO_3 water type of sub-group SG2 with lithology Shale, Shale + Marl + Limestone and Dolerite as final solution in the inverse modelling.

Table 19: Outputs of inverse modeling flow path 2

Phase	Mole transfer	Minimum	Maximum	Molecular Formula
$\text{CO}_2(\text{g})$	-3.792e-03	-5.610e-03	-2.616e-03	CO_2
H_2O	-4.200e+01	-7.198e+01	-2.326e+01	H_2O
Calcite	-2.905e-03	-4.021e-03	-2.242e-03	CaCO_3
Dolomite	-1.871e-04	-5.257e-04	2.504e-05	$\text{CaMg}(\text{CO}_3)_2$
Gypsum	1.268e-03	7.420e-04	1.533e-03	$\text{CaSO}_4 \cdot 2\text{H}_2\text{O}$
Halite	-6.037e-04	-1.039e-03	-3.193e-04	NaCl
Sylvite	4.773e-05	1.777e-05	6.805e-05	KCl

The inverse modeling result indicating that solution SG1 was concentrated by 1.757 fold to produce solution SG2. Thus 1.757 kg of water in SG1 is reduced to 1 kg of water in SG2. The model shows 42 mol or 0.757 kg water (43 % of solution SG1) water is removed along the flow path. The main hydrogeochemical processes observed during removal of water between the end members with uncertainty of 0.05 (5%) are carbon dioxide outgassing (0.0038 mol), loss of water (evaporation and pumping of water), dissolution of Gypsum (0.0013 mol) and Sylvite (0.000048 mol), and precipitation of calcite (0.0029 mol) and Halite (0.0006 mol), resulting in the increase of TDS, Ca^{2+} and SO_4^{2-} and decrease of HCO_3^- and Cl^- .

Model 3

Inverse geochemical modeling was conducted between SG1 and SG5 along the flow path 3 (F3). The low TDS value 522.7 mg/l and Ca- HCO_3 water type of sub-group SG1 with lithology of Shale, Shale + Marl + Limestone, Dolerite and Limestone + Shale was used as initial solution. The relatively higher TDS 1610.4 mg/l and Ca- SO_4 - HCO_3 water type of sub-group SG5 with lithology Shale, Marl + Limestone and Limestone + Shale as final solution in the inverse modelling.

Table 20: Outputs of inverse modeling flow path 3

Phase	Mole transfer	Minimum	Maximum	Molecular Formula
$\text{CO}_2(\text{g})$	1.103e-00	-1.489e-003	2.496e-003	CO_2
H_2O	4.625e+001	1.981e+001	5.550e+001	H_2O
Dolomite	2.314e-003	1.951e-003	2.513e-003	$\text{CaMg}(\text{CO}_3)_2$
Gypsum	4.912e-003	4.228e-003	5.306e-003	$\text{CaSO}_4 \cdot 2\text{H}_2\text{O}$
Halite	4.329e-003	4.015e-003	4.711e-003	NaCl
Sylvite	1.165e-004	9.089e-005	1.291e-004	KCl

The inverse modeling result indicating that solution SG1 was concentrated by 0.1665 fold to produce solution SG5. Thus 0.1665 kg of water in SG1 is increase to 1 kg of water in SG4. The model shows 46.25 mol or 0.83 kg (500 % of solution SG1) water is added along the flow path. The main hydrogeochemical processes observed between the end members with uncertainty of 0.05 (5%) are dissolving of Carbon dioxide (1.1 mol), dilution of water (recharge from surface and rain water and water release during chemical reactions), and dissolution Dolomite (0.0023 mol), Gypsum (0.0049 mol), Halite (0.0043 mol) and Sylvite (0.00012 mol) along the flow direction. These cause increase of TDS, Ca^{2+} , Mg^{2+} , Na^+ , K^+ , HCO_3^- , SO_4^{2-} and Cl^- .

Model 4

Inverse geochemical modeling was conducted between SG1 and SG3 along the flow path 4 (F4). The low TDS value 522.7 mg/l and Ca- HCO_3 water type of sub-group SG1 with lithology of Shale, Shale + Marl + Limestone, Dolerite and Limestone + Shale was used as initial solution. The relatively higher TDS 1570.3 mg/l and Ca- SO_4 water type of sub-group SG3 with lithology Shale, Shale + Limestone + Marl as final solution in the modeling.

Table 21: Outputs of inverse modeling flow path 4

Phase	Mole transfer	Minimum	Maximum	Molecular Formula
$\text{CO}_2(\text{g})$	-9.670e-03	-1.549e-02	-7.107e-03	CO_2
H_2O	-1.562e+02	-2.519e+02	-1.178e+02	H_2O
Calcite	-8.355e-03	-1.205e-02	-6.836e-03	CaCO_3
Dolomite	-2.264e-04	-1.262e-03	2.580e-04	$\text{CaMg}(\text{CO}_3)_2$
Gypsum	5.295e-03	3.626e-03	5.962e-03	$\text{CaSO}_4 \cdot 2\text{H}_2\text{O}$
Halite	-1.484e-03	-2.756e-03	-9.131e-04	NaCl
Sylvite	-3.881e-05	-1.177e-04	-2.396e-06	KCl

The inverse modeling result indicating that solution SG1 was concentrated by 3.81 fold to produce solution SG3. Thus 3.81 kg of water in SG1 is reduced to 1 kg of water in SG2. The model shows 156.2 mol or 2.81 kg (73.9 % of solution SG1) water is removed along the flow path. The main hydrogeochemical processes observed between the end members with uncertainty of 0.05 (5%) are carbon dioxide outgassing (0.0097 mol), loss of water (evaporation and pumping of water), dissolution of Gypsum (0.0053 mol), and precipitation of calcite (0.0084 mol), Dolomite (0.00023 mol), Halite (0.0015 mol) and Sylvite (0.000039 mol). As a result, TDS, Ca^{2+} and SO_4^{2-} have increased, while HCO_3^- decreased.

Generally, the main hydrogeochemical processes or reactions that control the water chemistry in the study area along the four flow paths among different sub groups are dissolving and outgassing of carbon dioxide, loss and dilution of water, dissolution and precipitation of Calcite, Dolomite, Halite and Sylvite, dissolution of Gypsum and anthropogenic effect.

6.7. Relation and Fractionation Between Stable Isotopes Deuterium and Oxygen ($\delta^{18}\text{O}$)

There was no any recorded of isotopic data for precipitation in study area. Thus, a Local Meteoric Water line for this research was produced from precipitation (rainfall) isotopes data of 2002 for KOBO station which is located at GPS coordinates of latitude $12^{\circ}8'37''$ and longitude $39^{\circ}38'27''$ with an elevation of 1500 m a.s.l. It is found approximately at air distance of 150 km from Mekelle region. The data was downloaded from <http://isohis.iaea.org> with project number GNIP and World Metrological Organization (WMO) code of 6333304 which is monitored by International Atomic Energy Agency (IAEA). Monthly mean of the year 2002 precipitation isotope data of $\delta^{18}\text{O}$ and δD are plotted to produce a LMWL, which is represented by $\delta^2\text{H}=5.65*\delta^{18}\text{O}+9.377$ equation (Table 22 and Figure 29).

In order to better understand the variation in δD and $\delta^{18}\text{O}$, the rainfall data from KOBO station were compared with VSMOW and GMWL. Besides, isotopes data from different water resources were compared with LMWL and VSMOW. When LMWL was compared with GMWL which is represented by $\delta^2\text{H}=8*\delta^{18}\text{O}+10$, the LMWL fall below the GMWL at the right upper part of the plot indicating the Ethiopian rainfall has lower D-excess than GMWL. However, the LMWL fall above the GMWL at the left bottom of the plot showing the Ethiopian rainfall has higher D-excess than the GMWL (Figure 29). It was also observed that the D-excess differs from 10‰ due to variations in humidity and temperature condition on the evaporation region or different source characteristics of moisture (Mook, 2000). Hence, higher and lower D-excess observed in the area is mainly due to seasonal variations of the main rain season (summer) influenced by Atlantic Westerlies and spring (hot season) or light rains influenced by easterlies respectively. The rainfall during summer season shows depletion in oxygen-18 when compared to VSMOW and ranges between -1.82 and -0.45‰. But the rainfall during spring shows enrichment in oxygen-18 that range from 1.88 to 3.23‰ than VSMOW, indicating the rainfall subjects to secondary processes of evaporation (Mazor, 1991; Mook, 2000)(Table 22).

Table 22: Isotopes abundances for precipitation of KOBO station

Station ID	Sample ID	Date	Sample Type	δD	$\delta^{18}\text{O}$	D-excess
GNIP	KOBO	2002-05-15	Precipitation - rain	24.5	2.91	1.2
GNIP	KOBO	2002-06-15	Precipitation - rain	25.4	3.23	-0.4
GNIP	KOBO	2002-07-15	Precipitation - rain	23.5	1.88	8.5
GNIP	KOBO	2002-08-15	Precipitation - rain	3.7	-1.15	12.9
GNIP	KOBO	2002-09-15	Precipitation - rain	-3.3	-1.82	11.3
GNIP	KOBO	2002-10-15	Precipitation - rain	0	-1.28	10.2
GNIP	KOBO	2002-12-15	Precipitation - rain	10.6	-0.45	14.2

In order to trace the origin of the water resources (how water mixes from different water resources) and to determine the fractionation effect in different water resources in the study area, a total of 24 primary water sample data of deuterium and oxygen-18 from boreholes, hand-dug wells, rivers, springs and rain, and 13 secondary isotopes data of 2002 for boreholes, springs and rivers were used (Figure 30).

The isotopic composition of different water resources is either a direct or modified of precipitation isotopic composition due to fractionation effect. Hence, plotting water resource isotopes data along the reference line (MWL) in $\delta^{18}\text{O}$ versus δD diagram is a common practice (Mazor, 1991; Mook, 2000). Based on this, the isotopes for 37 water samples from both primary and secondary data were plotted along LMWL of KOBO which is the nearest area (Figure 31).

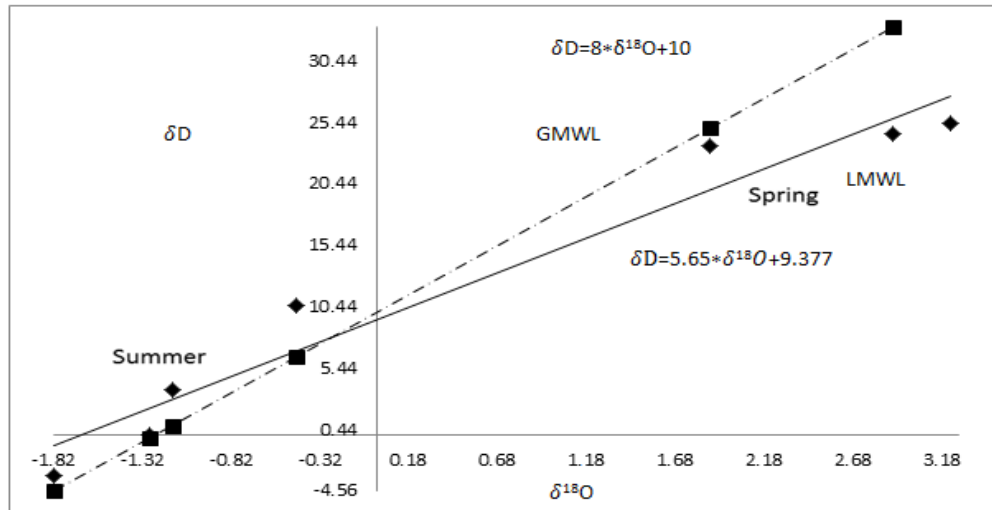


Figure 29: Plot of isotopic signature (LMWL) of rainfall year 2002 for KOBO and GMWL

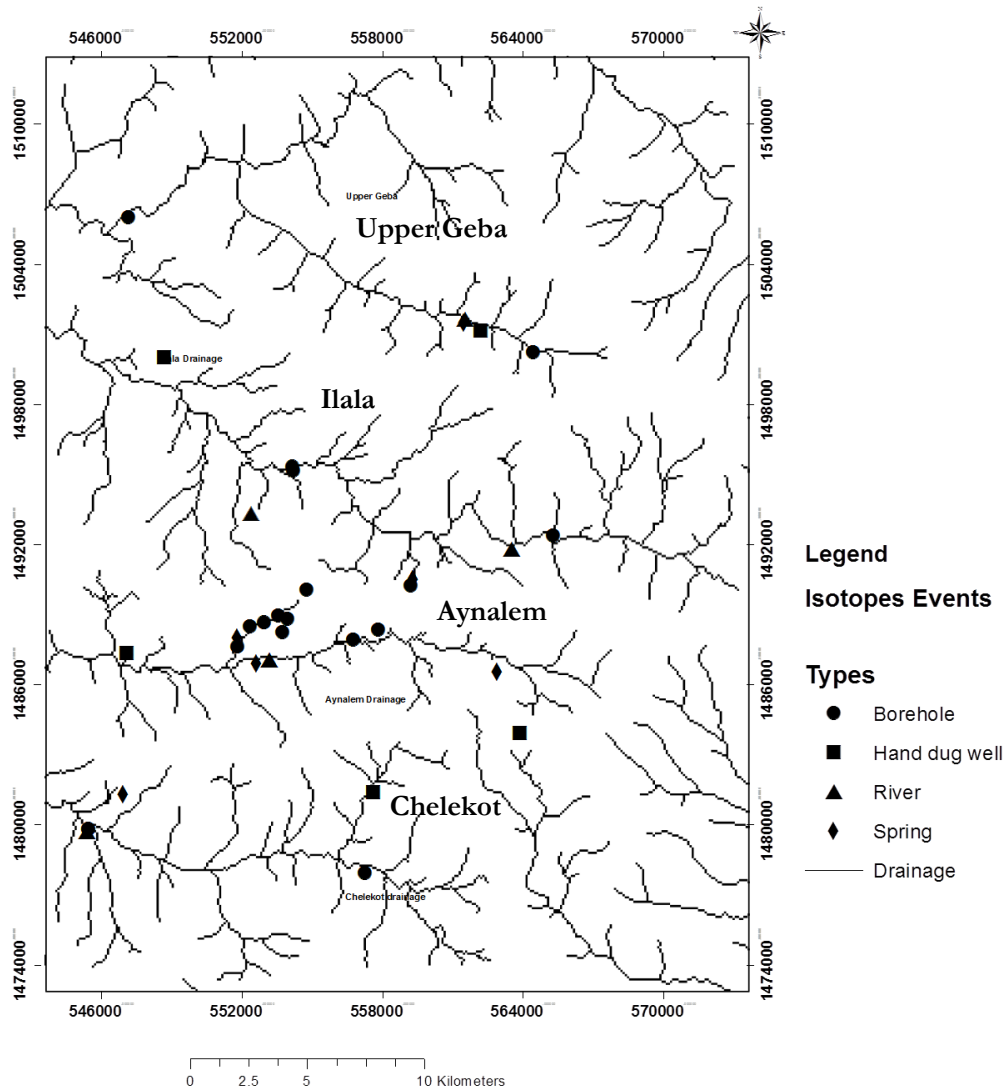


Figure 30: Isotopes data sample point distribution in the study area

Table 23: Summary of Isotopes Deuterium and Oxygen-18 for the study area

Types	δD			$\delta^{18}O$			D-Excess		
	Maximum	Minimum	Mean	Maximum	Minimum	Mean	Maximum	Minimum	Mean
BH	-0.08	-18.19	-6.38	-1.48	-3.90	-2.23	9.96	-1.45	6.23
HDW	5.68	-8.96	0.33	0.04	-2.47	-1.23	10.23	3.42	7.29
SP	3.08	-6.33	-1.76	-1.14	-2.05	-1.75	12.63	4.57	8.10
RI	13.83	-3.40	1.98	1.92	-1.74	-0.59	7.92	2.99	5.32
Rain	0.58	0.58	0.58	-0.86	-0.86	-0.86	5.41	5.41	5.41

NB. The D-excess is calculated using LMWL slopes and the unit for Deuterium is δD_{V-SMOW} (‰) and Oxygen-18 is $\delta^{18}O_{V-SMOW}$ (‰).

Table 24: summary output of Anova (single factor) for Oxygen-18

Groups	Count	Sum	Average	Variance
BH	17	-37.96	-2.23	0.27
HDW	5	-6.16	-1.23	1.03
SP	7	-12.22	-1.75	0.10
RI	7	-4.13	-0.59	1.62

Source of Variation	SS	DF	MS	F	P-value	F-critical
Between Groups	14.55	3	4.85	8.25	0.0003	2.90
Within Groups	18.80	32	0.59			
Total	33.35	35				

NB. SS is sum of square, DF (degrees of freedom), MS (mean of square), F (factor of the total deviation) and P (probability).

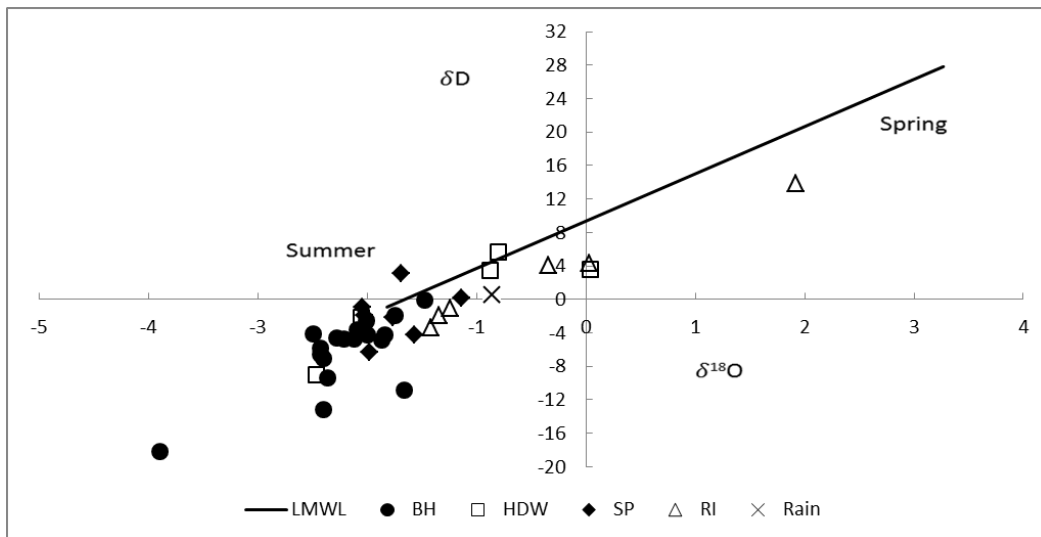


Figure 31: Plot of different water resource against LMWL using isotopes of deuterium versus oxygen-18

The result indicates that all the isotopes from boreholes (BH), hand-dug wells (HDW), river (RI) and springs (SP) fall below the local meteoric water line and have lower D-excess than the LMWL. Except borehole (BHMM1) from Upper Geba, hand-dug wells (HDWA1 and HDWAF1) from Aynalem and springs (SPIL1, SPCH1 and SPM1) from Ilala, Chelekot and Upper Geba sub-basins fall above the LMWL and have higher D-excess than LMWL. The composition of the water resources plotted below the

meteoric water line are subjected to secondary processes of evaporation prior to infiltration / isotopes exchange with aquifer rocks, (Mazor, 1991). In addition, difference in altitude, temperature and amount of rainfall play a major role in controlling the isotopic composition of the water resources. Hence, the groundwater composition from most boreholes (BH) in the study area were plotted below the local meteoric water line (Figure 31) and have lower D-excess, indicating there was a secondary fractionation by evaporation prior to infiltration or presence of ancient water that originated in deferent climatic regime (Mazor, 1991). However, they show depletion in both deuterium and oxygen-18 compared to VSMOW, which ranges between -18.19‰ and -0.08‰ for δD and -3.9‰ and -1.48‰ with variance of 0.27 for $\delta^{18}O$ due to fractionation effect. The isotopes from hand-dug wells that are plotted below the LMWL have lower D-excess than the local rainfall, implying the hand-dug wells are subjected to secondary process of evaporation before reaching the surface resulting enrichment of oxygen-18. However, the hand-dug wells show a depletion in oxygen-18 compared to VSMOW which range from -2.47 to -0.8‰ and variance of 1.03 except hand-dug well (HDWMM1) showing both Deuterium and Oxygen-18 enrichment (Appendix-7). Similarly, the springs from all sub-basins show depletion in both deuterium and oxygen-18 compare to VSMOW, which ranges from -6.33 to -0.91‰ for δD and from -2.05 to -1.14‰ and variance of 0.1 for $\delta^{18}O$. However, the springs from Aynalem (MKB 011/GWS) and Ilala (SPIL1) sub-basins are enriched in deuterium with a value of 0.2‰ and 3.08‰ respectively compared to VSMOW (Appendix-7). All the water samples from the rivers in the sub-basins show relatively higher variance (1.62) and a depletion of both deuterium and oxygen-18, while the water sample from Aynalem River (RIA1 and MKB 012/SRE) show enrichment in both Deuterium and oxygen-18. The water sample from Ilala River shows enrichment in Deuterium. The rivers have lower D-excess and were plotted below LMWL, implying the effect of secondary fractionation by evaporation during the flow of water from the upper to the lower part of the sub-basins in the study area. The result also show that the isotopic signature of a single rainfall sample from the study area has lower D-excess compared to the LMWL of KOBO, indicating the rainfall from the study area is subjected to secondary fractionation than the rainfall from KOBO station or it may be due to the time difference of between the rainfall data. The rainfall for the study area shows enrichment in Deuterium but depletion in Oxygen-18 when compared to VSMOW (Table 23, Appendix-7 and Figure 31).

The negative relationships between D-Excess and $\delta^{18}O$ shows the water resources are subjected to secondary evaporation prior to infiltration at surface. The degree of evaporation is relatively higher in surface water than groundwater in the study area. However, some of the groundwater from boreholes shows lower D-Excess than the groundwater from hand-dug wells, springs and rivers water. This is due to isotopic exchange with aquifers or presence of ancient water that originated in deferent climatic regime (Figure 32). Moreover, the groundwater from boreholes, hand-dug wells and springs show similar isotopic signature with the local rainfall from KOBO, indicating that the origin of groundwater from the boreholes, hand-dug wells and springs are local rainfall during main rainy season (Figure 31). Since the study area fall in the arid to semi-arid region, the rainfall is very low and has limited surface water. However, the perianal rivers observed in the study area during dry season are from the springs emerged as sub-surface and base flow from shallow and deep groundwater due to geological, structural and geomorphological changes.

Moreover, the result of analysis of variance (ANOVA) for single factor of oxygen-18 among different water resources indicated that the F-test (factors of the total deviation) value which is 8.25 is greater than F-critical (the number that the test statistic must exceeds to reject the test) which is 2.90. The result is significant at 5% significance level and it can be conclude that the values for the stable isotope oxygen-18 among the water resources differ (Table 24).

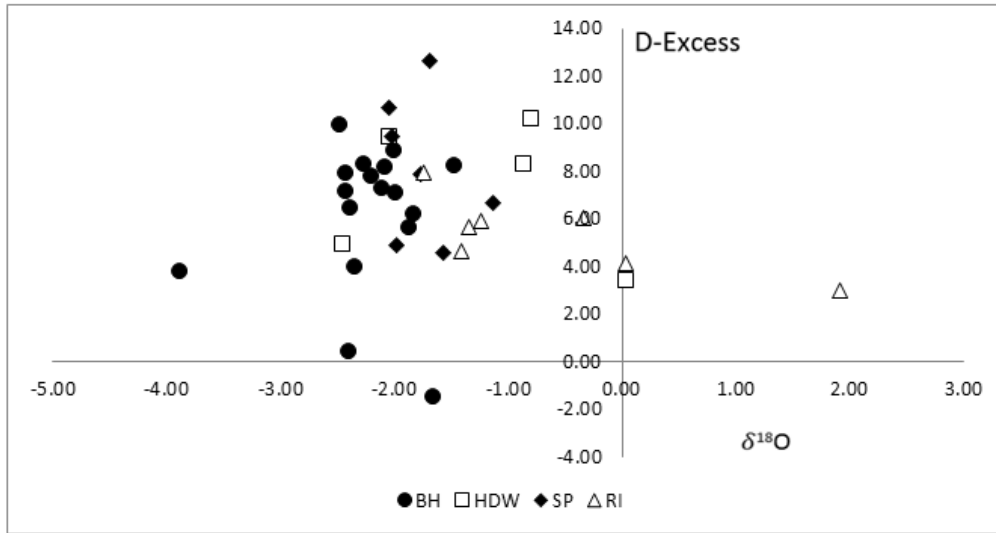


Figure 32: Evaporation trends for surface and groundwater samples in the study area

6.8. Mixing of Water Among Different Resources

A linear relationship between major ions with TDS indicates either mixing of water from different resources or the water resources have the same major ion sources (Mazor, 1991). Based on this analogy, the linear correlation between calcium and TDS and magnesium and TDS show mixing of water between boreholes, hand-dug wells, springs and rivers (Figure 21 A and B). However, the correlations of sodium, chloride, bicarbonate and sulphate ions with TDS showed clustering in two groups of rivers with springs, and boreholes with hand-dug wells rather than linear relation. This indicates the ions for the groups have different sources.

Even though the isotopic signature of the water samples from the rivers show heavy (positive) isotopes composition as compared to boreholes, hand-dug wells and springs water at dry season, the linear correlation among the water resources such as boreholes, hand-dug wells, springs and rivers indicate different water mixing. For instance springs and hand-dug wells water from boreholes and rivers water, and spring water from boreholes and hand-dug wells water show mixing in the study area (Figure 33).

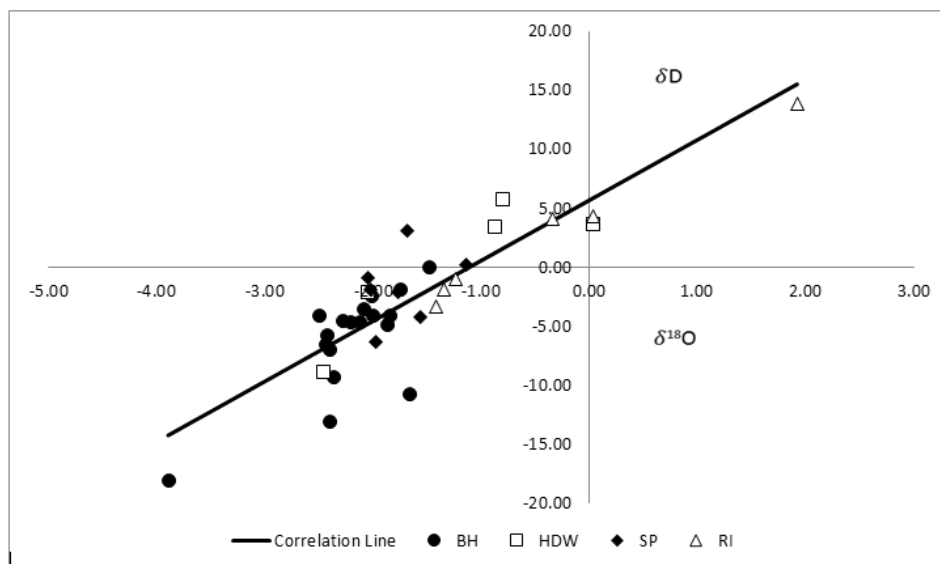


Figure 33: Linear correlation of stable isotopes of hydrogen and oxygen for different water resources in Mekelle region

6.9. Water Quality Assessment Evaluation (Criteria Testing)

Water sample parameters are analyzed in a laboratory and at the field but some parameters are determined including temperature, conductivity, alkalinity, dissolved oxygen, pH, cations and anions, hardness, TDS, sodium adsorption ratio and aggressive and corrosive index. These parameters were used to evaluate the suitability of the water for drinking, irrigation and pipe lines and construction materials purposes.

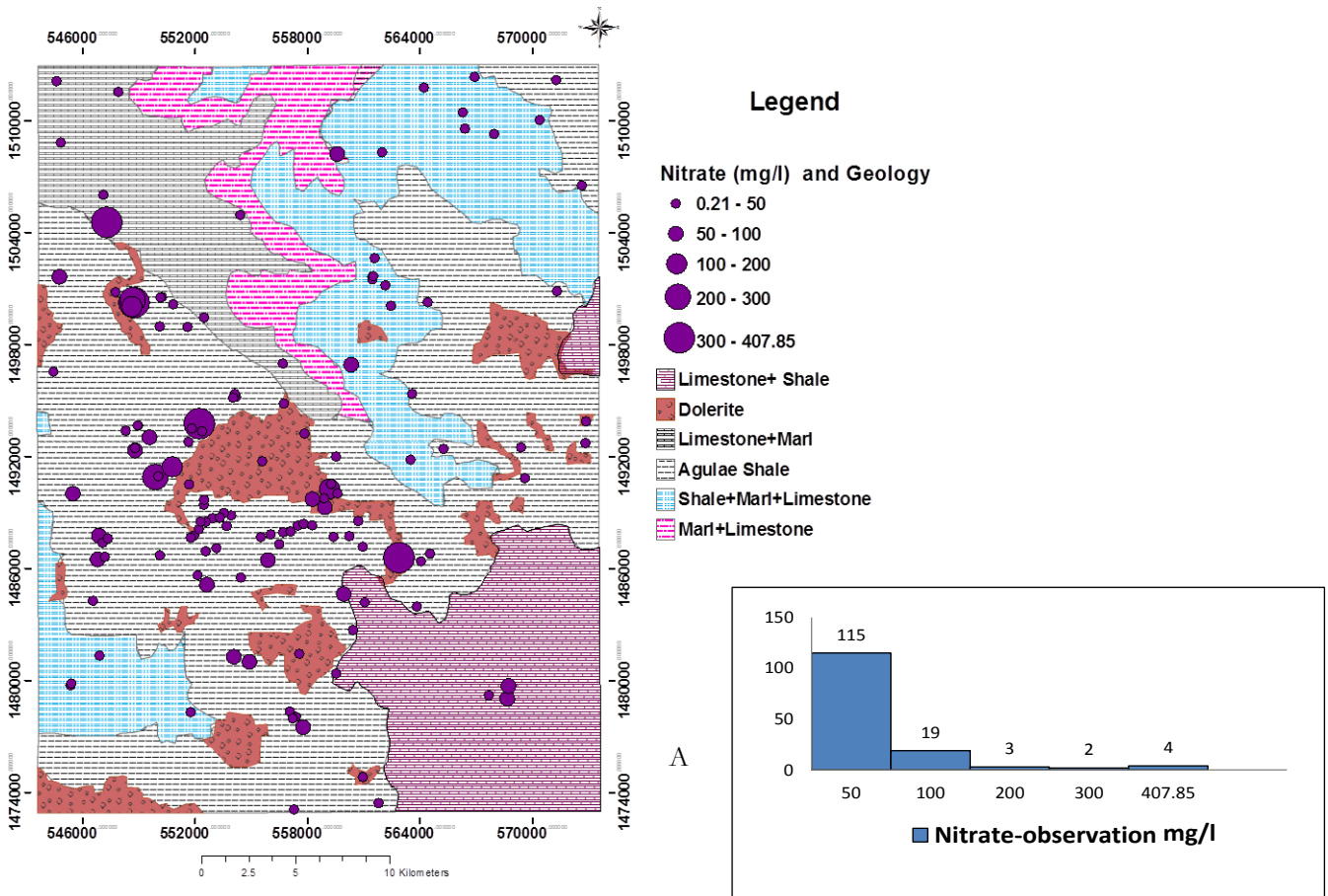
6.9.1. Domestic Use

To assess the quality of water for domestic use is very important due to its direct impact on human welfare. The water to be used for drinking purposes must fulfill the chemical, physical and biological standards of WHO (2011) and Ethiopian standards published on Negarit Gazeta No. 12/1990 and Guidelines of Ministry of Water Resource (MoWR, 2002) as cited in (Addisu, 2012; Yonas, 2009).

Most of the water resource samples from springs, hand-dug wells, boreholes, rivers and tap waters fulfill the physical properties such as colorless, odorless, tasteless and pH except one river sample from Aynalem sub-basin with a pH 9.15 due to spills and waste disposals from the Aynalem village (Figure 14 and Appendix-2 A) and the temperature ranges from 19.8 to 27°C. In contrast to this, many of the water samples have chemical parameters exceeding both the WHO and Ethiopian standards (Table 25). Especially, for sulphate ion sixty (60) water samples exceed the WHO standard, which is mainly due to dissolution of Gypsum layer intercalating with Agulae shale formation (Tewolde, 2012). Similarly, 55 and 118 samples exceed the WHO standard for TDS and hardness respectively due to high concentration of sulphate ion in the water sample. Moreover, 63 water samples exceed the Ethiopian standards for Ca^{2+} due to high dissolution of calcite minerals, which is the main contributor to water hardness. Six water samples from BHA1, BHIL1, BHIL3, BHIL5, BHCH1 and BHCH2 exceed both standards for iron, which promotes growth of iron bacteria, and results in deposit a slimy coating on piping and stains laundry and plumber fixtures (WHO, 2011). A significant number of water samples for nitrate ion exceed both standards. This could be due to soil leaching and anthropogenic effects, such as:- mixing of irrigation chemicals, sewage and animal wastes to the water resources (Chapman, 1996). The concentration of nitrate above the standards found at the lower and central parts of upper Geba, Ilala and Aynalem sub basins, at upper part of Aynalem and central part of Chelekot sub basins of the study area, mainly at urban land-use and on shale, limestone + shale, shale + marl + limestone and dolerite formations (Figure 34 A and B, Appendix-2 D). The result further indicates that the turbidity ranges from 0.35 to 76.8 NTU and 14 samples exceed the WHO standards which may be caused by suspended particles and colloidal matter and results in obstructs light transmission. Microorganisms (bacteria, viruses, protozoa) are typically attached to particulates. Thus, removal of turbidity by filtration can significantly reduce microbial contamination in treated water (WHO, 2011). Generally, the result indicated that a significant number of water resources in study area are saline and hard. This in turn results in precipitation, deposition or encrustation of calcium carbonate in water supply pipe lines, boilers and heaters. Moreover, it increases boiling point of the water, low lather formation with soaps and precipitation of soap scum and consumes excess soap to cleaning (WHO, 2011)(Appendix- 8).

Table 25: Study area parameters comparisons with guidelines of WHO (2011) and Ethiopian standards.

Parameters	WHO Standards	Ethiopia Standards	Range	Mekelle region	
				WHO	Ethiopia Standards
Turbidity	5	-	0.35 - 78.6	14	
TDS	1000	1500	289 - 3454	55	19
pH	6.5 - 8.5	6.5 - 8.5	6.74 - 9.15	1	1
Na ⁺	200	358	5.39 - 260	3	0
Fe ²⁺	0.3	0.4	-0.11 - 9.87	6	6
F ⁻	1.5	3	0.04 - 1.2	0	0
Cl ⁻	250	533	1.7 - 557.5	2	0
NO ₃ ⁻	50	50	0.21 - 407.85	27	27
SO ₄ ²⁻	250	483	11.6 - 1607	60	27
NH ₄ ⁺	1.5	-	0 - 10.076	3	
CaCO ₃ ⁻ (TH)	300	500	111.93 - 2050	118	47
Mn ²⁺	0.1	0.5	-0.08 - 0.36	3	0
Mg ²⁺		150	1.9 - 120		0
Ca ²⁺		200	37.54 - 631.8		63



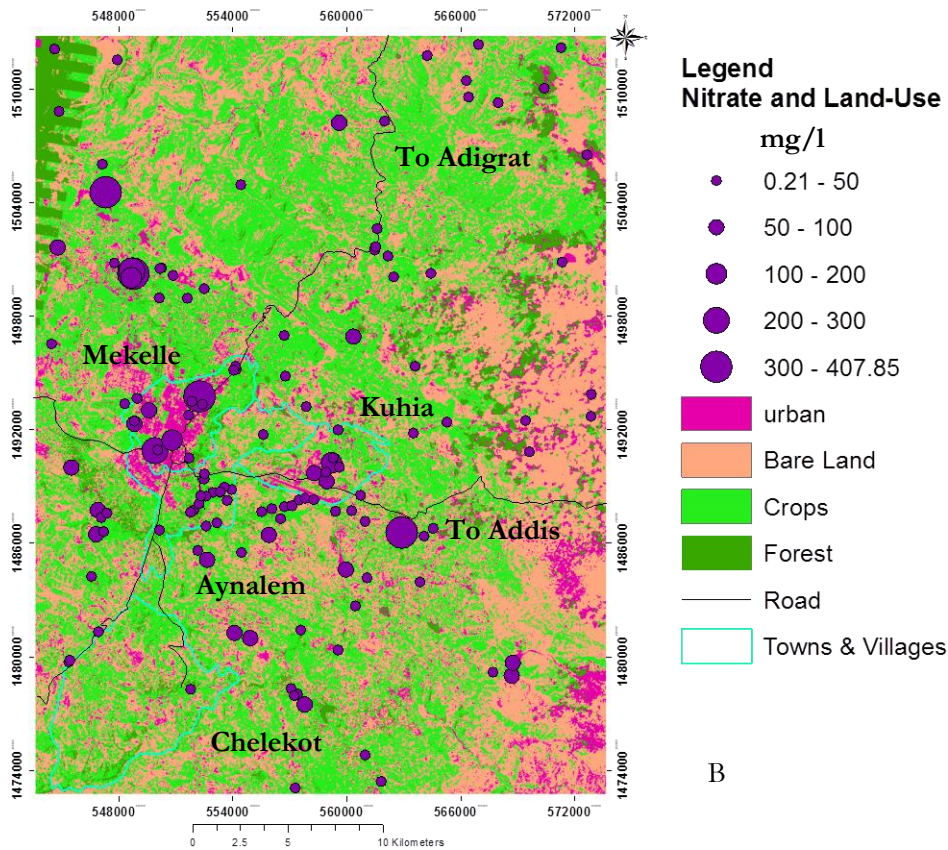


Figure 34: Distribution of Nitrate with Geology (A) and Land-use (B) in the study area

6.9.2. Irrigation Use

Based on the methodology of salinity hazard and sodium hazard of Wilcox diagram, all the water samples from Mekelle region are plotted on low sodium (alkalinity) hazard water (S1) indicating good for irrigation (Figure 37A & B, and Appendix-2 E). The result further indicates that most of the water samples in study area plotted on high and very high salinity hazard water of C3 and C4 respectively (Figure 35). Especially water samples from upper Geba (Agulae) sub-basin such as springs (SPE2, and SPK1), boreholes (SW1, SWK1, SWO1 and SWK3) and hand-dug well (HDWMM2), and borehole (BHIL5) and spring (SPA2) from Ilala and Aynalem sub-basins are unsatisfactory for irrigation. These water resources are located within urban and agricultural land-use and there is high dissolution of Gypsum which is intercalated with shale, limestone and marl and anthropogenic effects (Figure 16 and Appendix-2B). Generally, water sample from hand-dug well (HDWCH1) located at Chelekot sub-basin fall in category C1S1, indicating low salinity and alkali water. Similarly, 11% of the water samples from boreholes (BH-4, BH-15, BH-32, BH-48, BH-59 and BH-64), springs (SP01 and SP-4), hand-dug well (HDWAF1) and river (RIA1) located at Aynalem sub basin, borehole (BH-84) and springs (SP-24 and SP-25) from Ilala sub-basin and borehole (SW-45 and SW-49) and spring (SP-8) from upper Geba (Agulae) sub-basin fall at category C2S1. This indicates medium salinity and low alkalinity water and can be used for irrigation in all types of soil. However, 89% of the water samples fall within the categories of C3S1 and C4S1, indicating high and very high salinity and low alkalinity water. As a result, high salinity and low alkalinity water cannot be used with soils having restricted drainage. According to A. Singh et al. (2012), the presence of salt in water affects the soil permeability, structure, and aeration that indirectly affect the plant growth. Thus, it needs special management for salinity control including planting of salt tolerant crops and applying excess irrigation water to provide considerable leaching.

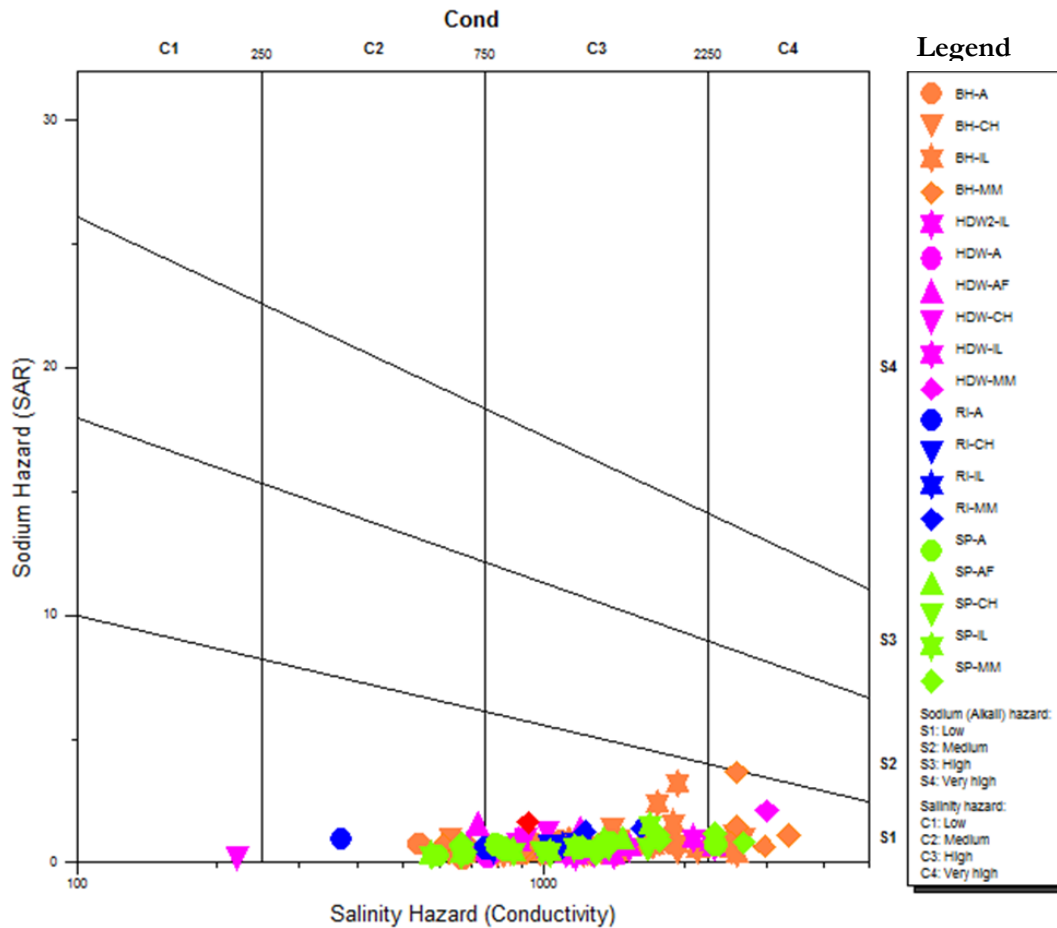


Figure 35: Wilcox diagram of Sodium Adsorption ratio (Sodium Hazard) versus Salinity Hazard of Mekelle region.

6.9.3. Implication of Groundwater Problems in Pipe Lines and Engineering Works

As discussed in the methodology the Larson and Langelier Indices were used to determine the corrosive and aggressive character of the water resources. Based on Larson index calculation, out of the 143 observations about 119 or 83 % (46.2 % boreholes, 13.2 % Hand dug wells, 16 % springs, 5.6 % rivers and 2% tap water) observations have LI above 0.5 (Table 26 and Figure 36 A). This indicates corrosive character of water for iron, pipe lines and foundation materials (Singley et al., 1985). High values were observed from observations located at limestone and shale formations and the effect is seen practically on the field where distribution lines and irons for construction are damaged (Berhane et al., 2013) (Appendix-8). Moreover, the Langelier Index was used to study the aggressive or corrosive character of water based on saturation with respect to calcite mineral. Accordingly, the result indicate that all water samples from boreholes, hand dug wells, springs, rivers and tap water show a positive index values that is likely precipitation of calcite (Table 26 and Figure 36 B). This indicates less aggressive character to corrode the pipes through which it passes (Hounslow, 1995). Generally the corrosive characteristics of the water lead to rusty water, tuberculation and lose in carrying capacity of materials. Moreover, corrosion products cause retarding of heat transfer for heating and cooling (Larson, 1975).

Table 26: Summarized values of LSI and LI for water resources in the study area

Type	Langelier Index			Larson Index		
	Maximum	Minimum	Mean	Maximum	Minimum	Mean
BH	3.04	1.68	2.83	12.84	0.09	3.09
HDW	3.16	2.27	2.87	17.88	0.15	2.70
SP	2.99	2.63	2.83	8.18	0.10	2.04
RI	2.90	2.16	2.69	6.52	0.61	2.60
Tap	2.87	2.84	2.85	4.60	4.12	4.28

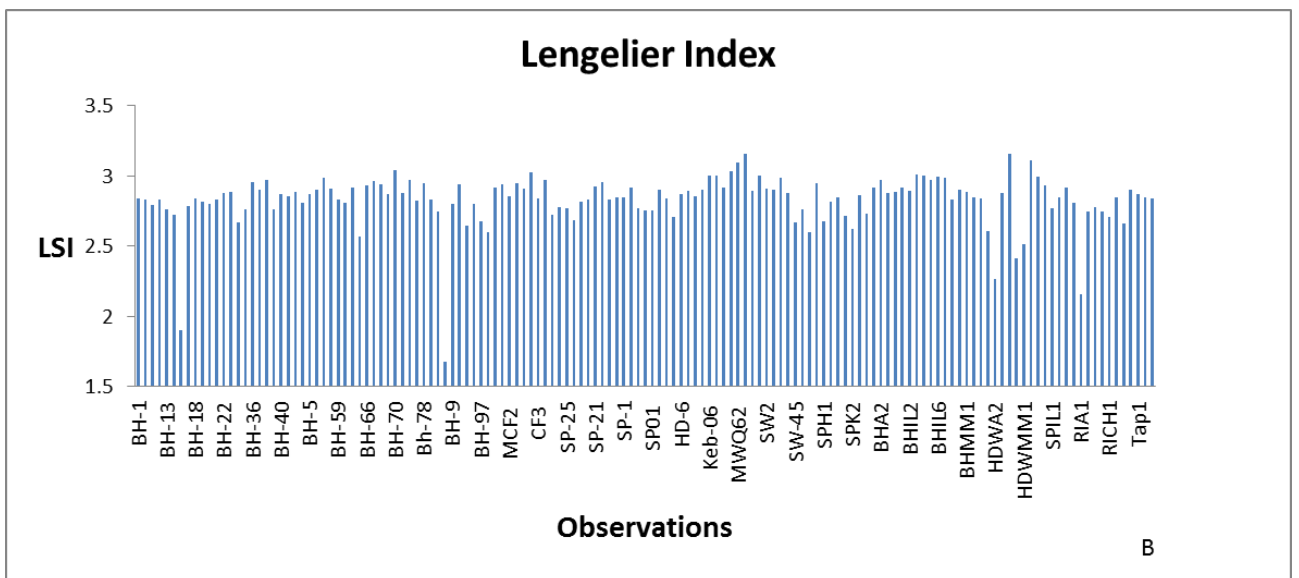
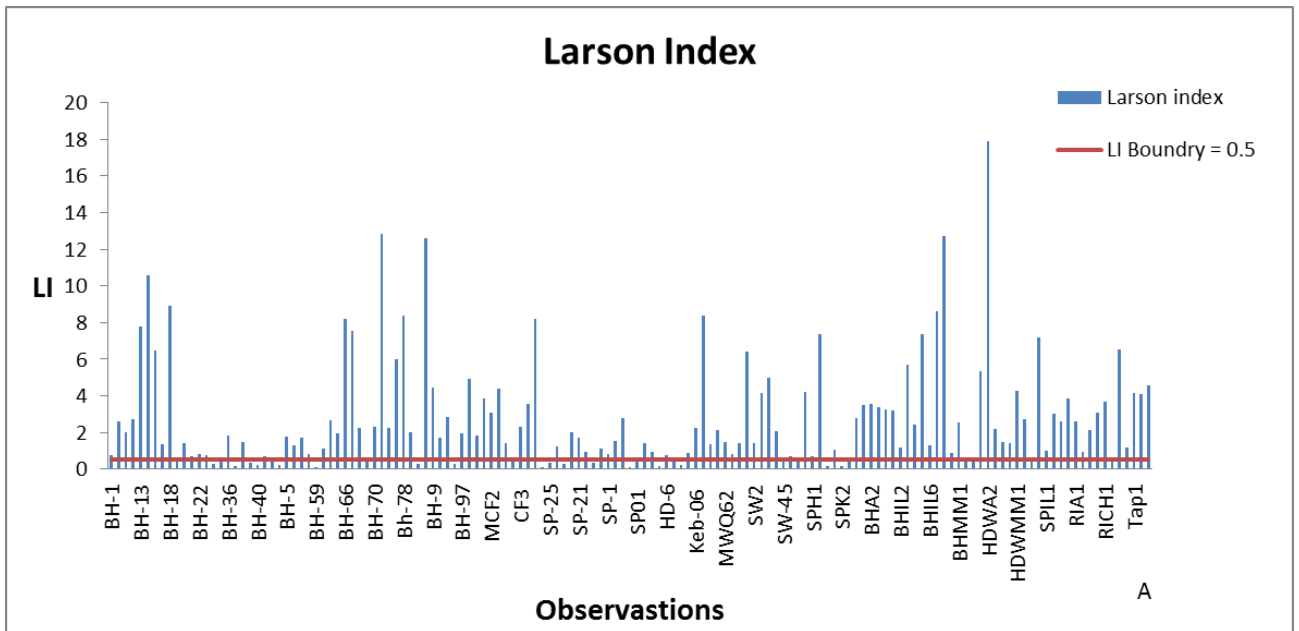


Figure 36: Plots of Larson index (A) for corrosive and Langelier Index (B) for aggressive characteristics of observations

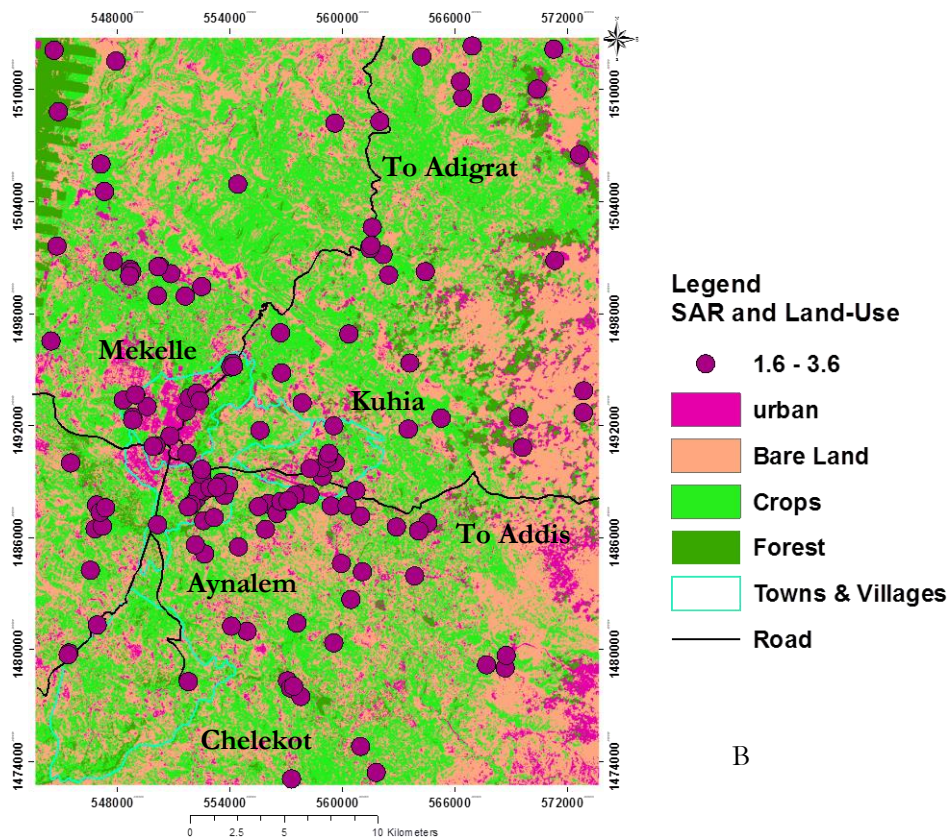
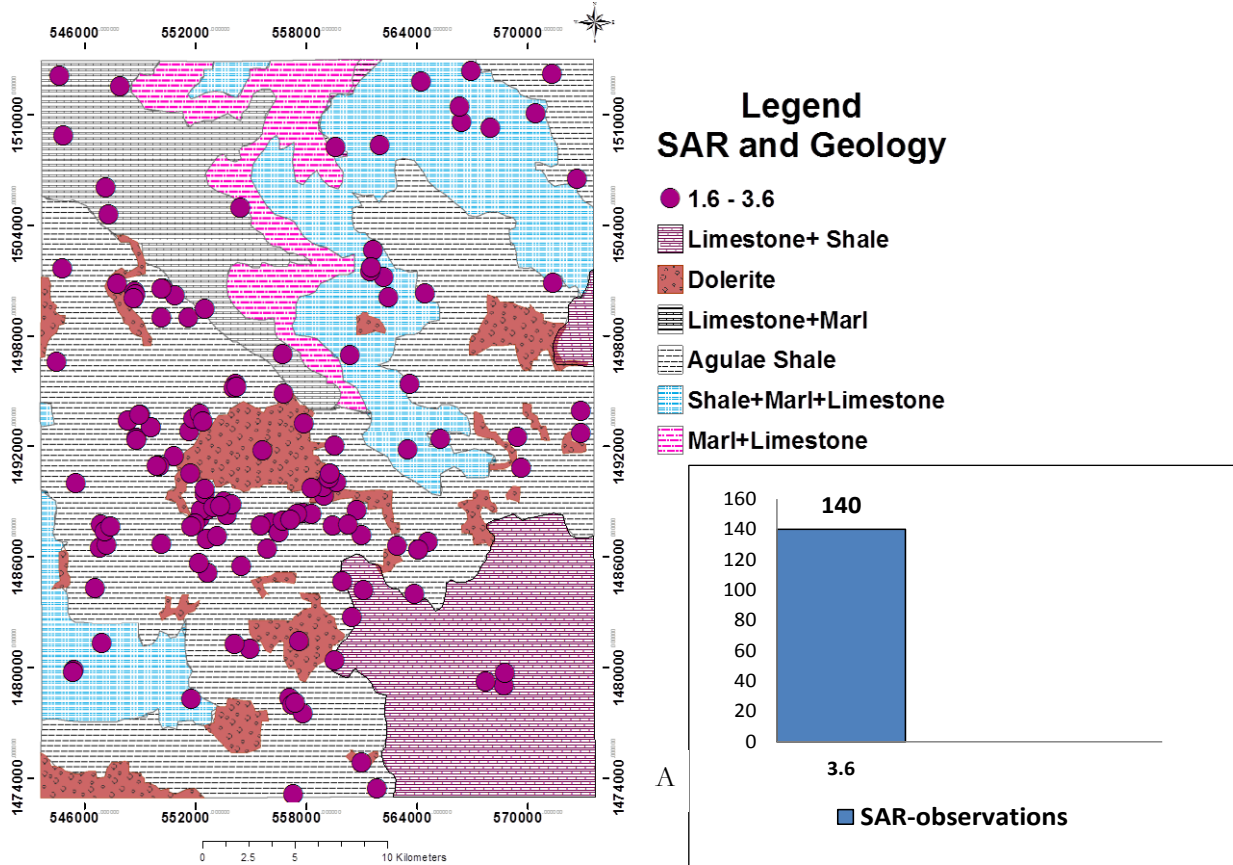


Figure 37: Sodium Adsorption Ratio map with Geology (A) and Land-use (B) in the study area

7. CONCLUSION AND RECOMMENDATION

7.1. Conclusions

The demand of water for domestic and irrigation purpose is growing very fast and is causing over-pumping of the water resources in the study area. As a result, water quality issues like groundwater salinity is a major concern for water resources development projects (irrigation, floriculture) as well as for human health (drinking water supply). This study attempted to examine water use problems related to water quality, hydrogeochemical processes and evolutions, origins and mixing of water resources in Mekelle region, Northern Ethiopia (Tigray). Hydrogeochemical (PHREEQC) and Aquachem modelling combined with stable water isotopes fractionation and geospatial data analysis were used as a methodological approach in the assessment. The main findings of the research can be summarized as follows:

- Data analysis and hydrochemical water typing
 - The AQUACHEM database constructed of the secondary and primary datasets permitted to verify the reliability of the data and to check possible inaccuracies. Most of the samples data passed the quality control tests are were permitted for further analysis using classic hydrochemical plotting and multivariate analysis techniques.
 - The study indicates that Ca^{2+} , SO_4^{2-} and HCO_3^- followed by Na^+ , Mg^{2+} , Cl^- , NO_3^- , SiO_2 and with lower levels of K^+ , Al^{3+} , Mn^{2+} , Fe^{2+} and PO_4^{3-} are the dominant dissolved ions in the study area. It is observed that both Ca^{2+} ($R = 0.92$) and SO_4^{2-} ($R = 0.88$) are linearly correlated with TDS values indicating as the primary salinity contributors for groundwater.
 - A HCA analysis was used to see whether different grouping and associations between water resources and points existed. Five distinct water types were found, illustrating an evolution of Ca- HCO_3 based waters towards Ca- SO_4 dominated and higher salinity waters (higher EC and TDS).
 - The HCA indicated one interesting small group (SG5) with a distinct and most probably contamination signature, with distinctly higher sodium, chloride and nitrate concentrations. This is an interesting finding for environmental control, as a well conducted HCA permits to pinpoint to contaminated areas and water points.
 - Limestone, Dolomite and Gypsum are found to be the main Source-rocks to explain the ion composition in the water resources. It is mainly due to carbonate weathering and dissolution of evaporite Gypsum. Anthropogenic processes also play a major role in the study area.
- Hydrogeochemistry, chemical evolution and processes
 - A critical analysis of the chemical element speciation and concentrations in the ground waters, the mineral saturation indices, in combination with the inverse model results, indicate that the $\text{CO}_2(g)$ dissolution, outgassing, plays probably an important role in the chemical kinetics of the calcification reactions (precipitation of calcite or aragonite and dolomite) and the dissolution kinetic of gypsum and anhydrite in the aquifer, wells and spring waters. Most waters samples as

well as reaction mechanisms deciphered with inverse modelling suggest a coupled calcite precipitation – gypsum dissolution kinetic governed by the TIC (total inorganic carbon) and dissolved CO_2 (g) and bicarbonate in the aqueous system. The unequal reaction kinetics of the removal of Ca (and Mg) with bicarbonate out of solution by chemical precipitation and the dissolution of gypsum (adding Ca and sulfate) to the solution can explain the non-equilibrium S.I observed in almost all sample points.

- Also the inverse model tends to point in the same direction, whereby Ca- HCO_3 dominated water (in possible recharge areas) undergoes an evolution to Ca-sulfate-bicarbonate type waters, with significant higher TDS loadings. In inverse models 2 and 4, we observe a loss of water (evaporation, pumping) whereas in inverse models 1 and 3 suggest some kind of recharge (adding of water or refreshing), even if the total TDS increases along the pathway due to appearance of gypsum in the system.
- Use of water isotope
- The isotope analysis was based on a set of existing isotope data (2002) and a limited set of 24 own analysis data representing Sep, 2013 conditions. Also rainfall isotope data were available for one year of a location some 150 km south of the study area, but also at a similar highland elevation. The rainfall isotope datasets shows the seasonal variations and differences in rainfall origins at the beginning, middle and end of the summer monsoon rain season, originating from the ITCZ (Intertropical Convergence Zone migrations across these latitudes).
 - It is also observed that the water resources in the study area show depletion in Oxygen-18 comparing to VSMOW. These water resources have lower deuterium excess than the local rainfall of KOBO due to fractionation by secondary evaporation, resulting in enrichment of oxygen-18. Besides, the result reveals that the water resources have a similar isotopic signature to the rainfall during summer season, indicating that the origin of the water resources is mainly rainfall. Based on the linear relationship of major ions with TDS and isotopic signature of the water resources, it can be concluded that there is a mixing of borehole and river water that can be observed in hand-dug well and spring water in the study area.
- Water quality assessment
- The waters around Mekelle distinctly show a very high hardness, and moreover sulfate (or permanent hardness). Although these waters are not immediately a high health risk, they provoke problems in water distribution systems and industrial water uses. A combination of sulfate with chlorides leads to high corrosive waters and damaging water distribution systems (pipes).
 - The waters show a high salinity for irrigation and many samples classify in the C3 (high) conductivity class. The sodium hazard is however low and pH and chloride levels are low to moderate. Therefore, these waters can be used for irrigation on course to medium textured soils, when large amounts are used and leaching requirements are respected and drainage conditions are present. If not enough water is available or applied, rapid damage to the soils (salinization) can be expected. Of course, leached waters will eventually increase the shallow groundwater salinity and deteriorate the quality.

7.2. Recommendations

In order to improve the above-mentioned problems in the study area, the following are recommend as major areas for intervention.

- Water softening: Mixing the hard with less hard and soft water could be done in the north-west of study area located at sandstone formation can help to reduce the hardness of water for domestic use in the study area. More expensive techniques such as RO are possible for e.g. industrial and or drinking waters. It reduces calcite precipitation and encrustation in pipelines, heaters and boilers.
- It is observed that many of the water points are located within urban and agricultural land-use. Hence, it is recommended to delineate a well field area and include in the master plan of the towns and land-use management plan of villages. This will helps to avoid anthropogenic effects.
- It is observed that irrigation practice within a small farm land and drinking water supply using groundwater mainly from private hand-dug wells and shallow boreholes causes over-pumping, evaporation and anthropogenic pollution of shallow groundwater. Hence, it is suggested to use communal hand-dug wells and motorized deep boreholes and construction of artificial recharge structures.
- Similarly, a special management including planting of salt tolerant crops and applying excess irrigation water that provides considerable leaching should be used to control the salinity problem for irrigation needs.

➤ Future Studies

- It can be recommended to further use the stable water isotopes ratio of oxygen and hydrogen combined with stable isotopes of carbon in monitoring and hydrogeochemical modelling of the water resources in the study area.
- The study area is covered by different geological formation therefore detailed mineral and chemical composition of the rocks is recommended as the weathering product of these rocks form an important contribution to the water quality of the water resources in the study area.
- The study area is located near to the north Rift Valley of Ethiopia. Moreover, minor joints and faults are extended almost perpendicularly from the Rift Valley into the study area. It is therefore recommended to carryout similar study for the whole Mekelle outlier and compare with water quality parameters of Rift Valley. This will help to understand the groundwater interconnection and interaction that may cause additional source for high salinity observed in the study area.

LIST OF REFERENCES

- Addisu, D. (2012). Hydrogeochemical and isotope hydrology in investigating groundwater recharge and flow processes; lower Afar, Eastern Ethiopia Retrieved 10/20, 2013
- Allison, L., Brown, J., Hayward, H., et al. (Eds.). (1954). *Diagnosis and improvement of saline and alkali soils*. United State, Washington D.C: U. S. Government Printing Office.
- APHA, AWWA, & WEF. (1992). *Standard methods for the examination of water and waste water* (18th ed.): A-merican Public Health Association, Washington, DC
- Appelo, C. A. J., & Postma. (1993). *Geochemistry, Groundwater and Pollution*. Rotterdam, Netherlands: A.A.BALKEMA.
- Barcelona, M. J., Gibb, J. P., Helfrich, J. A., et al. (1985). Practical guide for ground-water sampling (E. a. N. Resources, Trans.) (pp. 103): Illinois State Water Survey.
- Berhane, G., Abera, T., & Gebreselassie, S. (2013). Implications of groundwater quality to corrosion problem and urban planning in Mekelle area, Northern Ethiopia. *Momona Ethiopian Journal of Science*, 5(1), 51-70.
- Bricker, O. P. (1999). An overview of the factors involved in evaluating the geochemical effects of highway runoff on the environment.
- Carol, E., Kruse, E., & Mas-Pla, J. (2009). Hydrochemical and isotopical evidence of ground water salinization processes on the coastal plain of Samborombón Bay, Argentina. *Journal of Hydrology*, 365(3–4), 335-345. doi: <http://dx.doi.org/10.1016/j.jhydrol.2008.11.041>
- Chapman, D. (1996). *Water Quality Assessments* (second ed.). London and New York: E & FN SPON.
- Cloutier, V., Lefebvre, R., Therrien, R., et al. (2008). Multivariate statistical analysis of geochemical data as indicative of the hydrogeochemical evolution of groundwater in a sedimentary rock aquifer system. *Journal of Hydrology*, 353(3–4), 294-313. doi: <http://dx.doi.org/10.1016/j.jhydrol.2008.02.015>
- Demlie, M., Wohnlich, S., & Ayenew, T. (2008). Major ion hydrochemistry and environmental isotope signatures as a tool in assessing groundwater occurrence and its dynamics in a fractured volcanic aquifer system located within a heavily urbanized catchment, central Ethiopia. *Journal of Hydrology*, 353(1–2), 175-188. doi: <http://dx.doi.org/10.1016/j.jhydrol.2008.02.009>
- Federico, C., Pizzino, L., Cinti, D., et al. (2008). Inverse and forward modelling of groundwater circulation in a seismically active area (Monferrato, Piedmont, NW Italy): Insights into stress-induced variations in water chemistry. *Chemical Geology*, 248(1–2), 14-39. doi: <http://dx.doi.org/10.1016/j.chemgeo.2007.10.007>
- Fetter, C. (2001). Applied hydrogeology+ Visual Modflow, Flownet and Aqtesolv student version software on CD-ROM: Prentice Hall, Upper Saddle River.
- Freeze, R. A., & Cherry, J. A. (1980). Groundwater : Englewood Cliffs, NJ: Prentice-Hall, 1979, 604P Freeze R.A., Cherry J.A. *International Journal of Rock Mechanics and Mining Sciences & Geomechanics Abstracts*, 17(6), A111. doi: [http://dx.doi.org/10.1016/0148-9062\(80\)90606-3](http://dx.doi.org/10.1016/0148-9062(80)90606-3)
- Gebregziabher, B. (2003). Integrated geophysical methods to investigate the geological structures and hydrostratigraphic unit of the Aynalem area, Southeast Mekelle. *Unpublished Msc thesis AAU*.
- Gebreyohannes, T., De Smedt, F., Hagos, M., et al. (2010). Large-scale geological mapping of the Geba basin, northern Ethiopia. *Tigray Livelihood Papers*, 9.
- Güler, C., Thyne, G., McCray, J., et al. (2002). Evaluation of graphical and multivariate statistical methods for classification of water chemistry data. *Hydrogeology Journal*, 10(4), 455-474. doi: 10.1007/s10040-002-0196-6
- Hem, J. D. (1985). Study and interpretation of the chemical characteristics of natural water Retrieved 6-1-2013, from <http://pubs.er.usgs.gov/publication/wsp2254>
- Hidalgo, M. C., & Cruz-Sanjulián, J. (2001). Groundwater composition, hydrochemical evolution and mass transfer in a regional detrital aquifer (Baza basin, southern Spain). *Applied Geochemistry*, 16(7–8), 745-758. doi: [http://dx.doi.org/10.1016/S0883-2927\(00\)00078-0](http://dx.doi.org/10.1016/S0883-2927(00)00078-0)

- Hounslow, A. W. (1995). *Water quality data; analysis and interpretation*. Unites States of America: LEWIS.
- Iliopoulos, V., Stamatis, G., & Stournaras, G. (2011). Marine and human activity effects on the groundwater quality of Thriassio Plain, Attica, Greece. [Advances in the Research of Aquatic Environment]. *Environmental Earth Sciences*, 409-419.
- Jeong, C. H. (2001). Effect of land use and urbanization on hydrochemistry and contamination of groundwater from Taejon area, Korea. *Journal of Hydrology*, 253(1-4), 194-210. doi: [http://dx.doi.org/10.1016/S0022-1694\(01\)00481-4](http://dx.doi.org/10.1016/S0022-1694(01)00481-4)
- Kahsay, G. H. (2008). Groundwater resources assessment through distributed steady state flow modeling, Anylam Wellfield (mekele, Ethiopia) M. Sc Thesis. *International Institute for Geo-Information and Earth Observation, Enschede Netherlands*, 45-50.
- Kebede, S., Travi, Y., Alemayehu, T., et al. (2005). Groundwater recharge, circulation and geochemical evolution in the source region of the Blue Nile River, Ethiopia. *Applied Geochemistry*, 20(9), 1658-1676. doi: <http://dx.doi.org/10.1016/j.apgeochem.2005.04.016>
- Krishnaraj, S., Murugesan, V., K, V., et al. (2011). Use of Hydrochemistry and Stable Isotopes as Tools for Groundwater Evolution and Contamination Investigations. *Geosciences*, vol. 1, 16-25. doi: 10.5923/j.geo.20110101.02
- Larson, T. E. (1975). *Corrosion by domestic waters* (Vol. 59): Illinois State Water Survey Urban Bull.
- Larson, T. E., & Skold, R. V. (1957). *Corrosion and tuberculation of cast iron*: State of Illinois, Department of Registration and Education.
- Larson, T. E., & Skold, R. V. (1958). *Laboratory studies relating mineral quality of water to corrosion of steel and cast iron*: State of Illinois, Department of Registration and Education.
- Lawrence, A., Gooddy, D., Kanatharana, P., et al. (2000). Groundwater evolution beneath Hat Yai, a rapidly developing city in Thailand - NERC Open Research Archive Retrieved 6-1-2013, from <http://nora.nerc.ac.uk/7769/>
- Madrid, Y., & Zayas, Z. P. (2007). Water sampling: Traditional methods and new approaches in water sampling strategy. *TrAC Trends in Analytical Chemistry*, 26(4), 293-299. doi: <http://dx.doi.org/10.1016/j.trac.2007.01.002>
- Mazor, E. (1991). *Applied Chemical and Isotopic Groundwater Hydrology*. USA, Canada and Latin America: HALSTED PRESS.
- McNeill, L. S., & Edwards, M. (2001). Review of iron pipe corrosion in drinking water distribution systems. *J. AWWA*, 93(7), 88-100.
- Mook, W. G. (2000). *Environmental Isotopes in the Hydrological Cycle Principles and Applications* (Vol. 1). Vienna: IAEA-UNESCO.
- Nies, H., Newman, B., & Araguas, L. (2011, 27 March - 1 April). *Isotopes in Hydrology, Marine Ecosystems and Climate Change Studies* Monaco.
- Parkhurst, D. L., & Appelo, C. (1999). User's guide to PHREEQC (Version 2): A computer program for speciation, batch-reaction, one-dimensional transport, and inverse geochemical calculations.
- Prasanna, M. V., Chidambaram, S., Gireesh, T. V., et al. (2011). A study on hydrochemical characteristics of surface and sub-surface water in and around Perumal Lake, Cuddalore district, Tamil Nadu, South India. *Environmental Earth Sciences*, 63(1), 31-47. doi: 10.1007/s12665-010-0664-6
- Schlumberger. (2006). AquaChem v.5.1 Demo Tutorial (Version v.5.1). Kitchener, Ontario, Canada: Waterloo Hydrogeologic, Inc.
- Sharp, J. M. (1997). *Ground-water supply issues in urban and urbanizing areas*.
- Singh, A., Mondal, G. C., Singh, T. B., et al. (2012). Hydrogeochemical processes and quality assessment of groundwater in Dumka and Jamtara districts, Jharkhand, India. *Environmental Earth Sciences*, 67(8), 2175-2191. doi: 10.1007/s12665-012-1658-3
- Singh, A. K., Tewary, B., & Sinha, A. (2011). Hydrochemistry and quality assessment of groundwater in part of NOIDA metropolitan city, Uttar Pradesh. *Journal of the Geological Society of India*, 78(6), 523-540.
- Singley, J. E., Beaudet, B., Markey, P., et al. (1985). *Corrosion prevention and control in water treatment and supply systems*: Noyes Publications Park Ridge, NJ.

- Subramani, T., Rajmohan, N., & Elango, L. (2010). Groundwater geochemistry and identification of hydrogeochemical processes in a hard rock region, Southern India. *Environmental Monitoring and Assessment*, 162(1-4), 123-137. doi: 10.1007/s10661-009-0781-4
- Tahir, M., Imam, E., & Hussain, T. (2013). Evaluation of land use/land cover changes in Mekelle City, Ethiopia using Remote Sensing and GIS. *Computational Ecology and Software*, 3(1), 9-16.
- Tewolde, T. G. (2012). Regional groundwater flow modeling of the Geba Basin, Northern Ethiopia | Vrije Universiteit Brussel Retrieved 6-2-2013, from <http://www.vub.ac.be/node/3860>
- V.Kazmin. (1973). Explanation of the Geological Map of Ethiopia (pp. 14): Ministry of Mines, Energy and Water Resources Geological Survey of Ethiopia.
- WHO. (2011). Guidelines for drinking-water quality WHO (Ed.) Retrieved from http://www.who.int/water_sanitation_health/publications/2011/dwq_guidelines/en/
- Wilde, F. D. (2010). Water-quality sampling by the US Geological Survey: standard protocols and procedures. *US Geological Survey Fact Sheet*, 312(2).
- Worash, G., & Valera, R. (2002). Rare earth element geochemistry of the Antalo Supersequence in the Mekele Outlier (Tigray region, northern Ethiopia). *Chemical Geology*, 182(2-4), 395-407. doi: [http://dx.doi.org/10.1016/S0009-2541\(01\)00328-X](http://dx.doi.org/10.1016/S0009-2541(01)00328-X)
- Yidana, S. M. (2010). Groundwater classification using multivariate statistical methods: Southern Ghana. *Journal of African Earth Sciences*, 57(5), 455-469. doi: <http://dx.doi.org/10.1016/j.jafrearsci.2009.12.002>
- Yitbarek, A., Razack, M., Ayenew, T., et al. (2012). Hydrogeological and hydrochemical framework of Upper Awash River basin, Ethiopia: With special emphasis on inter-basins groundwater transfer between Blue Nile and Awash Rivers. *Journal of African Earth Sciences*, 65(0), 46-60. doi: <http://dx.doi.org/10.1016/j.jafrearsci.2012.01.002>
- Yonas, M. (2009). Hydrogeological investigation of Chacha Catchment a volcanic aquifer system, central Ethiopia.
- Zhu, B., Yang, X., Rioual, P., et al. (2011). Hydrogeochemistry of three watersheds (the Erlqis, Zhungarer and Yili) in northern Xinjiang, NW China. *Applied Geochemistry*, 26(8), 1535-1548. doi: <http://dx.doi.org/10.1016/j.apgeochem.2011.06.018>
- Zhu, C. (2002). *Environmental applications of geochemical modeling*: Cambridge: Cambridge University Press.

LIST OF APPENDICES

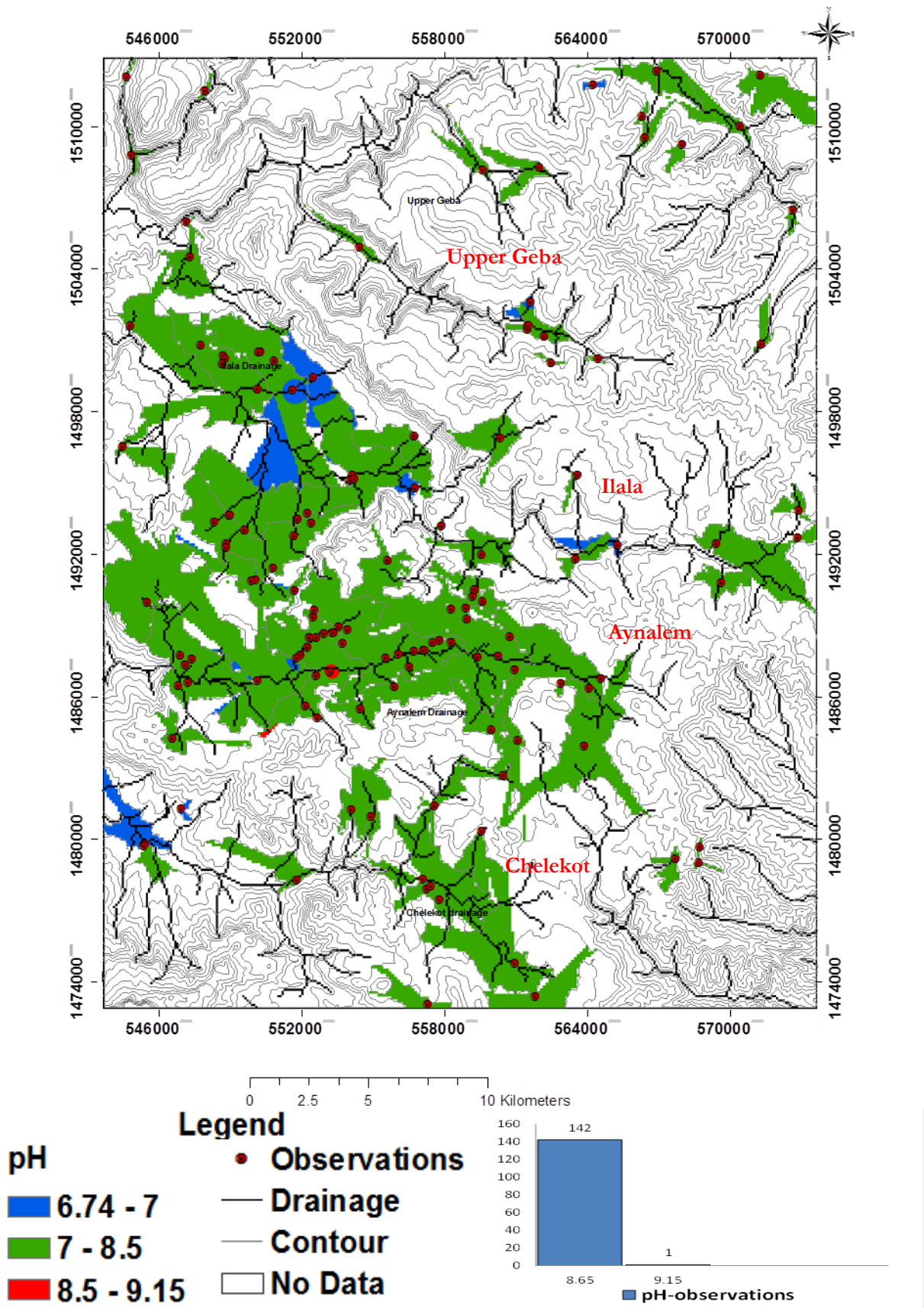
Appendix-1

Duplicated Samples for Quality Control and Assessment

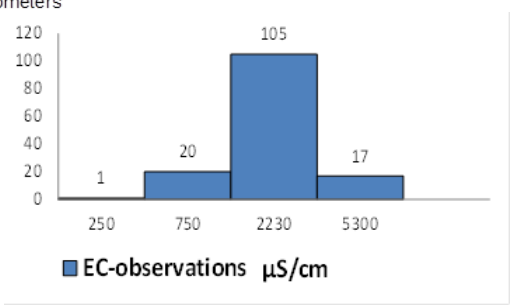
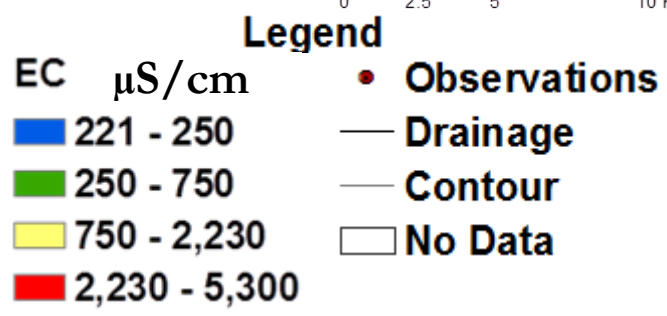
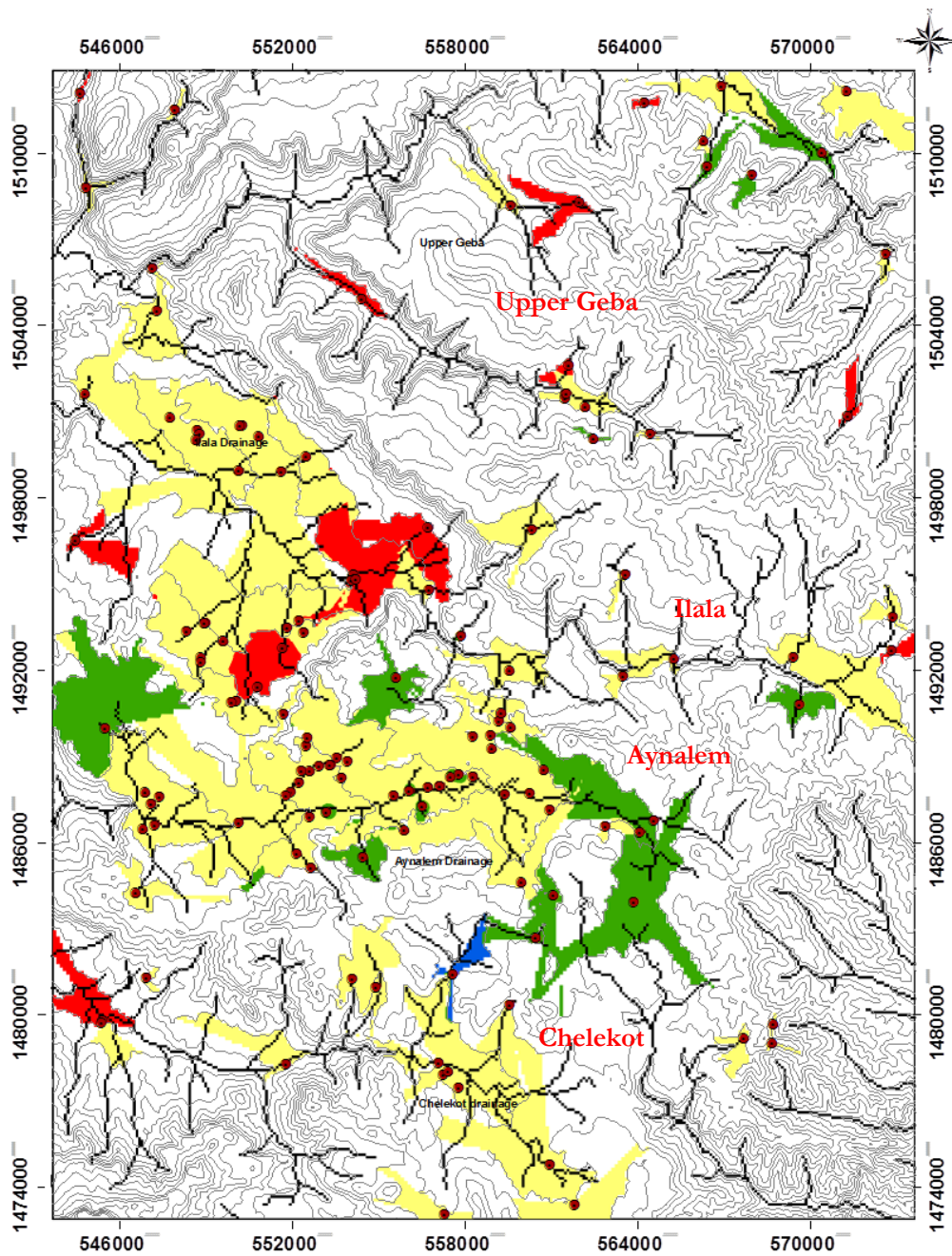
Station ID	Longitude m	Latitude m	Elevation m	Ca ²⁺ mg/l	Mg ²⁺ mg/l	Na ⁺ mg/l	K ⁺ mg/l	SiO ₂ mg/l	Cl ⁻ mg/l	HCO ₃ ⁻ mg/l	SO ₄ ²⁻ mg/l	NO ₃ ⁻ mg/l
BHA4	546892	1487735	2136	279	39	25	1	10	17	268	430	75
BHIL5	554194	1495168	1985	529	48	78	3	15	9	293	1075	25
BHMM2	547130	1505997	1809	146	26	30	12	6	22	366	100	27
BHA 4 D	546892	1487735	2136	272	40	27	2	9	23	268	490	373
BHIL 5D	554194	1495168	1985	401	59	92	2	16	9	178	1305	296
BHMM 2D	547130	1505997	1809	136	24	33	8	6	18	366	80	45

Appendix-2

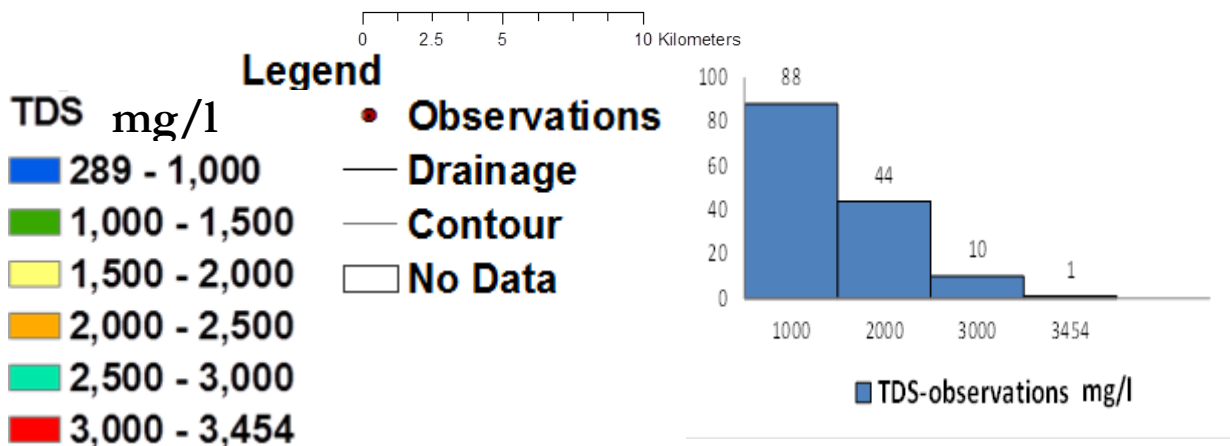
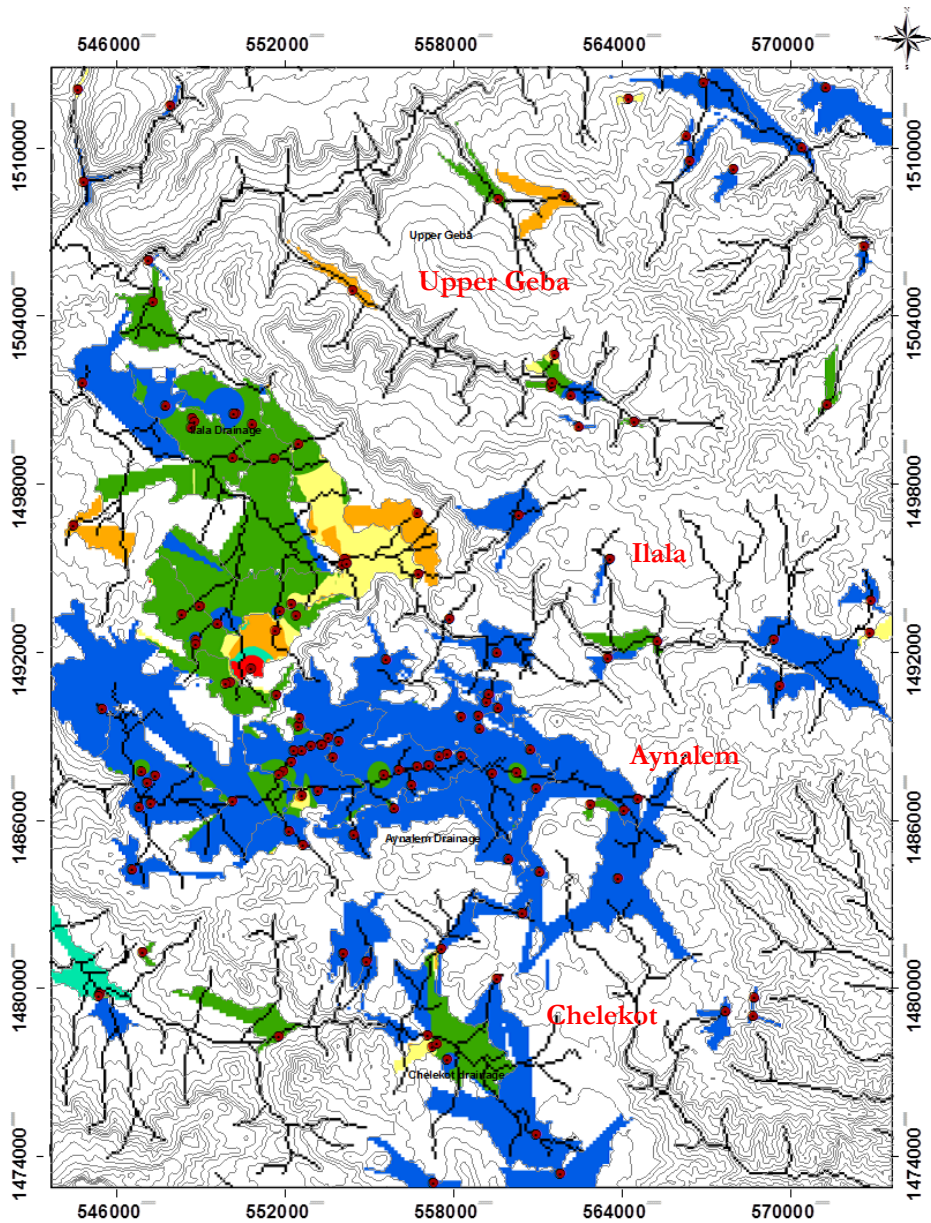
A- Interpolation map of pH



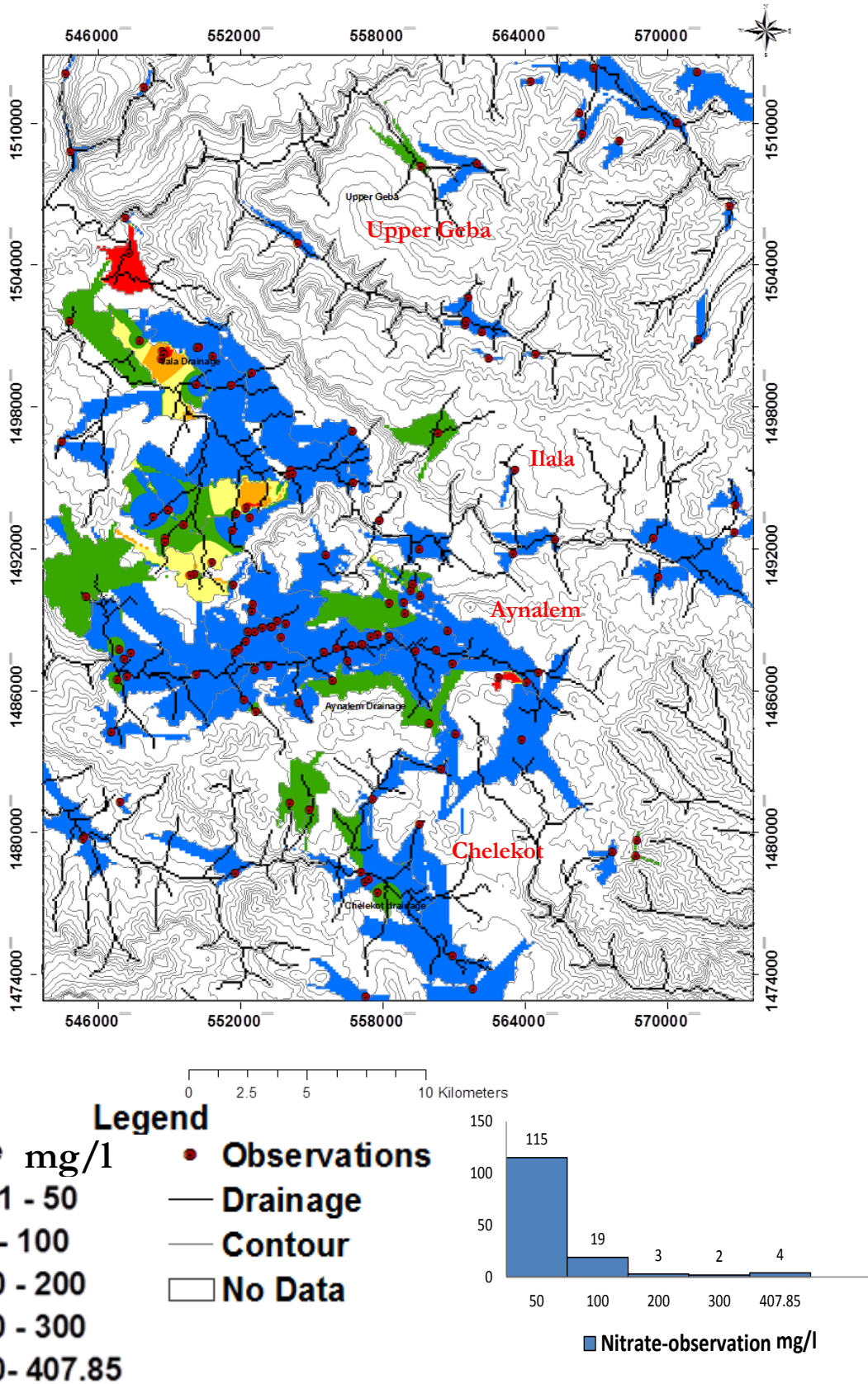
B- Interpolation map of EC (salinity hazard)



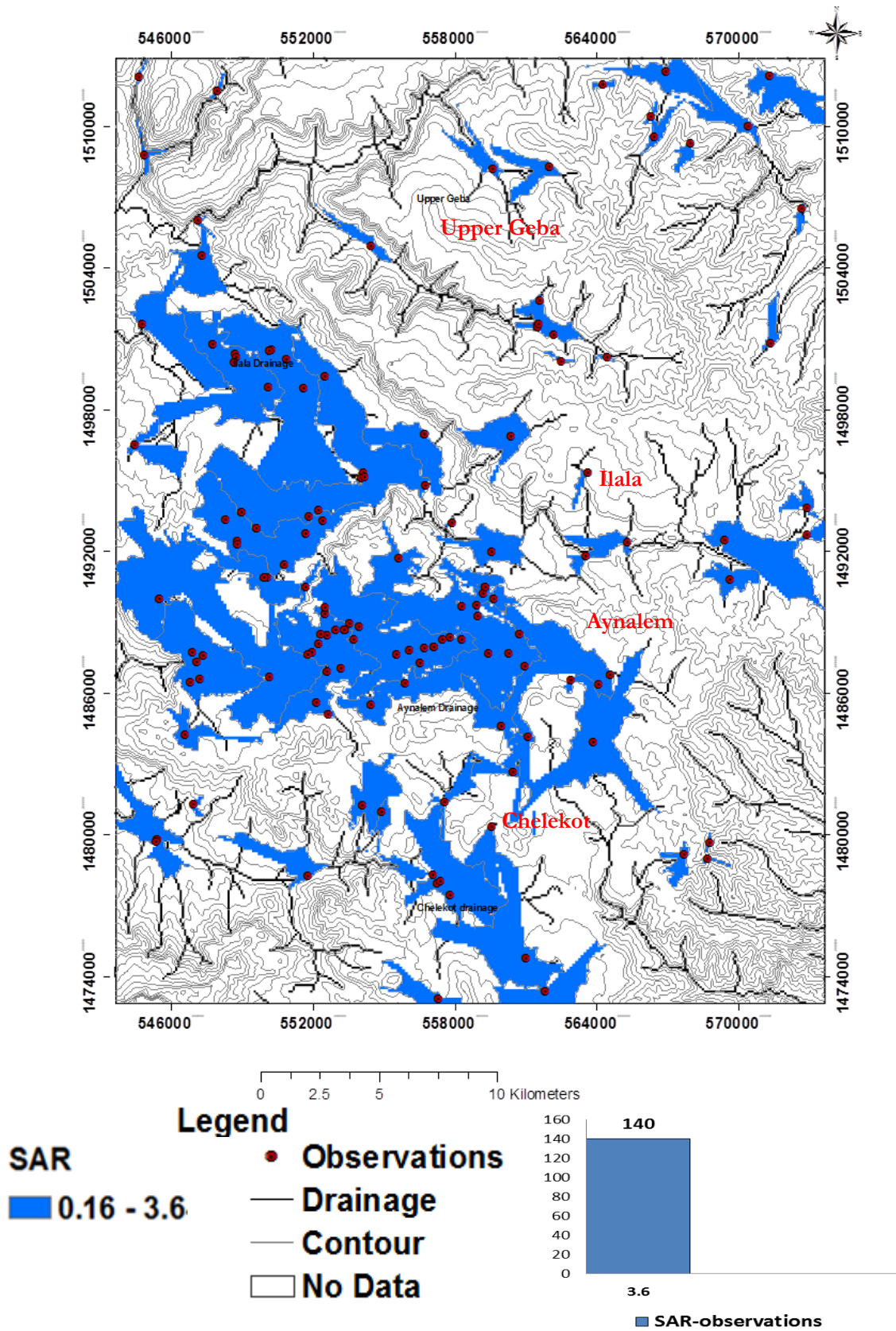
C- Interpolation map of TDS



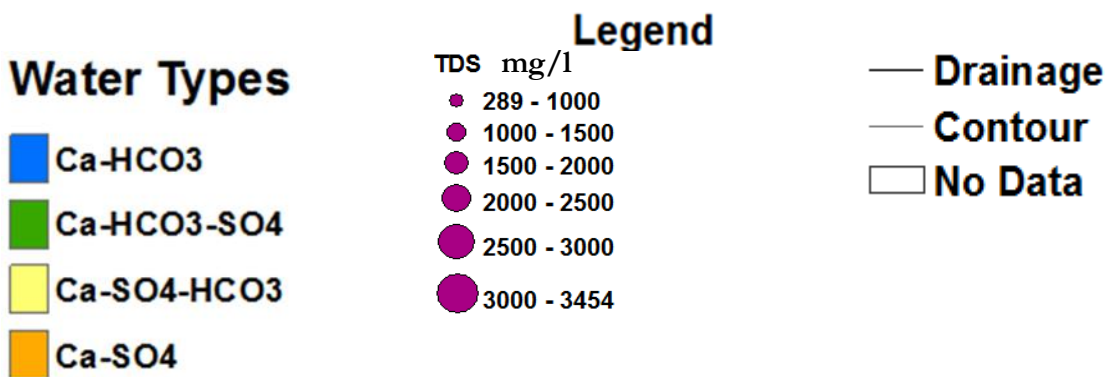
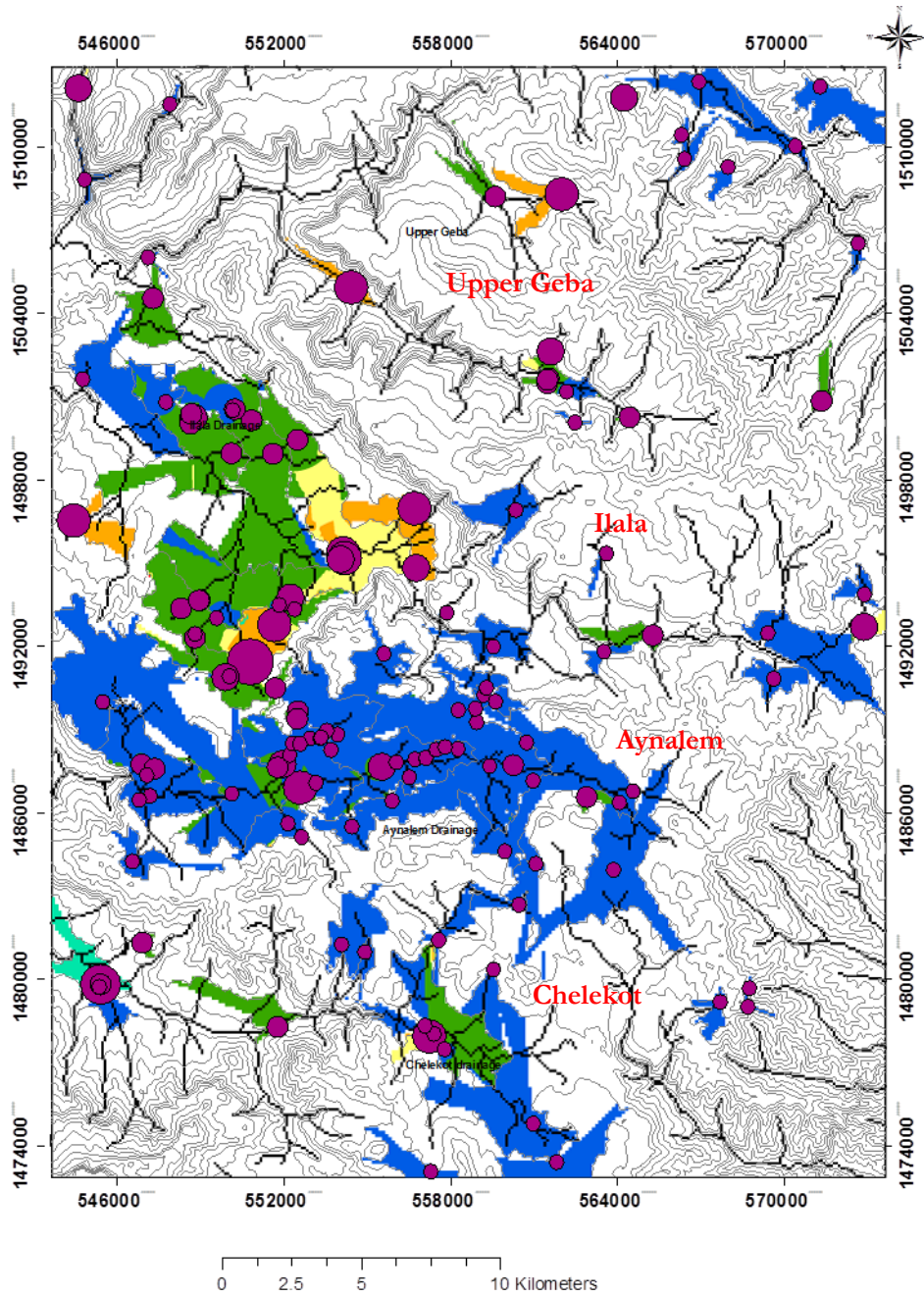
D- Interpolation map of Nitrate



E- Interpolation map of Sodium Adsorption Ratio



F- Interpolation of water type and point maps of TDS



Appendix-3 Classification of water samples in to groups and sub-groups based on water type using anions

Anion	Water Type	Cation	Borehole	Hand-dug Well	Spring	River
Bicarbonate (HCO ₃)	Ca-HCO ₃	Ca	BH-2,BH-4,BH-7,BH-32, BH-37,BH-40,BH-47,BH-48,BH-59,BH-84,BH-95,SW-45,SW-49,SW-70	HD-12,HDWAF1	SP4,SP01,SP-11	RIMM2
	Ca-Mg- HCO ₃	Ca, Mg	SW-48	HDWLL1, kebe-06, HDWMM2	SP-23, SPK2,SPA1	
	Ca-Na- HCO ₃	Ca, Na	BH-30		SPBM1	
Bicarbonate - Sulphate	Ca-HCO ₃ - SO ₄	Ca	BH-1,BH-3,BH-6,BH-16,BH-20,BH-21,BH-22,BH-38,BH-51,BH-58,BHCH2,BH2, BHL6,SW2	HD-4,HD-7, MWQ45,MWQ61,MWQ62, HD23, Kebe-05, MWQ41, MWQ63, HDWAF, HDWCH1	SP-1, SP-2, SP-17,SP-21, SP-22, SPL1	RIA2,RIC H2
	Sulphate- Bicarbonate	Ca	BH-5,BH-8,BH-9,BH-10,BH-11,BH-12,BH-63,BH-64,BH-69,BH-70,BH-94,BH-97,BH-98, CF3, MCF1, Tw-1(2005), BHA1,BHA2,BHA4,BH11, BHM1,SWK1	HD-6, MWQ29, MWQ10,HDWMM1	SP-12,SP-25,SPCH1,SPE2, SPK1,SPMM1	RICH1,RI II,1, Tap1,Tap2, Tap3
Sulphate	Ca-Mg-SO ₄ - HCO ₃	Ca, Mg	BH-72,BHA4,RH2		SP-3	
	Ca-Na-SO ₄ - HCO ₃	Ca, Na	BH-36, MCF2,RIA1,		SP-8,SPH2	
	Ca-SO ₄	Ca	BH-13,BH-14,BH-18,BH-66, BH-67,BH-71,BHCH1 ,BHCH2,BH23,BH25,SW1, BH-15,BH24,SW01	HD-1,HDWA1, HDWA2	SP-19, SPA2	RIMM1
Ca-Mg-Na- SO ₄	Ca, Mg					
Ca-Na-SO ₄	Ca		BH-73,BH-89,	jibrak-2001	SPH2	RIA1

Appendix-4 Water resources (n=132) cluster in to two group and five members of sub-groups

SG1	BH-1	BH-16	BH-2	BH-21	BH-3	BH-30	BH-32	BH-37	BH-4	BH-40	BH-43	BH-
47	BH-48	BH-5	BH-59	BH-6	BH-7	BH-8	BH-84	BH-95	TW-1(2005)		SP-24	SP-
25	SP-8	SP-11	SP-23	SP-1	SP-4	SP01	HD-4	HD-6	HD-7	HD-12	SW-45	SW-
48	SW-49	SW-70	SPK2	SPBM1	HDWAF1		SPIL1					
SG2	BH-10	BH-11	BH-12	BH-15	BH-20	BH-64	BH-9	BH-94	BH-97	BH-98	SPH1	
	SWK2	BHMM2	HDWA1	HDWCH1	HDWMM1							
SG3	BH-13	BH-14	BH-18	BH-66	BH-71	Bh-78	BH-89	MCF1	MCF2	MWQ10	SP-5	
	SP-19	HD-1	SW1	SPK1	SW01	BHCH3	BHA2	BHA3	BHIL1	BHIL3	BHIL5	
	BHCH1	BHCH2	BHMM1	HDWA2	SPA2	SPIL2	SPCH1	SPMM1				
SG4	BH-22	BH-36	BH-38	BH-51	BH-58	BH-63	BH-69	BH-70	BH-72	MWQ41		
	MWQ61		SP-12	SP-21	SP-22	SP-17	MWQ45		Keb-05	HD23	MWQ29	
	MWQ62		MWQ63		SPE1	SW2	Sp-47	BHA4	BHIL2	BHIL6	BHCH3	
SG5	BH-52	BH-67	BH-73	BH-90	CF3	SP-2	SP-3	Keb-06	Jibruk_2001		SPE2	
	SWK1	SWK3	BHIL4	HDWIL1		HDWIL2		HDWMM2	SPA1	BHA1		

Appendix-5 Source-rock Deduction Summary of Reasoning (Hounslow, 1995)

Parameters	Values	Conclusion
$\text{HCO}_3^-/\text{SiO}_2$	>10	Carbonate Weathering
	>5 and <10	Ambiguous
	<5	Silicate Weathering
$\text{SiO}_2/(\text{Na}^+ + \text{K}^+ - \text{Cl}^-)$	<1	Cation Exchange
	>1 and <2	Albite Weathering
	>2	Ferromagnesian Minerals
$(\text{Na}^+ + \text{K}^+ - \text{Cl}^-)/(\text{Na}^+ + \text{K}^+ - \text{Cl}^- + \text{Ca}^{2+})$	>0.2 and <0.8	Plagioclase Weathering Possible
	<0.2 or >0.8	Plagioclase Weathering Unlikely
$\text{Na}^+ / (\text{Na}^+ + \text{Cl}^-)$	>0.5	Sodium Source other than Halite-Albite, Ion Exchange
	=0	Halite Solution
	<0.5 TDS >500	Revers Softening, Seawater
	<0.5 TDS >500 >50	Analysis Error
	<0.5 TDS <50	Rainwater
$\text{Mg}^{2+} / (\text{Ca}^{2+} + \text{Mg}^{2+})$	$\text{HCO}_3^-/\text{SiO}_2 > 10$	Carbonate Weathering
	=0.5	Dolomite Weathering
	<0.5	Limestone-Dolomite Weathering
	>0.5	Dolomite Dissolution, Calcite Precipitation or Seawater
	$\text{HCO}_3^-/\text{SiO}_2 < 5$	Silicate Weathering
	>0.5	Ferromagnesian Minerals
$\text{Ca}^{2+} / (\text{Ca}^{2+} + \text{SO}_4^{2-})$	<0.5	Granitic Weathering
	=0.5	Gypsum Dissolution
	<0.5 pH <5.5	Pyrite Oxidation
	<0.5 neutral	Calcium Removal-Ion Exchange or Calcite Precipitation
$(\text{Ca}^{2+} + \text{Mg}^{2+}) / \text{SO}_4^{2-}$	>0.5	Calcium Source other than Gypsum-Carbonate or Silicate
	>0.8 and < 1.2	Dedolomitization

Appendix- 6

A- Initial Species having higher concentrations and activities

Name	Species	SG1		SG2		SG3		SG4		SG5	
		Molality	Activity								
C(4)	H ₂ O	5.55E+01	9.99E-01								
		1.83E-02		3.16E-03		1.79E-02		1.86E-02		1.88E-02	
	HCO ₃ ⁻	9.41E-03	7.62E-03	2.44E-03	1.99E-03	9.31E-03	7.53E-03	9.50E-03	7.69E-03	9.47E-03	7.62E-03
	CO ₂	7.92E-03	8.05E-03	4.88E-04	4.95E-04	7.67E-03	7.80E-03	8.17E-03	8.31E-03	8.37E-03	8.52E-03
Ca	CaHCO ₃ ⁺	5.23E-04	4.26E-04	1.23E-04	1.01E-04	5.14E-04	4.18E-04	5.36E-04	4.36E-04	5.57E-04	4.52E-04
	MgHCO ₃ ⁺	3.92E-04	3.11E-04	9.17E-05	7.34E-05	3.85E-04	3.05E-04	4.01E-04	3.18E-04	4.18E-04	3.29E-04
		1.55E-02		1.39E-02		1.55E-02		1.57E-02		1.64E-02	
	Ca ⁺²	1.05E-02	4.51E-03	9.23E-03	4.08E-03	1.04E-02	4.48E-03	1.06E-02	4.58E-03	1.13E-02	4.78E-03
Cl	CaSO ₄	4.54E-03	4.62E-03	4.55E-03	4.62E-03	4.54E-03	4.62E-03	4.54E-03	4.62E-03	4.54E-03	4.62E-03
	CaHCO ₃ ⁺	5.23E-04	4.26E-04	1.23E-04	1.01E-04	5.14E-04	4.18E-04	5.36E-04	4.36E-04	5.57E-04	4.52E-04
		6.38E-04		5.65E-04		9.15E-04		1.12E-03		4.81E-03	
	Cl ⁻	6.38E-04	5.05E-04	5.65E-04	4.50E-04	9.15E-04	7.24E-04	1.12E-03	8.85E-04	4.81E-03	3.78E-03
Mg		1.28E-02		1.16E-02		1.28E-02		1.29E-02		1.35E-02	
	Mg ⁺²	7.89E-03	3.51E-03	6.98E-03	3.18E-03	7.86E-03	3.49E-03	8.02E-03	3.57E-03	8.54E-03	3.72E-03
	MgSO ₄	4.52E-03	4.59E-03	4.52E-03	4.59E-03	4.52E-03	4.59E-03	4.52E-03	4.59E-03	4.51E-03	4.59E-03
	MgHCO ₃ ⁺	3.92E-04	3.11E-04	9.17E-05	7.34E-05	3.85E-04	3.05E-04	4.01E-04	3.18E-04	4.18E-04	3.29E-04
Na		1.07E-03		1.34E-03		2.74E-03		1.20E-03		4.50E-03	
	Na ⁺	1.03E-03	8.32E-04	1.30E-03	1.05E-03	2.65E-03	2.13E-03	1.17E-03	9.38E-04	4.37E-03	3.50E-03
		2.31E-02		2.42E-02		2.33E-02		2.29E-02		2.27E-02	
	SO ₄ ⁻²	1.40E-02	5.83E-03	1.50E-02	6.45E-03	1.42E-02	5.88E-03	1.38E-02	5.75E-03	1.35E-02	5.51E-03
S(6)	CaSO ₄	4.54E-03	4.62E-03	4.55E-03	4.62E-03	4.54E-03	4.62E-03	4.54E-03	4.62E-03	4.54E-03	4.62E-03
		4.52E-03		4.52E-03		4.52E-03		4.52E-03		4.52E-03	
	MgSO ₄	4.52E-03	4.59E-03	4.52E-03	4.59E-03	4.52E-03	4.59E-03	4.52E-03	4.59E-03	4.51E-03	4.59E-03
		4.52E-03		4.52E-03		4.52E-03		4.52E-03		4.51E-03	

B- Initial Phases, their saturation indices and concentration for sub-groups

		saturation indices					initial phases concentration				
		SG1	SG2	SG3	SG4	SG5	SG1	SG2	SG3	SG4	SG5
Phase	Mineral	SI	SI	SI	SI	SI	mole	mole	mole	mole	mole
Anhydrite	CaSO4	-1.82	-1.32	-0.70	-1.23	-0.95	0.015136	0.047863	0.199526	0.058884	0.112202
Aragonite	CaCO3	0.44	0.55	0.40	0.73	0.61	2.754229	3.548134	2.511886	5.370318	4.073803
Calcite	CaCO3	0.59	0.70	0.55	0.88	0.76	3.890451	5.011872	3.548134	7.585776	5.754399
CO2(g)	CO2	-2.02	-2.53	-1.93	-2.08	-1.90	0.00955	0.002951	0.011749	0.008318	0.012589
Dolomite	CaMg(CO3)2	0.46	0.74	0.44	1.12	1.10	2.884032	5.495409	2.754229	13.18257	12.58925
Gypsum	CaSO4·2H2O	-1.50	-1.00	-0.38	-0.91	-0.62	0.031623	0.1	0.416869	0.123027	0.239883
H2(g)	H2	-23.05	-23.65	-22.65	-23.25	-22.85	8.91E-24	2.24E-24	2.24E-23	5.62E-24	1.41E-23
H2O(g)	H2O	-1.55	-1.55	-1.55	-1.55	-1.55	0.028184	0.028184	0.028184	0.028184	0.028184
Halite	NaCl	-7.83	-7.80	-7.33	-7.56	-6.39	1.48E-08	1.58E-08	4.68E-08	2.75E-08	4.07E-07
O2(g)	O2	-37.79	-36.59	-38.59	-37.39	-38.19	1.62E-38	2.57E-37	2.57E-39	4.07E-38	6.46E-39
Sylvite	KCl	-8.59	-8.18	-8.05	-8.27	-7.26	2.57E-09	6.61E-09	8.91E-09	5.37E-09	5.5E-08

Appendix-7 Isotopes Deuterium and Oxygen-18 for the study area

Sample ID	Code	Types	δD	$\delta^{18}O$	D-excess
BHA1	AG1	Borehole	-13.14	-2.40	0.43
BHA3	AG2	Borehole	-10.83	-1.66	-1.45
BHIL1	AG3	Borehole	-9.32	-2.36	4.01
BHIL5	AG4	Borehole	-0.08	-1.48	8.25
BHCH1	AG5	Borehole	-7.05	-2.40	6.50
BHCH2	AG6	Borehole	-6.60	-2.43	7.14
BHMM1	AG	Borehole	-4.13	-2.49	9.96
BHMM2	AG8	Borehole	-18.19	-3.90	3.82
HDWAF1	AG9	Dug well	-2.11	-2.05	9.48
HDWA1	AG10	Dug well	5.68	-0.80	10.23
HDWIL1	AG11	Dug well	3.41	-0.87	8.33
HDWCH1	AG12	Dug well	-8.96	-2.47	4.96
HDWMM1	AG13	Dug well	3.64	0.04	3.42
SPA1	AG14	Spring	-6.33	-1.98	4.86
SPA2	AG15	Spring	-2.11	-1.76	7.86
SPIL1	AG16	Spring	3.08	-1.69	12.63
SPCH1	AG17	Spring	-1.96	-2.03	9.49
SPMM1	AG18	Spring	-0.91	-2.05	10.66
RIA1	AG19	River	13.83	1.92	2.99
RIL1	AG20	River	-1.96	-1.34	5.62
RICH1	AG21	River	-1.09	-1.24	5.93
RIMM1	AG22	River	-3.40	-1.42	4.61
BHIL2	AG23	Borehole	-1.91	-1.74	7.92
Rain	AG24	Rain	0.58	-0.86	5.41
MKB 01/GWB	PW-2	Borehole	-4.7	-2.21	7.79
MKB 02/GWB	PW-3	Borehole	-4.7	-2.12	7.28
MKB 03/GWB	PW-4	Borehole	-4.2	-1.84	6.20
MKB 04/GWB	PW-8	Borehole	-4.2	-2	7.10
MKB 05/GWB	PW-12	Borehole	-2.5	-2.01	8.86
MKB 06/GWB	TW-3	Borehole	-3.6	-2.09	8.21
MKB 07/GWB	Mai Shibti	Borehole	-5.8	-2.43	7.93
MKB 08/GWB	Enda Tarekgn	Borehole	-4.6	-2.28	8.28
MKB 09/GWB	Lachi	Borehole	-4.9	-1.87	5.67
MKB 010/GWS	Quiha spring	Spring	-4.3	-1.57	4.57
MKB 011/GWS	Aynalem spring	Spring	0.2	-1.14	6.64
MKB 012/SRE	Aynalem river	River	4.3	0.03	4.13
MKB 013/SRE	Illala river	River	4.1	-0.34	6.02

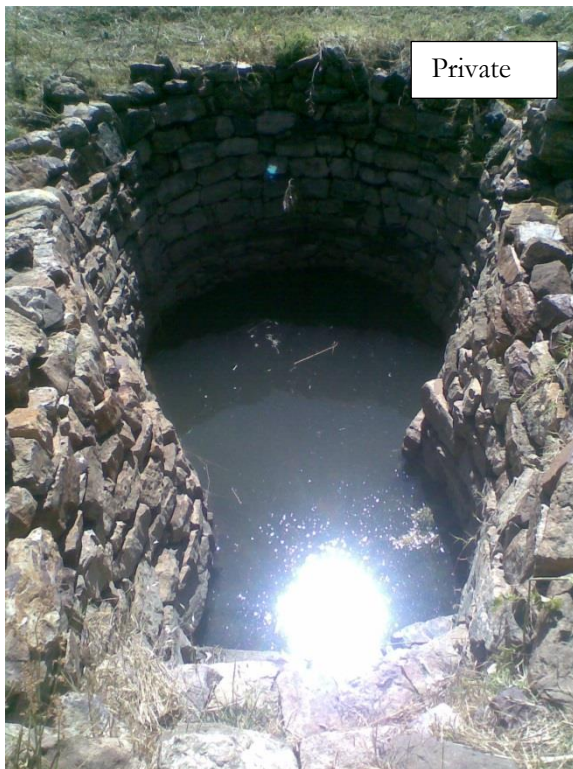
NB. The D-excess 1 and 2 are calculated using LMWL slope and the unit for Deuterium is δD_{V-SMOW} (‰) and Oxygen-18 is $\delta^{18}O_{V-SMOW}$ (‰).

Appendix-8



Figure: a, PVC Pipes to replace damaged metallic pipes due to corrosion (salinity) problem and d, metallic pipe change to soil due to corrosion problem (Berhane et al., 2013)

Appendix-9 Hand Dug Wells



Appendix -10: Primary data

40 Water samples collected by Asmelash Gebreyohanns Abreha in the Mekelle region Ethiopia, September 2013																													
Station ID No.	Sampling Date	Sample ID No.	Sample Location	Geology	UTM-E meter	UTM-N meter	Elevation	Tedegree Celsius	pH	EC μ S/cm	TDS	Hard- ness	Alka- linity	Ca mg/l	Mg mg/l	Na mg/l	K mg/l	SiO ₂ mg/l	Al mg/l	Mn mg/l	Fe mg/l	Cl mg/l	CO ₃ mg/l	HCO ₃ mg/l	SO ₄ mg/l	NH ₄ mg/l	NO ₃ mg/l	PO ₄ mg/l	
BH-A	15-9-2013	BHA1	Dandera	Limestone	545422	1479809	23.3	23.3	7.1	1352	1209	859	615	288	33	32	4.0	24.3	0.3	0.04	0.8	20	369	300	520	0.15	16	0.03	
BH-A	15-9-2013	BHA2	Asiago New	Limestone	502056	1487705	2271	24.5	6.9	1508	1205	978	550	335	34	46	3.1	18.5	0.3	0.02	0.03	15	330	288	570	0.06	13	0.02	
BH-A	15-9-2013	BHA3	May Gassa New	Limestone Shell	551783	1487625	2163	21.5	6.9	1364	1309	825	660	256	45	58	2.3	20	0.3	0.15	0.1	10	396	322	540	0.13	1	0.03	
BH-A	15-9-2013	BHA4	Tienamo	Limestone	546892	1487735	2136	21.8	7.0	1359	1079	862	550	279	39	25	1.5	9.9	0.3	0.01	0.09	17	330	288	430	-0.01	75	0.02	
BH-L	16-9-2013	BHL1	Sinba	Limestone Shell	565273	1492382	2262	23.5	7.0	1450	1249	858	650	280	38	65	3.9	17.2	0.3	0.02	1.6	21	390	317	500	1.63	21	0.02	
BH-L	16-9-2013	BHL2	May Bandera	Limestone	559201	1490233	2228	23.5	7.0	1217	949	642	580	211	27	22	1.9	13.4	0.3	0.01	0.03	73	348	283	133	0.04	132	0.03	
BH-L	16-9-2013	BHL3	Felig Daero	Limestone Shell	556765	1494810	2049	22.5	6.8	1935	1883	1483	580	486	55	66	3.1	16.3	0.3	0.07	3.02	20	348	283	950	0.83	21	0.02	
BH-L	16-9-2013	BHL4	Sewhi Adi	Limestone	548765	1500224	1957	24.1	7.0	2143	1715	1422	560	390	90	45	1.8	18.6	0.3	0.01	0.05	210	336	273	290	-0.04	406	0.03	
BH-L	16-9-2013	BHL5	Lachi	Limestone Shell	554194	1495168	1985	22.7	7.1	2290	2060	1615	540	529	48	78	3.1	15.3	0.2	0.01	1.07	9	324	263	1075	0.25	25	0.03	
BH-L	16-9-2013	BHL6	Adi Daero	Limestone Shell	548819	1492299	2072	20.5	7.0	1261	1067	724	680	245	27	27	2.3	11.8	0.1	<0.01	<0.01	50	408	332	235	0.03	64	0.02	
BH-CH	17-9-2013	BHCH1	Mirgaf Negado	Limestone Shell	545422	1479809	1910	24.6	6.7	2570	2628	1859	670	611	80	105	8.9	19.9	0.2	<0.01	5.26	7	402	327	1408	0.67	1	0.03	
BH-CH	17-9-2013	BHCH2	Meskia	Limestone Shell	557238	1477930	2218	24.5	7.0	1943	2291	1398	460	503	34	37	8.4	30.4	0.2	<0.01	1.82	5	276	224	1425	0.22	1	0.03	
BH-CH	17-9-2013	BHCH3	Mereb Mety High Sch.	Limestone Shell	557785	1477471	2248	24.2	7.0	797	880	558	680	182	24	15	3.7	15.8	0.1	<0.01	0.05	17	408	332	140	0.11	69	0.02	
BH-MM	17-9-2013	BHMM1	Mesaru	Limestone Shell	564431	1500241	2276	22.5	7.6	1182	1005	753	510	243	25	41	23.1	8.8	0.1	<0.01	<0.01	40	306	249	340	0.87	40	0.02	
BH-MM	18-9-2013	BHMM2	Chentefrese	Sandstone	547130	1356997	1809	24.5	7.5	808	813	472	750	146	16	30	12.0	6.1	0.1	<0.01	<0.01	22	450	366	100	0.06	27	0.02	
HDW-AF	15-9-2013	HDWAF1	Dolefrie	Dolefrie	563859	1488933	2340	25	7.1	686	750	412	740	138	16	37	2.2	9.1	0.1	<0.01	<0.01	17	444	361	80	0.00	16	0.02	
HDW-A	15-9-2013	HDWA1	Mekeyh	Limestone	547075	1487343	2134	19.8	7.7	1013	791	652	250	199	34	24	4.2	5	0.1	<0.01	<0.01	25	150	122	380	0.01	28	0.03	
HDW-A	18-9-2013	HDWA2	Tienamo	Limestone	547366	1487383	2130	26.6	8.1	1331	1016	620	150	190	35	39	1.6	6.4	0.2	<0.01	<0.01	8	90	73	650	0.23	2	0.02	
HDW-L	16-09-2013	HDWL1	May Avri	Limestone Shell	548648	1500004	1950	22.5	7.8	1531	1172	1033	500	258	83	45	3.2	15.4	0.1	<0.01	<0.01	215	300	244	230	0.09	151	0.02	
HDW-L	18-09-2013	HDWL2	Anna Aregawi	Limestone	549904	1490878	2096	22.5	6.8	2066	1724	1233	800	420	34	79	3.5	13.4	0.2	<0.01	<0.01	234	480	390	218	0.05	284	0.03	
HDW-CH	17-09-2013	HDWCH1	Hayki Hiltet	Dolefrie	557382	1481403	2254	27	8.4	221	355	112	270	68	6	5	2.4	5.7	0.0	<0.01	<0.01	2	162	132	122	250	0.06	46	0.02
HDW-MM	17-09-2013	HDWMM1	Mengedi drba	Limestone Shell	562172	1501155	2204	22.2	8.1	793	579	443	250	147	18	32	5.8	4.4	0.1	<0.01	<0.01	22	150	122	250	0.06	46	0.02	
HDW-MM	18-09-2013	HDWMM2	Asgerba-Sewhi	Limestone Shell	554425	1504918	2001	23.8	7.3	3010	2485	1322	1200	417	67	175	13.1	11.6	0.2	0.36	<0.01	588	720	585	525	10.08	1	0.02	
SP-A	15-09-2013	SPA1	May Atat	Limestone Shell	562895	1486554	2311	22.2	7.1	1397	1465	538	990	208	58	50	9.5	13.6	0.1	0.22	0	114	594	483	100	2.77	408	0.05	
SP-A	15-09-2013	SPA2	Avriam	Limestone Shell	552596	1488936	2160	23	6.9	2350	2379	1353	770	414	76	59	1.0	15.2	0.1	0.03	0	7	462	376	1350	0.06	9	0.02	
SP-L	16-09-2013	SPL1	May Bandera	Limestone	559285	1490499	2227	23	7.0	862	734	370	630	126	13	20	1.6	13.6	0.1	0.02	0.02	21	378	307	140	0.08	34	0.03	
SP-L	16-09-2013	SPL2	May Degene	Limestone Shell	551701	1490485	2119	23.3	7.5	1692	1344	478	700	200	20	31	87	3.2	22.8	0.1	0.02	0.01	24	420	341	575	-0.02	4	0.24
SP-CH	17-09-2013	SPCH1	Dagwegis	Limestone Shell	546923	1481307	1990	24.5	6.8	1379	1148	667	690	235	19	32	2.7	17.9	0.1	0.02	0.09	13	414	336	429	0.22	3	0.36	
SP-MM	17-09-2013	SPMM1	May Diba	Limestone	561475	1504471	2217	21.7	6.8	1759	1382	629	690	215	22	64	6.0	11.8	0.1	0.02	0.07	56	414	336	525	0.03	10	0.03	
R-A	15-09-2015	RA1	Avriam	Basalt	553164	1487065	2174	28	9.2	370	289	156	131	52	6	27	10.7	9.7	5.2	0.03	0.97	17	86	79	120	0.22	33	0.03	
R-A	15-09-2015	RA2	Kalamino	Limestone	550141	1486676	2123	21.8	7.9	755	711	391	590	124	19	26	8.6	9.9	0.1	0.09	0.12	13	354	288	127	0.05	38	0.03	
R-L	16-09-2016	RL1	Senna	Limestone Shell	563514	1491804	2224	21.4	7.8	1180	975	442	660	149	17	41	2.7	13.2	0.1	0.05	0.08	10	396	322	335	0.06	24	0.02	
R-L	16-09-2017	RL2	Hiba	Limestone Shell	552966	1493321	1978	21.6	8.1	1100	987	593	500	183	33	39	3.8	12.6	0.1	0.05	0	15	300	244	370	0.20	44	0.03	
R-CH	17-09-2018	RCH1	Mirgaf Negado	Limestone Shell	545377	1479714	1904	21.6	8.1	1030	954	542	460	176	25	36	3.6	11.1	0.1	0.04	0.02	20	276	224	400	0.08	17	0.02	
R-CH	17-09-2019	RCH2	Ruba Meskia	Limestone Shell	557402	1478023	2216	22.4	7.8	783	754	457	670	150	19	22	2.9	7.6	0.1	0.08	0.25	18	402	327	90	-0.03	49	0.02	
R-MM	17-09-2020	RMM1	May Mekden	Limestone Shell	561529	1501640	2220	21.5	7.6	1621	1405	616	650	208	33	83	1.8	8.2	0.1	0.02	0.02	75	312	284	670	0.20	2	0.05	
R-MM	18-09-2021	RMM2	May Trakele	Limestone Dolefrie	547306	1504527	1870	25.5	7.9	1227	1470	535	910	190	36	71	1.1	9.5	0.0	0.05	0.02	41	546	444	210	-0.05	346	0.02	
Tap	18-09-2022	Tap1	Adi Haki		550508	1491255	2098	24.5	7.2	1303	1303	804	580	273	29	37	1.2	18.2	0.1		0.05	7	348	283	580	0.01	27	0.03	
Tap	18-09-2023	Tap2	Adi Shinduhun		546572	1493806	2050	23.5	7.4	1270	1263	743	560	253	27	37	3.0	18.1	0.1	0.02	0.11	5	336	273	560	0.01	43	0.03	
Tap	28-09-2024	Tap3	Avder		551112	1494015	2070	22.5	7.4	1275	1267	790	520	271	27	37	3.2	18.1	0.1	0.01	<0.01	7	312	254	580	0.05	30	0.03	

Appendix-11

Secondary dat of accepted samples																			
Station ID No.	UTM-E meter	UTM-N meter	Elevation meter	EC µS/cm	TDS mg/l	Hard-ness	pH	Ca mg/l	Mg mg/l	Na mg/l	K mg/l	HCO ₃ mg/l	Cl mg/l	SO ₄ mg/l	NO ₃ mg/l	F mg/l	NH ₄ mg/l	PO ₄ mg/l	
BH-1	558941	1489255	2265	851	600	399	7.4	151	5	20	1.2	293	22	103	59	0.65	0.04	0.44	
BH-10	552219	1488072	2183	1056	812	542	7.5	211	9	35	3.0	269	17	317	4	0.65	0.47	0.51	
BH-11	552590	1488475	2194	917	620	460	7.4	168	10	34	2.8	266	12	260	4	0.83	0.40	0.57	
BH-12	552313	1488491	2195	1053	796	552	7.5	210	7	37	3.1	266	19	325	3	0.67	0.45	0.57	
BH-13	552490	1489376	2208	1210	836	650	7.5	319	12	48	3.4	179	18	686	4	1.00	0.77	0.58	
BH-14	552506	1489646	2209	1900	1404	964	7.7	370	10	56	4.3	155	19	810	5	1.27	0.90	0.41	
BH-15	556050	1487809	2211	542	350	210	7.6	54	18	24	2.0	50	17	153	5	0.66	2.08	0.04	
BH-16	553706	1488251	2210	830	586	431	7.9	152	13	20	1.6	266	13	174	16	0.06	0.33	0.13	
BH-18	555526	1487648	2221	1890	1522	1113	7.6	428	10	55	3.7	202	15	892	4	0.79	1.30	0.41	
BH-2	558901	1489740	2256	752	510	370	7.5	134	8	20	1.2	307	19	74	32	0.19	0.39	0.32	
BH-20	553549	1488948	2208	844	540	431	7.8	151	13	28	2.8	297	17	206	11	0.19	0.46	0.25	
BH-21	559618	1490000	2247	863	534	410	7.6	143	13	20	1.1	319	21	98	30	0.51	0.36	0.45	
BH-22	559953	1484601	2312	1090	698	519	7.6	168	24	26	2.6	348	65	113	53	0.59	0.45	0.29	
BH-3	558284	1489689	2271	985	708	462	7.5	168	10	22	1.3	322	42	98	82	0.52	0.42	0.42	
BH-30	560456	1482673	2317	631	385	271	7.7	84	15	34	2.0	348	10	45	7	0.52	0.35	0.29	
BH-32	564070	1486356	2323	680	434	328	7.5	109	13	17	1.4	343	10	69	11	0.21	0.34	0.45	
BH-36	561812	1473402	2284	1405	970	615	7.3	227	12	78	2.4	395	68	330	17	0.74	0.49	0.28	
BH-37	557291	1473063	2324	883	534	376	7.5	134	10	21	2.4	469	29	30	18	0.17	0.33	0.32	
BH-38	554920	1480973	2249	1292	840	622	7.5	227	13	19	3.1	369	35	259	66	0.33	0.45	0.38	
BH-4	557809	1488359	2237	688	447	309	7.4	109	9	18	1.6	319	13	48	24	0.35	0.44	0.39	
BH-40	554088	1481242	2255	820	516	363	7.6	134	7	11	2.2	381	21	32	59	0.35	0.33	0.41	
BH-43	552650	1485112	2255	1090	710	470	7.5	160	17	42	2.7	322	81	70	75	0.12	0.37	0.20	
BH-47	555901	1486423	2252	900	540	412	7.3	151	8	16	1.0	348	37	53	86	0.36	0.33	0.25	
BH-48	556519	1487277	2249	649	400	336	7.4	117	10	17	1.0	351	12	37	24	0.34	0.30	0.37	
BH-5	556722	1487915	2227	1089	785	515	7.5	193	8	29	1.2	290	18	251	19	0.25	0.48	0.51	
BH-51	547768	1500782	1946	1132	790	498	7.2	185	9	46	2.1	348	48	198	48	0.12	0.44	0.36	
BH-52	548688	1500360	1956	1713	1149	794	7.3	286	19	47	1.7	313	127	206	70	0.40	0.76	0.30	
BH-58	546813	1486455	2106	1183	757	536	7.5	178	18	26	2.7	351	57	116	70	0.38	0.38	0.30	
BH-59	545504	1489984	2131	672	426	344	7.4	122	7	7	0.4	337	7	12	56	0.30	0.30	0.15	
BH-6	558268	1488286	2243	769	528	401	7.6	151	6	21	1.4	272	13	150	18	0.06	0.44	0.50	
BH-63	548820	1492435	2070	1243	924	670	7.5	243	10	27	1.6	310	40	396	49	0.71	0.30	0.19	
BH-64	553347	1488703	2202	687	456	326	7.7	105	13	28	1.7	182	15	169	4	0.40	0.30	0.22	
BH-66	554141	1495331	2016	2540	2068	1487	7.3	502	45	81	2.2	278	73	1100	4	0.40	1.93	0.20	
BH-67	551668	1492754	2068	2680	2136	1520	7.4	518	43	93	9.0	296	122	1051	12	0.46	2.38	0.21	
BH-69	548981	1493639	2049	1374	1044	777	7.4	243	36	33	1.9	366	33	396	34	0.90	0.29	0.29	
BH-7	557115	1487967	2233	785	500	395	7.4	143	9	20	1.0	351	17	63	25	0.53	0.53	0.46	
BH-70	548313	1493357	2038	1435	1136	851	7.2	308	13	30	2.1	395	22	448	37	0.41	1.35	0.23	
BH-71	544459	1496518	1995	2660	2150	1743	7.4	632	26	36	3.0	211	13	1347	2	1.10	1.70	0.47	
BH-72	550247	1500526	1980	1438	1015	840	7.4	260	46	29	2.3	410	35	448	31	0.46	0.97	0.18	
BH-73	550130	1498943	1960	1896	1432	901	7.8	302	35	111	2.3	284	102	738	15	0.06	0.90	0.20	
BH-78	556707	1496957	2081	2520	2195	1491	7.6	504	49	49	4.0	305	23	1266	4	0.57	2.20	0.22	
BH-8	553941	1488821	2214	1034	763	531	7.6	176	2	31	1.4	287	20	280	18	0.46	0.50	0.50	
BH-84	569617	1490817	2434	627	373	315	7.8	105	13	20	0.6	319	11	37	38	0.14	0.34	0.27	
BH-89	551965	1487745	2172	1734	1523	960	7.3	319	39	60	2.5	15	57	897	4	0.28	1.14	0.02	
BH-9	552945	1488663	2202	1219	960	641	7.6	253	13	40	3.4	217	17	475	6	1.08	0.53	0.48	
BH-90	559605	1508191	2119	1730	1302	811	7.3	235	54	80	4.2	407	150	280	80	0.34	0.74	0.20	
BH-94	553320	1488680	2203	863	596	431	7.6	146	13	32	2.4	184	15	253	15	0.44	0.37	0.30	
BH-95	557487	1488269	2248	705	448	361	7.4	122	11	17	1.4	322	15	40	29	0.26	0.30	0.30	
BH-97	559405	1487676	2262	823	612	363	7.7	134	7	26	2.1	202	22	187	34	0.16	0.59	0.12	
BH-98	557115	1487960	2232	965	760	456	7.8	168	9	37	3.2	152	12	369	4	0.18	0.43	0.32	

Secondary data of 103 accepted samples, continuation

Station ID No.	UTM-E meter	UTM-N meter	Elevation meter	EC µS/cm	TDS mg/l	Hardness	pH	Ca mg/l	Mg mg/l	Na mg/l	K mg/l	HCO ₃ mg/l	Cl mg/l	SO ₄ mg/l	NO ₃ mg/l	F mg/l	NH ₄ mg/l	PO ₄ mg/l
TW-1(2005)	560968	1487142	2237	1016	782	539	7.3	209	4	20	1.3	320	20	280	13	0.50	0.26	0.04
MCF1	551617	1498923	1984	1774	1376	284	6.9	316	45	62	4.6	346	38	652	18			
MCF2	550855	1500131	1977	1751	1296	317	7.0	223	50	152	3.9	387	74	562	3			
MWQ10	554049	1495122	2005	2290	1633	1058	7.9	350	44	62	2.0	321	55	675	0			
MWQ41	560730	1488518	2284	762	543	533	8.1	178	21	11	2.0	404	15	274	0			
MWQ61	550174	1500497	1981	1174	837	657	8.2	201	37	16	1.7	588	25	183	30			
CF3	552500	1499429	2022	1937	1382	410	7.0	188	69	202	7.7	500	77	533	22			
SP-5	561486	1501596	2222	1775	1312	947	7.6	324	26	61	5.8	343	67	580	48	0.25	0.85	0.17
SP-19	551781	1478274	2015	1672	1308	922	7.8	311	35	38	3.6	179	36	712	4	0.39	0.86	0.24
SP-24	555605	1491726	2247	575	330	307	7.7	105	11	13	0.9	354	6	15	9	0.35	0.41	0.39
SP-25	557864	1493201	2112	668	396	347	7.9	111	17	14	0.9	334	15	46	32	0.26	0.55	0.25
SP-8	562470	1500055	2327	682	464	344	7.6	112	13	17	1.3	261	18	150	19	0.12	0.35	0.21
SP-11	546564	1484237	2183	790	472	368	8.1	122	13	31	0.7	361	17	45	38		0.34	0.34
SP-12	547201	1486597	2112	1190	782	601	7.6	186	29	32	0.9	299	27	290	23		0.41	0.19
SP-21	560347	1496897	2340	1165	835	590	7.6	218	11	34	1.2	316	36	251	53	0.07	0.45	0.20
SP-22	563602	1495337	2373	1032	705	567	7.4	193	20	22	1.2	401	20	174	40		0.43	0.15
SP-23	552160	1485603	2184	821	528	412	7.3	126	23	26	0.8	413	36	59	18	0.04	0.73	0.23
SP-17	557078	1478316	2203	992	676	521	7.3	162	25	22	1.7	334	30	169	28	0.20	0.38	0.29
SP-1	559289	1490495	2223	863	556	412	7.8	151	8	21	1.1	316	21	116	38	0.22	0.37	0.35
SP-2	568690	1479000	2230	1476	990	699	7.6	218	37	60	2.9	357	100	230	99	0.34	0.61	0.39
SP-3	568746	1479672	2286	1346	936	651	7.8	193	41	58	2.5	258	87	317	78	0.64	0.67	0.24
SP-4	554457	1485491	2258	596	352	294	7.5	101	10	11	2.8	331	11	15	24	0.16	0.34	0.38
SP01	564560	1486767	2321	683	570	328	7.4	105	16	13	1.2	355	14	61	5			
MWQ45	559542	1491972	2138	1304	930	617	8.5	175	43	34	1.0	476	83	298	0			
HD-1	567696	1479172	2320	1199	780	504	7.7	143	36	72	3.3	457	37	200	7	0.43	0.42	0.44
HD-4	561072	1484157	2335	722	436	252	7.8	84	10	58	4.0	425	15	24	6	0.28	0.34	0.25
HD-6	559545	1480345	2288	917	596	433	7.5	151	13	46	0.9	378	21	135	18	0.54	0.36	0.57
HD-7	560974	1474794	2271	1020	660	228	7.3	151	12	58	2.2	413	64	53	42	0.61	0.38	0.17
HD-12	544780	1501607	1906	885	600	347	7.5	126	8	37	2.6	416	23	34	52	1.00	0.34	0.54
Keb-05	551843	1493480	2023	1036	873	538	7.1	166	30	24	1.0	415	21	178	37			
Keb-06	552246	1493738	2027	2320	1668	1120	7.4	350	60	50	3.1	340	298	230	336			
Jibruk_200	550806	1491426	2071	5300	3454	2041	7.4	620	120	260	4.7	412	231	1607	199			
HD23	549588	1493004	2045	1154	934	585	7.5	198	22	22	3.5	350	42	218	78			
MWQ29	550053	1490912	2075	1117	797	838	7.9	300	21	24	1.0	405	90	392	0			
MWQ62	549588	1493004	2045	1284	916	837	8.3	303	19	27	1.3	466	62	311	75			
MWQ63	548960	1493639	2032	1413	1010	845	8.2	288	30	20	0.7	691	25	281	9			
SPE1	569411	1492462	2382	1213	728		7.8	179	19	34	2.0	384	27	262	1	0.14		
SW1	572860	1492688	2389	2977	1786		7.3	504	26	55	2.7	313	40	982	3	1.3		
SW2	572878	1493857	2409	1240	744		7.7	193	27	34	0.7	372	37	247	14	0.51		
SPE2	571338	1500834	2361	2327	1396		8.0	308	53	85	3.7	325	98	630	48	0.69		
SPK1	561600	1502608	2253	2683	1610		6.8	410	47	66	2.6	343	80	820	0	1.24		
Sp-47	572655	1506501	2266	1297	778		7.8	206	33	21	1.6	320	32	312	10	0.7		
SW-45	570401	1510014	2392	630	378		7.6	99	10	16	1.3	243	29	53	17	0.49		
SW-48	566933	1512326	2278	920	552		7.4	122	29	18	1.9	335	63	86	18	0.39		
SW-49	566413	1509551	2234	610	366		7.5	75	13	26	2.4	300	11	59	4	0.54		
SWK1	564238	1511748	2007	2592	1555		6.9	336	51	110	3.3	370	129	716	15	0.68		
SPH1	544854	1508800	2103	817	490		7.6	100	22	29	7.0	297	46	85	14	0.46		
SW01	562000	1508280	1970	3353	2012		7.8	347	90	90	9.8	277	27	1002	1	0.97		
SW-70	571286	1512152	2367	753	452		7.4	130	13	11	0.3	361	22	25	24	0.21		
SWK2	566298	1510418	2000	907	544		7.1	120	19	25	4.9	266	34	125	23	0.85		
SPK2	567974	1509262	2222	667	400		7.8	76	28	31	0.5	351	24	13	6	0.46		
SPBM1	547918	1511516	2256	927	556		7.7	139	6	72	4.1	397	22	90	22	0.37		
SWK3	544623	1512094	2148	2593	1556		7.1	155	95	234	8.4	499	162	615	17	1.92		

Secondary data of rejected water samples																
Station ID No.	UTM-E meter	UTM-N meter	Elevation meter	EC $\mu\text{S/cm}$	TDS mg/l	Hardness	pH	Ca mg/l	Mg mg/l	Na mg/l	K mg/l	HCO ₃ mg/l	Cl mg/l	SO ₄ mg/l	NO ₃ mg/l	
NMWQ37	554369	1489536	2219	841	600	400	8.2	130	18	15	2	330	11	279	0.29	
NMWQ43	560528	1491641	2161	947	675	517	8.3	170	22	14	3	460	11	401	0.31	
NMWQ50	559092	1490160	2218	1099	784	400	7.9	125	21	16	2	345	52	322	0.29	
NMWQ42	559192	1490424	2215	891	635	458	8.2	150	20	14	2	391	27	252	0.33	
Jubruk_2011	550806	1491426	2071	2700	1961	926	8.5	285	52	18	0.5	593	197	514	0.29	
NMWQ30	549807	1490804	2088	1342	957	967	7.9	350	22	22	1	502	82	248	0.35	
NMWQ51	550035	1493830	2014	1833	1307	621	8.5	175	44	69	1	449	143	487	0.35	
NMWQ65	551033	1491964	2060	2390	1704	1650	7.2	600	36	107	0.4	658	219	420	124.2	
NMWQ66	551033	1491964	2060	2390	1704	1650	7.2	600	36	107	0.4	658	219	420	124.2	
NMWQ67	551033	1491964	2060	2390	1704	1650	7.2	600	36	107	0.4	658	219	420	124.2	
NMWQ68	551033	1491964	2060	2390	1704	1650	7.2	600	36	107	0.4	658	219	420	124.2	
NMWQ69	551033	1491964	2060	2390	1704	1650	7.2	600	36	107	0.4	658	219	420	124.2	
NMWQ70	551033	1491964	2060	2390	1704	1650	7.2	600	36	107	0.4	658	219	420	124.2	
NMWQ71	551033	1491964	2060	2390	1704	1650	7.2	600	36	107	0.4	658	219	420	124.2	
Gereb Beati	551339	1486555		390	320	175	6.9	180	10	15	4	80	16	480	13	
Era_Quihila	564688	1486570		580	290	197	7.1	132	12	18	5	65	9	300	35	
May Tuwaru	563738	1487881		600	300	218	7.4	150	7	8	1.2	40	16	180	13	
BH-2/2006	558901	1489740	2256	752	510	370	7.5	134		20	1.2		19	74	32.1	
BH-43/2006	552650	1485112	2205	1090	710	470	7.5	160		42	2.7		81	70	75.2	
BH-63/2006	548820	1492435	2070	1243	924	670	7.5	243		27	1.6		40	396	48.8	
BH-7/2006	557115	1487967	2233	785	500	395	7.4	143		20	1		17	63	24.6	
BH-84/2006	569617	1490817	2434	627	373	315	7.8	105		20	0.6		11	37	37.84	
BH-95/2006	557487	1488269	2248	705	448	361	7.4	122		17	1.4		15	40	29	
MCF1/2006	551617	1498923	1984	1774	1376	284	6.9	316		62	4.6		38	652	18.3	
SP-25/2006	557864	1493201	2112	668	396	347	7.9	111		14	0.9		15	46	31.68	
SP-17/2006	557078	1478316	2203	992	676	521	7.3	162		22	1.7		30	169	28.2	

Appendi- 12 Field Activity Photos



Appendix-13 Laboratory Activity Photos

